QUANTITATIVE FAILURE MODELS OF FEED-FORWARD NEURAL NETWORKS

by

Mark Jonathan Dzwonczyk

B. S. Electrical Engineering, summa cum laude

Tufts University (1984)

Submitted to the Department of Aeronautics and Astronautics

in partial fulfillment of the requirements for the degree of

MASTER OF SCIENCE

in Aeronautics and Astronautics

at the Massachusetts Institute of Technology

February, 1991

Signature of Author _____
Department of Aeronautics and Astronautics
January 15, 1991

Certified by _____
Wallace E. Vander Velde
Professor, Department of Aeronautics and Astronautics
Thesis Supervisor

Certified by _____
Professor Harold Y. Wachman
Chairman, Department Graduate Committee

QUANTITATIVE FAILURE MODELS OF FEED-FORWARD NEURAL NETWORKS

by

Mark Jonathan Dzwonczyk

Submitted to

the Department of Aeronautics and Astronautics on January 15, 1991

in partial fulfillment of the requirements for the degree of

Master of Science in Aeronautics and Astronautics

ABSTRACT

The behavior of feed-forward neural networks under faulty conditions is examined using quantitative models. The madaline multi-layer network for pattern classification is used as a representative paradigm. An operating model of the madaline network with internal weight failures is derived. The model is based upon the operation of a single n-input processing node in n-dimensional space. It quantitatively determines the probability of a node failure (incorrect classification) under specified fault conditions. Resulting errors are then propagated through network to determine the probability of madaline failure. The analysis is intentionally general so that the models can be extended to other neural paradigms.

Thesis Supervisor: Dr. Wallace E. Vander Velde, Professor of Aeronautics and Astronautics

ACKNOWLEDGEMENTS

Several people contributed to the successful completion of this thesis. Foremost, my thesis advisor, Professor Wallace Vander Velde, provided insightful guidance to focus the work and develop meaningful results. Professor Richard Dudley of the Department at Mathematics of MIT suggested methods for deriving the probability density functions in Chapter Three and patiently assisted with questions until the derivations were complete. I gratefully acknowledge their contributions.

This work was supported by the generous Staff Associate Program of the Charles Stark Draper Laboratory, Inc. I am thankful to the Laboratory for the privilege to pursue this research on a full-time basis. I am particularly appreciative to Dr. Jaynarayan Lala, Leader of the Fault-Tolerant Systems Division, for his patience during my extended leave.

Finally, I am deeply thankful for having a supportive family — including the two new additions, Natalie and Lianne — which has been indulgent of my unorthodox schedule for the past 18 months.

Special appreciation goes to Michelle Schaffer for her continued support of my goals.

TABLE OF CONTENTS

CHAPTER ONE
INTRODUCTION

Processing architectures inspired by biological neural systems, so-called *neural networks*, have been proven to excel at certain classes of computational problems. These systems can modify their outputs in order to minimize some error function, essentially performing non-linear optimization of a multi-dimensional function mapping. This ability to learn, by self-tuning the processing topology to minimize output error, makes the systems attractive for implementing functions that are not well understood or difficult to formulate mathematically. Furthermore, the systems exploit massive parallelism through distributed storage of global information to achieve a robust realization of this mapping.

Simulations of these architectures have demonstrated their utility for a variety of state identification problems, particularly in pattern recognition. Hardware prototypes which implement the algorithms in silicon are now being introduced for such problems. With the continued advancement of the technology, it is inevitable that operational hardware implementations will be deployed into meaningful systems in the next five years.

It has been conjectured that the fundamental properties of these systems make them inherently *fault-tolerant*. Since state information is dispersed throughout the connection weights of a large network, the argument goes, loss of any particular local data will not notably disturb the global state representation, so the systems can withstand a degree of locally distributed failures. Moreover, their internal thresholding logic is able to restrain the propagation of errors. The most celebrated property is the architecture's ability to learn. This means the systems can adapt to internal failures, effectively reconfiguring themselves around failed elements.

Although these claims may have merit, there has been no examination of neural network architectures resulting in quantitative metrics of performance under faulty conditions.

To date, the research has provided only qualitative analyses of particular properties and failure characteristics of select network instantiations; for examples see [11, 33, 35, 36]. Given the expansive progression of the systems and their likely deployment into substantive applications in the next several years, it is clear that a quantitative measure of their fault-tolerance is in order.

This thesis addresses the quantification of the performance of neural networks in the presence of faults. It is the start of the formulation of a set of criteria that can be applied to designing ultra-reliable systems.

The approach is to develop a model of the operation of a neural network under faulty conditions. A particular feed-forward network is chosen as a representative paradigm. A spatial analysis of the operation of a processing node, or neuron, is used to determine the effects of faults in the network. Network reliability is determined by a systematic propagation of the errors from failed nodes.

The purpose of this thesis is not a final pronouncement on the fault-tolerance of neural networks. The models developed here, and the methods used to construct the models, serve as an essential foundation for the rigorous analysis that must be partaken to determine the viability of neural networks as reliable processing architectures.

A general discussion of the computational model of a neural network is omitted from this work. The reader unfamiliar with the architecture and operation of these *connectionist* systems is referred to the many references now available on the subject, including newly available textbooks [20, 54], summary compilations [3, 46], and the seminal articles that span the forty years of research of these systems referenced therein.

Chapter Two provides a detailed description of the madaline neural network, the paradigm selected for study here. Since the failure models constructed later in the text are based upon the operation of madaline processing elements, called adalines, particular attention

is given to the description of the adaline in that Chapter. This includes adaline learning, although learning is not addressed in the failure models. It is hoped that this additional detail will provide the unfamiliar reader with a more substantive understanding of this particular neuron element.

Chapter Three comprises virtually all the novel work. The formal criteria for the madaline failure model are presented first. Next, a spatial analysis is used to determine the operation of an n-input adaline node. In §3.3, failure models of the adaline are constructed. These models require evaluating the expected values of functions of random variables, where the variables are the components of an adaline synaptic weight vector. The probability density functions of those components are next derived. In §3.5, the models are evaluated. Closed-form solutions for the probability of adaline failure are obtained. Monte Carlo simulations are used to evaluate those equations. In the final section of Chapter Three, the adaline failure models are combined to determine madaline failure.

Concluding remarks, including the identification of future research areas, are presented in Chapter Four.

CHAPTER TWO

THE ADALINE AND MADALINE MODELS

One early computational model which continues to pervade fine grain parallel architectures is the adaptive linear element, or *adaline*. The adaline was introduced by Widrow [60] over three decades ago during the first wave of connectionist activity and was shown to be a statistically-optimum, trainable classifier. Its utility as a statistical predictor led to its useful application in real-time adaptive signal processing problems. Currently it is overwhelmingly used in these contexts [64] and has had commercial success in the telecommunications industry, particularly as an adaptive equalizer for digital modems and as an echo canceller in long distance telephone transmissions. With the recent resurgence in neural networks, the adaline has again become in vogue as a classifier.

In addition to being one of the earliest models for neural processing, the adaline is also one of the simplest. This makes it ideal for study. Furthermore, it is so general in form, that other, more complex neural models can be considered specializations of it. For example, Rosenblatt's perceptron [38] can be considered to be an adaline with additional random fixed weights and asymmetric Boolean input and output values. Also, if a sigmoid function replaces the hard-limiter in an adaline, the popular back-propagation learning method [40] can be used to train a network of adalines. In fact, nearly all non-stochastic connectionist processing systems are generalized by the adaline model. For this reason, the adaline is chosen as a model for study here. The failure models which are developed in Chapter Three will similarly be broad representations which can be tailored to the parameters of other neural processing models.

This chapter describes the operation of the adaline in both recall and learning phases. After a review of single element operation and capabilities, the incorporation of the element into a network of many adalines (a *madaline*) is discussed. The acronyms adaline and madaline, incidentally, were coined by Widrow.

2.1. A Single Processing Element: The Adaline

The adaptive linear element is a processing node which performs a weighted sum of its inputs followed by a hard limiting threshold function. A diagram of an adaline is shown in Figure 2-1. The adaline has n inputs, x_i, i = 1, ..., n, and one output, y. The inputs and output take on binary values. Unlike conventional Boolean representations, however, the inputs and output are symmetrically-valued: each may be either +1 or -1. This approach simplifies the mathematical analysis and allows for inhibiting signals (at level -1) to be readily utilized.

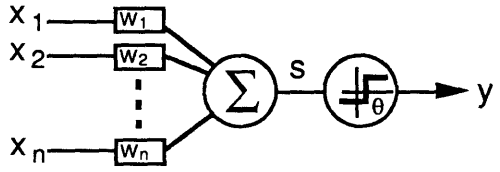

Figure 2-1: *An Adaptive Linear Element*

Each input is multiplied by a weight value. Thus, there are n weights, w_i, i = 1, ..., n, corresponding to the respective inputs. Weights have continuous values and can be positive or negative (or zero).

A sum of the weighted inputs is first performed in the node. The result is $s = \sum_{i=1}^{n} x_i w_i$.

If the inputs x_i and w_i are considered to be the elements of two n-dimensional vectors **x** and **w**,

$$\mathbf{x} \equiv \begin{bmatrix} x_1 \\ x_2 \\ \cdots \\ x_n \end{bmatrix} \qquad \mathbf{w} \equiv \begin{bmatrix} w_1 \\ w_2 \\ \cdots \\ w_n \end{bmatrix}$$

then the sum can be written as the dot product of the two vectors. Thus,

$$s = \mathbf{x} \circ \mathbf{w} = \mathbf{x}^T\mathbf{w} = \mathbf{w}^T\mathbf{x}$$

The sum is fed to a threshold element with parameter θ to yield the node output y. The threshold function is depicted in Figure 2-2. Thus, the output can be written as a function of the input and weight vectors and the threshold value:

$$y = SGN\{\mathbf{x} \circ \mathbf{w} - \theta\} \tag{2-1}$$

where $SGN\{\bullet\}$ simply takes the sign of its argument.

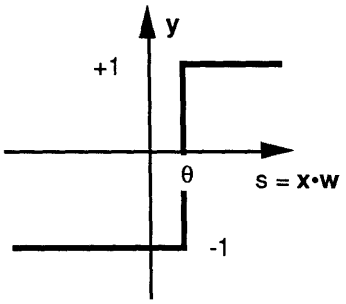

Figure 2-2: *Hard Limiting Threshold Function*

2.1.1 Adaline Classification

The adaline can classify input sets into two categories, a +1 or -1 category, as specified by the output. If the argument of eq. (2-1) is set to 0, the decision boundary in n-dimensional space, $\Re^n$, of the adaline is found:

$$\mathbf{x} \circ \mathbf{w} = \theta \tag{2-2}$$

This is an (n-1)-dimensional plane (a hyperplane) in input space $\Re^n$, given by the equation:

$$x_n = \frac{-x_1 w_1 - x_2 w_2 - \ldots - x_{n-1} w_{n-1} + \theta}{w_n} \tag{2–3}$$

Classification can be seen with a simple 2-input adaline example (Figure 2-3). The adaline schematic is shown in part (a) of the figure and the 4 possible input combinations, $(\pm 1, \pm 1)$, are shown in 2-dimensional space in part (b). Suppose input (+1, +1) is assigned to the set A and the remaining inputs to the complement set, $\overline{A}$. Any number of lines in the input space can be drawn to separate those inputs, that is, to make that decision boundary. A particular one is shown in the figure. The line has the equation $x_2 = -x_1 + 1$.

From eq. (2-2) the decision boundary of this example is $x_1 w_1 + x_2 w_2 = \theta$, which can be manipulated, as presented in eq. (2-3), to obtain a linear equation for x_2 in terms of x_1 and θ:

$$x_2 = -\frac{w_1}{w_2} x_1 + \frac{\theta}{w_2} \tag{2-4}$$

The resulting line (a hyperplane of dimension 1) has a slope of $-\frac{w_1}{w_2}$ and an x_2-intercept of $\frac{\theta}{w_2}$. If w_1, w_2, and θ are all set to 1, eq. (2-4) is $x_2 = -x_1 + 1$, precisely the line drawn in Figure 2-3b. Now if the set A is equated with a y value of +1 and the set $\overline{A}$ with a y value of -1, the adaline with $w_1 = w_2 = \theta = 1$ will perform the desired classification, creating the decision boundary shown in Figure 2-3b. By varying the parameters w_1, w_2 and θ, other decision boundaries can be drawn.

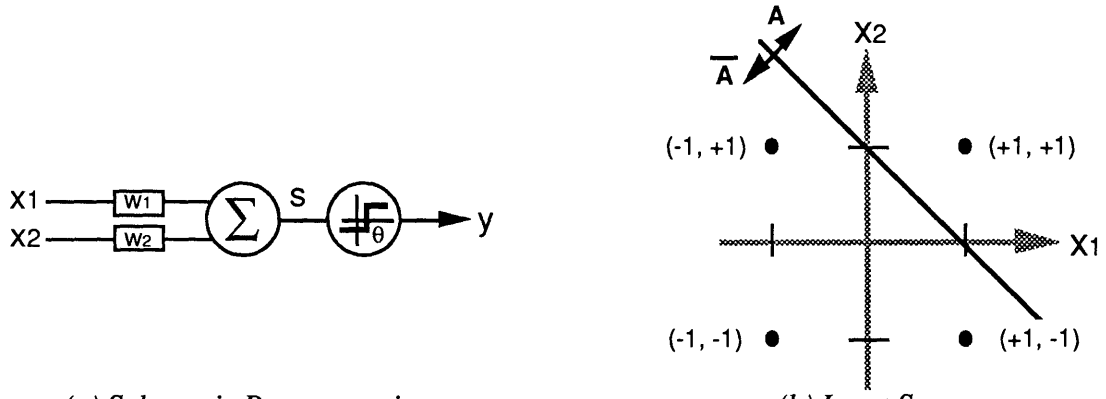

(a) Schematic Representation *(b) Input Space*

Figure 2-3: *The 2-input Adaline*

2.1.2 Simplifying the Adaline Equations

One of the characteristics of the adaline, and of all neural network processors, is regularity. Regularity affords easy replication and streamlines mathematical analysis. Although it may be obvious that the input weights of an adaline can be readily modified to perform a classification function, the requirement to change the threshold parameter, θ, for each adaline does not appear to be a simple task. In the model described by eq. (2-4), a new threshold function must be constructed (with a new θ) in order to move the x_2 intercept of the decision boundary.

In fact, the model can be altered to make the adaline structure more regular. The threshold function is simplified by setting $\theta = 0$ for all adalines. The variability of the

threshold parameter can be recovered by adding a new input, $x_0 \equiv +1$, and weighting that input by w_0. Thus, the strict definition of the adaline function, originally described by Widrow [60] is given by

$$y = SGN\left\{ \sum_{i=0}^{n} x_i w_i \right\} \tag{2-5}$$

The adaline is shown in Figure 2-4.

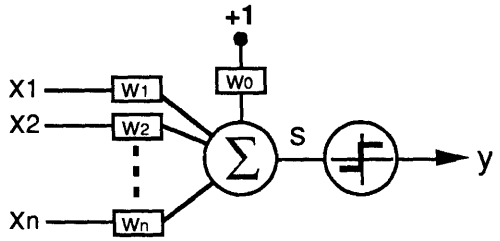

***Figure 2-4**: The Adaline*

The general n-1 dimensional hyperplane is determined by

$$x_n = \frac{-w_0 - x_1 w_1 - x_2 w_2 - \ldots - x_{n-1} w_{n-1}}{w_n} \tag{2-6}$$

The new weight, w_0, is $-\theta$ of the original model. In the 2-input example, eq. (2-4) becomes,

$$x_2 = -\frac{w_1}{w_2} x_1 - \frac{w_0}{w_2}$$

Figure 2-4 and eq. (2-5), where $x_0 \equiv +1$, will be used for the remainder of this work as the adaline definitions.

2.2 Training an Adaline using LMS Techniques

The adaline has the ability to classify its inputs into one of two categories. In the example of the previous section, a two input adaline was programmed to perform as a logical AND gate. That is, if -1 is equated with logical FALSE (F) and +1 is equated with logical TRUE (T) , then the output, y, is T if and only if input x_1 is T AND input x_2 is T; otherwise y is F. With $w_1 = w_2 = +1$ and $w_0 = -1$ (the weight values have no logical significance and are coincidentally +1 and -1), the AND function, tabulated below, has been constructed.

x_1	x_2	$y = (x_1$ AND $x_2)$
-1, F	-1, F	-1, F
-1, F	+1, T	-1, F
+1, T	-1, F	-1, F
+1, T	+1, T	+1, T

Figure 2-5: *Logical AND Function Constructed by the 2-input Adaline of §2.1*

In this example, the adaline was *programmed.* That is, eq. (2-6) was analytically solved for w_0, w_1, and w_2. (There were three unknowns and 1 equation, so two variables were arbitrarily set to +1.) Programming the weights of an adaline becomes difficult, however, as the number of inputs grows large. If the analytic classification function is not known (if the location of the hyperplane is not known) programming becomes impossible.[1] For example, suppose the input vector represents a 2-dimensional pattern of a binary image and it is desired to have an adaline determine if that image is a filled-in circle. It would be a very difficult task to identify a priori the placement of the hyperplane decision boundary on the input space.

As its name implies, however, the adaline can be made to adapt itself in order to perform the classification. When presented with the set of inputs and corresponding outputs, the adaline can adapt its weights so that the appropriate classification will be performed. This process is called *learning* and is one of the fundamental properties of neurocomputing systems. It obviates the need for analytical solutions to classification problems and the ensuing programming which is requisite for all conventional computing systems. The neural approach also allows, simply upon presentation of examples, abstraction of concepts to statistically resolve the key features of the input space and generalization to situations never before encountered.

---

1. If the hyperplane location is known, a look-up table or other less complex method could be used to perform the classification.

In this section, adaline learning is examined. It is shown that the adaline can learn a classification in an optimum manner by using only information available only locally, that is, by using only the input and weight vectors, the desired output, and the current output, which may be in error. The adaline adjusts its weights to minimize this error.

2.2.1 Training Based Upon Output Error

The adaline can learn a classification function simply upon repeated presentation of pairs of input vectors and corresponding desired outputs. This process is called *supervised learning* because a supervisor is required to present the adaline with the desired output category for the input vector.[2] Thus, the availability of an output training signal is assumed. For large input vectors (representing, for example, a two dimensional pattern) this is a non-trivial assumption: it is not always clear which is the appropriate classification, and if it were a look-up table may well suffice for the task.

Consider the following process. A specific input vector $\mathbf{x}_1$ with a desired classification, y_d, is presented to an arbitrarily configured adaline. The adaline settles to an output, y, based upon its arbitrary weights, $\mathbf{w}$. An error signal, ε, is constructed from y_d and y. The signal ε is a penalty or cost function of output y with respect to y_d , $\varepsilon = C(y, y_d)$. The weights are then systematically adjusted until the error is zero or the cost is minimized in some reasonable sense. If the error is zero, then the adaline has been properly adapted and it has "learned" the classification of that specific input vector $\mathbf{x}_1$. This process can be repeated for multiple pairs of vectors and desired classes, $\{\mathbf{x}_i, y_{di}\}$. If the cost is optimally minimized, the adaline has learned to the best of its ability. When the error is zero for all vectors, the adaline has learned the appropriate classification.

---

2. Another form of learning, called unsupervised or self-organized, obviates the need for the training input. Two of the more popular unsupervised learning methods are Kohonen's *self-organizing map* [26] and the *adaptive resonance theories* of Grossberg and Carpenter [52].

The principal challenge to creating a supervised learning scheme is the derivation of a systematic weight modification method which will converge to some optimally minimum net error. For example, in a poor learning scheme, the weight modifications which may be required to learn the classification of a second vector, $\mathbf{x}_2$, may completely destroy the learned classification of $\mathbf{x}_1$.

Consider the cost function as a surface above a multi-dimensional plane of its arguments. If the cost function is quadratic in its arguments, its surface will be a paraboloid with a single (global) minimum. The principal method of iteratively finding the minimum of such a surface from an arbitrary starting location is gradient descent [63]. In this method, a change in the arguments of the cost function is made in the opposite direction of the gradient of the surface, that is, in the direction of steepest downhill change. Figure 2-6 illustrates gradient descent with one argument only.

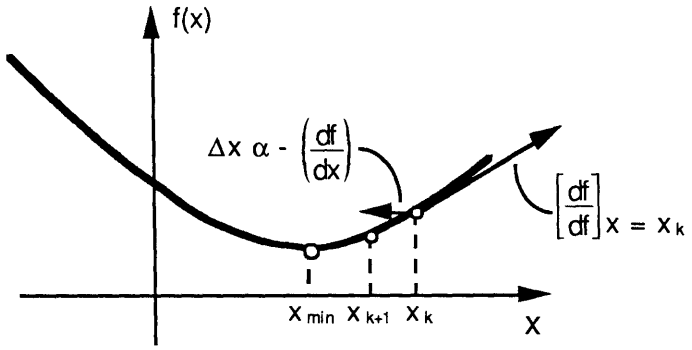

***Figure 2-6**: Gradient Descent Minimizing with One Argument*

Because the adaline performs a linear sum of weighted inputs, a cost function which is quadratic with adaline weights can be constructed and a gradient descent method can be used to iteratively modify the weights until the minimum is reached. Finding that cost function was the breakthrough of Widrow which has made the adaline widely applicable.

2.2.2 Gradient Descent for Least Mean-Squared Error

Consider the error with respect to the linear sum. Let the error signal be equal to the

difference between the desired output, y_d, and the sum, s, and be denoted ε_s. The presence of a possible negative value for ε_s is bothersome since minimizing this error would lead to driving the adaline to a negative error, not a minimum net error. To avoid this problem, it is appropriate to square the cost function. Thus the error signal can be defined as

$$(\varepsilon_s)^2 = (y_d - s)^2$$
$$= (y_d - \mathbf{x}^T\mathbf{w})^2$$

Clearly, $(\varepsilon_s)^2$ is a quadratic function of the weights **w**. It is a paraboloid with a global minimum **w*** (at a constant **x** and y_d), as illustrated in Figure 2-7.

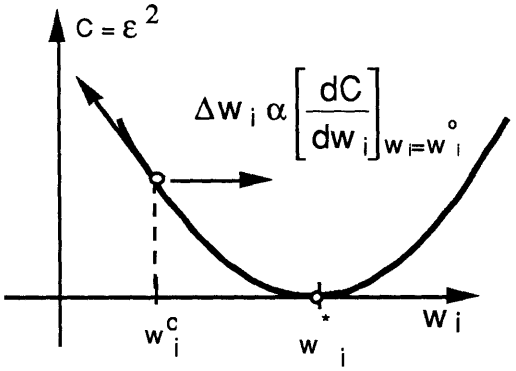

Figure 2-7: *Minimum of a Parabolic Cost Surface*

The actual output error is $\varepsilon_y \equiv (y_d - y)$. But, $(\varepsilon_y)^2$ is a monotonic function of $(\varepsilon_s)^2$ [60]. That is, as $(\varepsilon_s)^2$ increases, $(\varepsilon_y)^2$ increases; as $(\varepsilon_s)^2$ decreases, $(\varepsilon_y)^2$ decreases. Minimizing $(\varepsilon_s)^2$ will therefore minimize $(\varepsilon_y)^2$. This means that **w***, the minimum of the parabolic function $(\varepsilon_s)^2$, provides the *least mean-squared output error* of adaline.

In both the training and recalling phase of adaline operation, the input vector is assumed to be random. Thus $(\varepsilon_s)^2$ will be a random variable with an expected value $E\{(\varepsilon_s)^2\}$. From the definition:

$$E\{(\varepsilon_s)^2\} = E\{(y_d - \mathbf{x}^T\mathbf{w})^2\}$$

and since $\mathbf{x}^T\mathbf{w} = \mathbf{w}^T\mathbf{x}$ (a scalar),

$$E\{(\varepsilon_s)^2\} = E\{(y_d - \mathbf{w}^T\mathbf{x})\,(y_d - \mathbf{x}^T\mathbf{w})\}$$

$$= E\{(y_d)^2 - 2y_d\mathbf{x}^T\mathbf{w} + \mathbf{w}^T\mathbf{x}\mathbf{x}^T\mathbf{w}\}$$

$$E\{(\varepsilon_s)^2\} = E\{(y_d)^2\} - 2\,E\{y_d\mathbf{x}^T\}\mathbf{w} + \mathbf{w}^T\,E\{\mathbf{x}\mathbf{x}^T\}\mathbf{w}$$

The input vector is assumed stationary, that is, its statistics do not vary with time. If $\mathbf{p}$ is defined as the cross-correlation of the input vector and the desired response scalar and $\mathbf{R}$ is the input correlation matrix:

$$\mathbf{p} \equiv E\{y_d\mathbf{x}\}$$

$$\mathbf{R} \equiv E\{\mathbf{x}\mathbf{x}^T\}$$

then

$$E\{(\varepsilon_s)^2\} = E\{(y_d)^2\} - 2\,\mathbf{p}^T\mathbf{w} + \mathbf{w}^T\mathbf{R}\mathbf{w}$$

Recognize that $y_d = \pm 1$, so that $E\{(y_d)^2\} = 1$:

$$E\{(\varepsilon_s)^2\} = 1 - 2\,\mathbf{p}^T\mathbf{w} + \mathbf{w}^T\mathbf{R}\mathbf{w} \tag{2-7}$$

It is desired to minimize this expected value. Gradient descent in weight space is used. The gradient of $E\{(\varepsilon_s)^2\}$is

$$\nabla\, E\{(\varepsilon_s)^2\} \equiv \frac{\partial}{\partial \mathbf{w}} E\{(\varepsilon_s)^2\} \tag{2-8}$$

and from eq. (2-7)

$$\nabla\, E\{(\varepsilon_s)^2\} = -2\mathbf{p} + 2\mathbf{R}\mathbf{w} \tag{2-9}$$

The argument of the minimum value, $\mathbf{w}^*$, is reached when the gradient is zero:

$$0 = \nabla\, E\{(\varepsilon_s)^2\} = -2\mathbf{p} + 2\mathbf{R}\mathbf{w}$$

which yields

$$\mathbf{w}^* = \mathbf{R}^{-1}\mathbf{p}$$

The minimum error is found by inserting $\mathbf{w} = \mathbf{w}^*$ into eq. (2-7):

$$E\{(\varepsilon_s)^2\} = 1 - 2\,\mathbf{p}^T\mathbf{R}^{-1}\mathbf{p} + \mathbf{p}^T\mathbf{R}^{-1}\mathbf{R}\mathbf{R}^{-1}\mathbf{p}$$

$$= 1 - 2\,\mathbf{p}^T\mathbf{R}^{-1}\mathbf{p} + \mathbf{p}^T\mathbf{R}^{-1}\mathbf{p}$$

$$E\{(\varepsilon_s)^2\} = 1 - \mathbf{p}^T\mathbf{R}^{-1}\mathbf{p} \tag{2-10}$$

The gradient descent method dictates the change from an arbitrary weight vector, $\mathbf{w}_k$, to the next $\mathbf{w}_{k+1}$, where the index represents an iteration number:

$$\Delta\mathbf{w}_k = -\mu\nabla_k$$

$$\mathbf{w}_{k+1} = \mathbf{w}_k + \Delta\mathbf{w}_k$$

where μ is a constant which determines the rate of change and guarantees convergence. Using eq. (2-9)

$$\mathbf{w}_{k+1} = \mathbf{w}_k + \mu(2\mathbf{p} - 2\mathbf{R}\mathbf{w}) \tag{2-11}$$

Unfortunately, all statistics required to implement eq. (2-11) are not known. If they were, $\mathbf{w}^* = \mathbf{R}^{-1}\mathbf{p}$ could be used to minimize $E\{(\varepsilon_s)^2\}$ directly. Instead of the true gradient, an estimate of the gradient must be made.

The easiest estimate of the expected value of $(\varepsilon_s)^2$ is $(\varepsilon_s)^2$ itself. That is, define

$$\begin{aligned}
\hat{\nabla}_k &\equiv \frac{\partial}{\partial\mathbf{w}}(\varepsilon_s)^2 \approx \nabla E\{(\varepsilon_s)^2\} \\
&= \frac{\partial}{\partial\mathbf{w}}(y_d - \mathbf{x}^T\mathbf{w})^2 \\
&= -2\mathbf{x}(y_d - \mathbf{x}^T\mathbf{w}) \\
\hat{\nabla}_k &= -2\mathbf{x}\varepsilon_s
\end{aligned} \tag{2-12}$$

So that the weight change using the estimated gradient is

$$\Delta\mathbf{w}_k = -\mu\hat{\nabla}_k$$

so
$$\mathbf{w}_{k+1} = \mathbf{w}_k + 2\mu\mathbf{x}\varepsilon_s \tag{2-13}$$

Note the simplicity of this algorithm: all information required for each weight change is local to the adaline. The new weight is simply the current weight modified in the direction of the input vector ($\mathbf{x}$) proportioned by the adaline sum error (ε_s).

Although an estimate of the gradient is used in the iteration process, convergence to the minimum error, as dictated by the true gradient descent, is still guaranteed. To see this, take the expected value of the gradient estimate. From eq. (2-12),

$$E\{\hat{\nabla}_k\} = E\{-2\mathbf{x}(y_d - \mathbf{x}^T\mathbf{w})\}$$
$$= -2E\{\mathbf{x}(y_d - \mathbf{x}^T\mathbf{w})\}$$
$$= -2E\{\mathbf{x}y_d - \mathbf{x}\mathbf{x}^T\mathbf{w}\}$$
$$E\{\hat{\nabla}_k\} = -2E\{\mathbf{x}y_d\} + 2E\{\mathbf{x}\mathbf{x}^T\mathbf{w}\}$$

which from the definitions becomes

$$E\{\hat{\nabla}_k\} = -2\mathbf{p} + 2\mathbf{R}\mathbf{w}$$

which is the definition of the gradient from eq. (2-9). Thus

$$E\{\hat{\nabla}_k\} = \nabla_k$$

Eq. (2-13), often called the Widrow-Hoff or Delta rule, presents a method for adjusting the weights of an adaline which minimizes the output error. If the input training vectors are independent over time, for a large number of trials the Delta rule will converge to the minimum error given in eq. (2-10) [63].

2.3 LINEAR SEPARABILITY

The perceptive reader will note that a single line cannot create a decision boundary for all possible binary classifications of adaline input space in Figure 2-3. Only classifications which are determined with a single line can be implemented. Inputs which can be classified in this way are called *linearly separable.* In n-dimensional space, linearly separable inputs can be separated by an n-1 dimensional hyperplane.

The notorious example of linearly inseparable classification is the Boolean exclusive-or (XOR) function. In two dimensional adaline input space, the XOR function is TRUE (+1) for the set of inputs which differ in sign, namely, (-1,+1) and (+1,-1). The function is depicted in Figure 2-8. As can be seen, no single line can separate the two classes of inputs.

In their compelling 1969 treatise *Perceptrons* [32], Minsky and Papert argued that the inability of neuronal elements such as the adaline to perform linearly inseparable classifications

x_1	x_2	y
-1	-1	-1
-1	1	1
1	-1	1
1	1	-1

(a) Input/Output Function

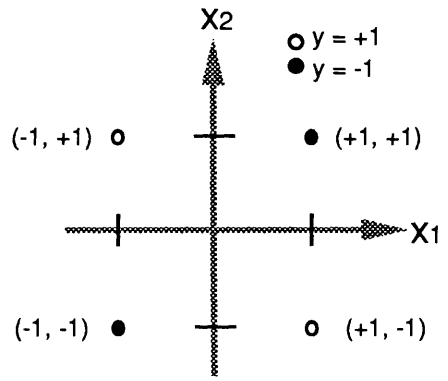

(b) Input Space Classification

Figure 2-8: *The 2-input XOR function*

severely limited their computational capacity. Their work was so convincing (because it was mathematically rigorous) that research at the time went into remission for well over a decade. The XOR problem epitomizes their arguments.

For the 2-input adaline, there are 2^2 possible input combinations. Since the output is binary each of the 4 input combinations can take on 1 of 2 values. Thus, there are $2^{(2^2)}$ possible classification functions. Of these 16, only 2 require classification of linearly inseparable functions: the XOR and its complement, the XNOR. However, in the more general n-input adaline, there are $2^{(2^n)}$ possible input classification functions and the number that require classification of linearly inseparable inputs becomes a larger fraction of the total. It has been shown that as n approaches infinity, the percentage of linearly *separable* classification functions in the ensemble becomes zero [56]. Thus, for a reasonably large adaline, Minsky and Papert's concerns are legitimate.

The inability of the adaline to perform linearly inseparable classifications is clear from the semantics: the decision boundary created by an adaline in its input space is linear and can therefore only separate inputs which are linearly separable. To implement a non-linear separation, a non-linear decision boundary must be constructed.

Recall that the decision boundary is determined by setting the argument of SGN{•} in eq. (2-1) to zero. In that equation, the argument is $s = \theta + w_1x_1 + \ldots + w_nx_n$, a linear

function of the inputs. If this argument is changed to a generalized non-linear function of the inputs, non-linear separation can be implemented.

For example, let the non-linear sum, s', be defined as

$$s' = w_0 + w_1x_1 + w_{11}(x_1)^2 + w_2x_2 + w_{22}(x_2)^2 + w_{12}x_1x_2$$

and the weights to be programmed as $w_0 = 0.25$, $w_1 = w_2 = 0$, $w_{11} = w_{22} = -0.5$, and $w_{12} = -0.875$. These parameters yield the decision boundary of Figure 2-9, where the inputs inside the ellipse are classified as $y = +1$.

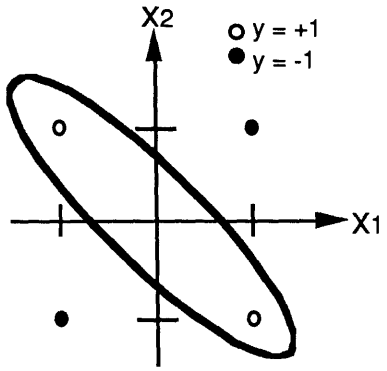

***Figure 2-9**: Non-Linear Decision Boundary for the XOR Function*

Clearly, the key to implementing linearly inseparable classifications is to apply a non-linear function to the inputs. The question then becomes how to create the non-linearity. After all, the elegance of the LMS algorithm is due to the linear combination of the inputs yielding a quadratic error surface in weight space.

In fact, a non-linearity is readily available in the form of the adaline threshold. The inputs can be "preprocessed" with adalines to obtain a non-linear function of the inputs. Since the threshold is not a generalized polynomial, not all classifications can be implemented with one layer of preprocessing. As shown in the next section, two preprocessing layers — for a total of three layers — are required to implement any arbitrary mapping.[3]

---

3. Viewed in another way, adalines which implement the logical NAND can be used as building blocks for larger functions [2]. Since all logical functions can be constructed from NAND elements, a network of

2.4 MANY ADALINES: IMPLEMENTING ANY CLASSIFICATION FUNCTION

It is clear that a non-linear operator must be applied to the inputs of an adaline in order for the device to perform a linearly inseparable classification. If adalines are used to realize this preprocessing, a layered network of many adalines - a madaline - is created.

A madaline is a network of layers of adalines. A three layer madaline with equal number of adalines per layer is shown in Figure 2-10. (Weights between adalines are not shown for simplicity.) In general, the number of adalines per layer can vary. Full connectivity between layers is usually assumed (a weight of 0 is equivalent to an open connection), but the topology is strictly feed-forward: no feedback paths are allowed.

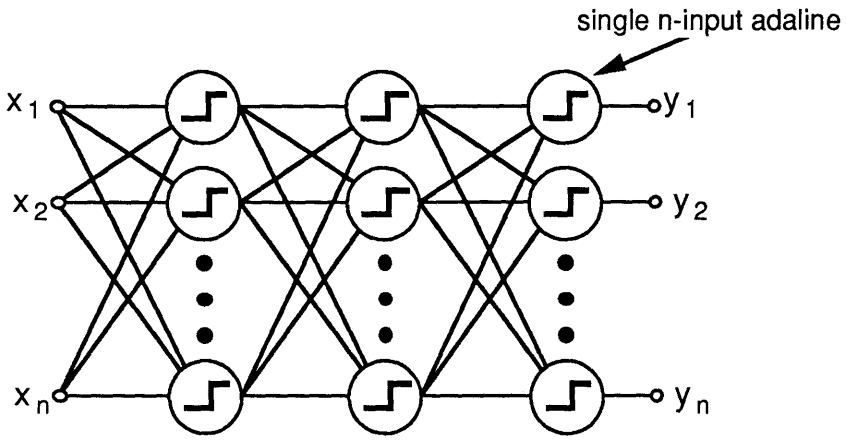

Figure 2-10: A Three Layer Madaline

In Figure 2-3, a single adaline formed a single line in the adaline input space. Two adalines with the same inputs can form two lines. In general, m adalines can form m decision hyperplanes.

Figure 2-3b is repeated below (Figure 2-11b) with a new decision line separating an additional classification, B and $\overline{B}$. Two adalines, configured as shown in Figure 2-11a, are used to create these two lines.

---

adalines can implement any logical function.

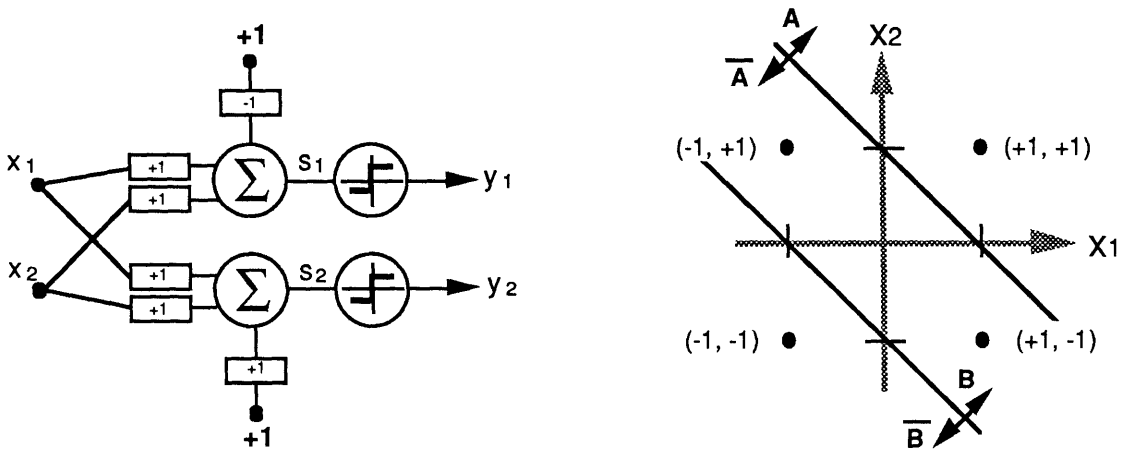

(a) Schematic Representation *(b) Input Space*

Figure 2-11: *Additional Classification of Adaline Input Space*

The two outputs, y_1 and y_2, which classify all four inputs into both classes A ($\overline{A}$) and B ($\overline{B}$), respectively, can be fed to a third adaline. Since A is represented by $y_1 = +1$ and B as $y_2 = +1$, these two outputs can be used as the inputs for the third adaline. To implement the XOR, the desired classifying set is $\overline{A}$ AND B, so the third adaline must implement the Boolean function $y_3 = \overline{y_1}$ AND y_2, a linearly separable function realized with $w_0 = -1$, $w_1 = -1$, and $w_2 = +1$. The three adaline structure with the classification of the inputs is shown in Figure 2-12. Thus the XOR function, which is linearly inseparable, can be implemented with 3 adalines assembled in a two layer structure.

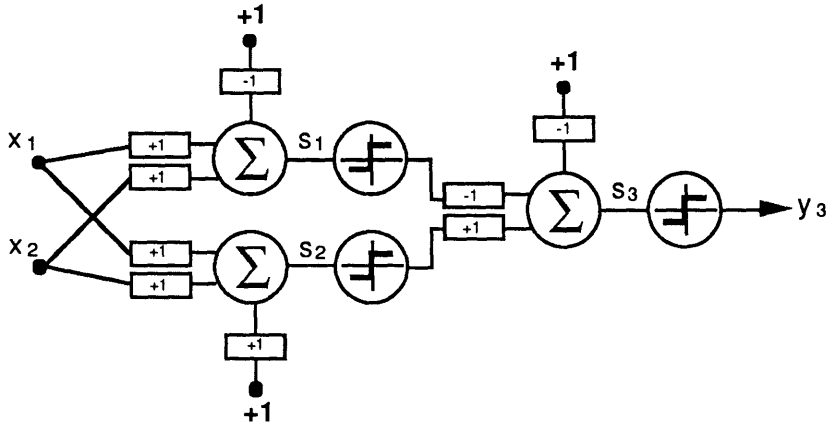

Figure 2-12: *A Three Adaline XOR*

The network of Figure 2-12 forms a region { $\overline{A}$ AND B} in adaline input space by

bounding it with 2 decision lines. Additional regions can be formed using additional adalines in the second layer. More complex regions can be formed using additional adalines in the first layer. In principle, a two layer madaline with sufficient number of adalines in each layer can form any number of convex regions in the input space. If convex decision regions are all that is required, a two layer network will suffice.

To implement decision regions which are more general than convex, an additional layer is needed [28]. An adaline can create arbitrary regions from convex regions, so the convex regions created in the second layer must be fed to a third layer. The second layer becomes "hidden", forming an internal representation of the input space [40]. The third layer which has formed decision boundaries of arbitrary geometry can implement any classification function and acts as an output layer.

Thus, a three layer madaline neural network with sufficient numbers of adalines in each layer can implement any classification function. A formidable problem, however, is determining the number of adalines required for a particular classification task. A larger problem is assigning the weight values. For n adalines in a network, the assignment of weights to implement a classification function requires satisfying $O(n^2)$ constraints. Similar to the single input adaline, if the analytic classification function is not known — if all of the boundaries of the classification region are not known a priori — learning must be used. This is the subject of the next section.

2.5 MADALINE LEARNING

Learning in a madaline network is similar to adaline learning in that it is based upon error feedback. Madaline learning, however, is plagued by the problem common to all non-linear multi-layer adaptive neural networks: credit assignment [32]. The dilemma is determining the effect of network parameters, namely, the synaptic weights, on the output error of the network.

In a single adaline, a parabolic cost function can be created and the minimum error can be found through gradient descent. In a multi-layer network, the cascaded non-linearities prohibit the construction of a parabolic error surface. The output error surface is arbitrarily-shaped. A global minimum may exist, but reaching it through gradient descent is virtually impossible due to the local minima which permeate the surface.

The back-propagation learning rule [40] exploits the sigmoidal nature of its neuron threshold function. Using the derivative chain rule, the change in output error for network parameters is propagated backward through the network layers.[4] Even so, convergence to an absolute minimum error is not guaranteed. The step threshold of the adaline has an infinite derivative and thus prohibits such an approach.

The madaline network has evolved in stages since its original introduction 30 years ago [56]. The learning rules have also evolved with the architecture. Through the history, however, all madaline learning rules have been based upon the simple principle of *minimal disturbance*. In Widrow's words [64]:

> When training the network to respond correctly to the various input patterns, the "golden rule" is to *give the responsibility to the neuron or neurons that can most easily assume it.* In other words, *don't rock the boat* any more than necessary to achieve the desired objective.

The minimal disturbance principle is best embodied by madaline learning rule II (MRII) [67]. Consider a network of adalines which is presented with an input pattern, **x**. If the output classification, **y**, is in error, then weights of the adalines in the first layer are perturbed to determine their effect on the output. The adaline in the first layer whose weighted sum is closest to zero is perturbed first. That is, the adaline whose weight change will have the minimum disturbance on the network is given a first attempt at reducing the error. The perturbation is such that adaline output changes sign. If this perturbation reduces the network

---

4. Since back-propagation uses the gradient descent techniques of Widrow, it is sometimes referred to as the generalized Delta rule.

output error, the weight changes are accepted; otherwise, the changes are rescinded. The first layer adaline whose weighted sum is the next closest to zero is then perturbed. This process continues for all first layer adalines and then to all subsequent layer adalines until the network error is zero or all adalines have been perturbed. This tedious process is not computable locally, but has shown acceptable results.

The next generation of madaline learning rules, MRIII [4], propagates an estimate of the error gradient backward through the network layers. It has been shown to converge to the weights which would have been found using back-propagation. That is, the madaline rules are globally calculated versions of the local back-propagation of errors. It is important to remember, however, that convergence of madaline to zero error using any rule — or for that matter, convergence of any multi-layer perceptron network to zero error — cannot be guaranteed, except for particularly well-behaved input sets.

CHAPTER THREE
FAILURE MODELS

In this chapter, a failure model of the adaline is constructed. The approach is to examine the operation of an n-input adaline in (n+1)-dimensional space and is an extension of Stevenson's weight sensitivity analysis work [50]. Given specific fault modes, the model can be evaluated to determine the probability of adaline failure under faulty conditions. The models of many adalines connected in a feed-forward topology are then combined into a madaline failure model. Since the madaline architecture is a generalization of many different feed-forward neural networks, the models can be used for further study of other networks.

Clarifying definitions of the failure model and fault modes which will be considered are presented first. Next, the operation of a single n-input adaline in $\Re^{n+1}$ is described. From this, a failure model of the adaline is developed which treats all failures as weight perturbations and describes the operation of an adaline as a function of the perturbation. After identification of the probability distribution for the adaline weights, the specific fault modes are inserted into the failure model and the probabilities of failure are determined. Extensions are then made to the madaline network.

3.1 MODEL CRITERIA

In this work, a failure model of an adaline is desired which can be extended in some manner to evaluate a madaline network of arbitrary size. Ideally, the adaline can be considered as a "black box" with inputs, outputs, and an internal mapping function. The goal is to determine the probability of failure of the black box. Extension to a madaline network failure model can be realized through a systematic assembly of black box models. The probability of madaline failure can be determined from a combinatorial aggregation of adaline failure probabilities.

A necessary foundation for achieving that goal is a clear understanding of the terms associated with dependable computing. In the vernacular of the technical community [5], the adaline is a *resource* which provides a *service*. This service is a mapping of an input vector, **x**, to an output scalar, y, by a *specification*, S, such that y = S(**x**). If the actual output, y', does not agree with the specified output (for the same input), then the output y' is in *error* and the resource has *failed*. The failure is caused by one or more internal resource *faults*.

Figure 3-1 depicts the adaline as a black box resource. It provides the specified service stated in eq. (2-5):

$$y = SGN\left\{ \sum_{i=0}^{n} x_i w_i \right\} \tag{2-5}$$

In this context, the adaline service is binary classification for the n-dimensional input vector. The linear summer and threshold units in the adaline provide the capability for that service. The particular classification function is the service specification and it is determined by the weight vector[1], $\mathbf{w} = [w_0\ w_1\ \ldots\ w_n]^T$. Note that the adaline is being considered only in its feed-forward (or recall) operation: no learning mechanism is associated with the resource of Figure 3-1.

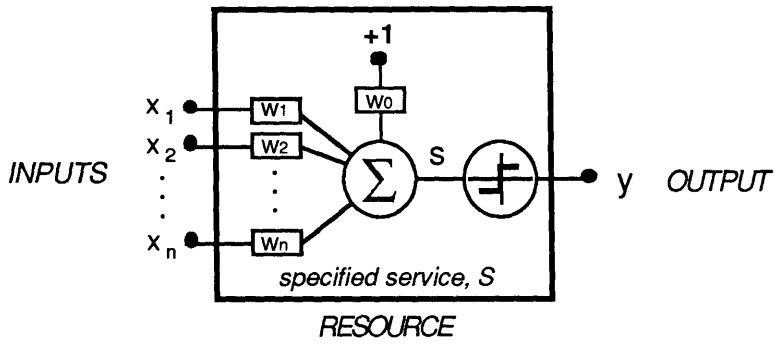

Figure 3-1: *The Adaline as a Black Box Resource*

With these basic definitions in hand, the purpose of the failure model can be stated

1. Normally one would say that the specification determines the weight vector, but this discussion is for general adaline operation. A weight vector can be determined through programming or training, but even an arbitrary weight vector will result in *some* service specification.

succinctly: *the model will determine the (conditional) probability of adaline failure, given some internal adaline fault.* In other words, assuming the adaline weights have been set such that a specified service is provided and given some internal adaline fault, the failure model will determine the probability of the misclassification of the input vector. Note the underlying assumption that *a fault-free adaline does not misclassify.* By definition, an adaline with a specified weight vector provides a specified service. It is true that a single adaline is incapable of providing a linearly inseparable classification service, but a fault-free adaline is guaranteed to perform the service specified by its weights.

Since the adaline is defined as the resource of interest in this work, it should be clear that the failure model does not consider adaline training. Although adaptability is an important fault-tolerance attribute, by no means does it guarantee that the adaline can learn around all possible faults. Consideration of adaline adaptability requires a thorough evaluation of a specific learning rule in the context of the assumed topology. Instead of examining the performance of particular learning schemes, this work is meant to evaluate the fault-tolerance of a neural network in the recall phase. The work can be compared to similar studies of heteroassociative or autoassociative memories (a.k.a., content addressable memories) when the input vector is incomplete.[2] Here, the probability of (correct) madaline recall will be determined, given some internal memory fault.

Since the failure model assumes some internal resource fault has occurred and determines the probability of correct operation (classification) conditioned on this event, the selection of the fault event is the underpinning of a valid failure model. In Chapter Two, the weight vector was shown to create a hyperplane which separates the adaline input space. Changes in the weight vector change the adaline classification by moving the hyperplane. A reasonable fault to consider, then, is a perturbation of the weight vector. In fact, except for

---

2. Kohonen [25] offers an extensive review of these systems.

pathological cases[3], faults in the summer or threshold units can be modelled as weight faults by moving the decision hyperplane to emulate their effect and altering the weight vector to produce the new hyperplane. For example, a stuck-at-one failure occurs when all inputs are classified as $y = +1$. A weight vector of $\mathbf{w} = [\alpha\ 0\ \ldots\ 0]^T$, $\alpha > 0$, could be used to model this failure. From a practical perspective, since weights far outnumber[4] other components in a physical implementation, weight faults are the most meaningful events for study. Furthermore, in a practical setting weights are likely to be more failure prone since they must be a dynamic media, while the summer and threshold units can be constructed from fixed electronic devices.

Thus, for this work, the following supposition applies: *Since the adaline failures are considered to be input misclassifications and are caused by some internal adaline fault, and adaline weights determine the classification function by positioning the decision hyperplane, then all faults are considered weight faults or can be emulated by weight faults.*

The next logical question concerns the type of weight fault: which weight faults should be considered in the analysis? In search of an answer to that question, consider an electronic implementation of an adaline. An input would be amplified by a weight value which can be positive or negative. A physical realization, however, must place a limit on the maximum and minimum values which can be achieved. For example, an operational amplifier will saturate at its rail voltages. One reasonable fault mode to consider, then, is the driving of the weight from its preset value to one of its possible rail values. This will be called a *rail fault.* For simplicity, assume the rails are at ± 1. A rail fault, then, is a change in a weight from its original value to its rail value, $w_i \rightarrow \pm 1$.

A second likely fault is the disconnection of a synapse such that the input at that

---

3. A pathological failure would be an adaline which no longer implements a linear hyper-"plane", i.e., the decision boundary is non-linear.

4. In a single madaline layer with n adalines, there are n^2 weights and n summers and threshold units. For $n = 20$, weights account for over 90% of the components; at $n = 100$, representing a pixelated 10 by 10 window for image recognition, weights account for 98% of the components.

synapse does not contribute to the internal summed value. This disconnection can be represented by a zero weight value for that synapse, $w_i \rightarrow 0$. This fault will be called a *zeroed-weight fault.*[5]

A failed adaline produces an output y' which has the opposite sign of its non-failed output. Adalines in the adjoining layer whose inputs are attached to the failed adaline thus receive an erroneous input. With some probability, a non-faulty adaline with an erroneous input will produce an output different than the output with error-free inputs. That is, with some probability the adaline with an erroneous input behaves as if it had failed. This failure can be modelled as a weight fault, the fault being a change of sign in the weight component. Although its physical manifestation is unlikely, such a fault is paramount for modelling errors which propagate through the network and will be considered as an adaline fault mode. This fault will be called a *sign-change fault.*

Of course, many other classes of weight faults exist and could be enumerated ad infinitum. The rail fault and the zero weight fault represent the extreme fault modes which could beset an adaline. Using these faults in the failure model should result in a conservative estimate of the probability of correct adaline operation since it is unlikely that a small weight perturbation would cause an adaline to fail while a weight change to -1, +1, or 0 would not. The sign-change fault is useful in propagating adaline failures through the network. These three fault modes will be used in the remainder of this work to determine their effect on adaline operation.

A final pronouncement on faults is in order before the model criteria are summarized. The model developed in the subsequent sections is a static one, that is, the analysis is performed for a fixed state of the system. This requires faults themselves to be invariant in time: the model assumes a fault occurs and stabilizes and the analysis on the faulty adaline is

---

5. Note that a dead short in a synapse is equivalent to a +1 rail fault.

performed. Dynamic faults, those which vary with time, require careful analysis but can be treated as a succession of static faults. Transient faults, those which are present for only a limited time, may produce transient errors; the failure model will determine the probability of adaline error while the fault is present.

The model criteria described in this section can be summarized as follows:

- The adaline is considered to be a resource which provides a service.
- The service specification is determined by the adaline weight vector, $\mathbf{w} = [w_0\ w_1\ \ldots\ w_n]^T$.
- The single adaline possesses only recall capability; no learning mechanism is assumed.
- The adaline fails if its output does not agree with the specified output for the same input; the output in such a case is considered in error.
- Since adaline weights determine the adaline service by positioning a decision hyperplane, all faults in the adaline are modelled by weight faults.
- Two fault modes, $\{w_i \rightarrow \pm 1$, and $w_i \rightarrow 0\}$, are assumed to cover the range of adaline faults and offer a conservative estimate of the probability of adaline failure. A third fault mode $\{w_i \rightarrow -w_i\}$ is used to propagate failures through the network.
- Faults are assumed to be static; model analysis occurs on a stable system.

With the criteria defined, the model can now be constructed.

3.2 Adaline Operation in n-dimensional Space

In Chapter Two, the weight vector of an adaline was shown to define the adaline classification function by positioning a decision hyperplane in its input space. Inputs on one side of the hyperplane are classified as $y = +1$; inputs on the other as $y = -1$. This section extends that type of spatial analysis to consider the classification directly in terms of the position of the weight vector, not merely the resulting hyperplane, in adaline input space. This allows the classification function to be studied as the weight vector is altered, that is, as weight faults are inserted.

The simple adaline example of §2.1 illustrated two-input classification. There, the adaline was assigned weights of $w_0 = -1$, $w_1 = 1$, and $w_2 = 1$ and thus performed the function:

$$y = SGN\{x_1 + x_2 - 1\}$$

The decision hyperplane is defined by the set of points where the argument of $SGN\{\bullet\}$ in eq. (5-1) is zero. Figure 3-2 shows that hyperplane in the adaline input space (originally, Figure 2-3b).

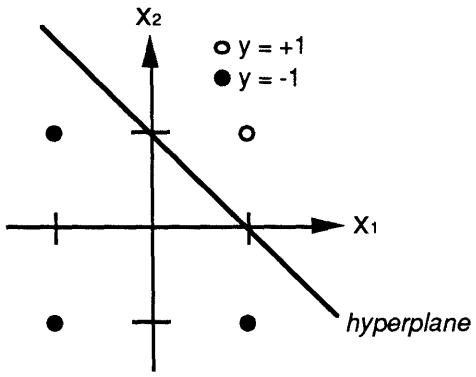

Figure 3-2: *Hyperplane $x_1 + x_2 - 1 = 0$ in $\Re^2$ Adaline Input Space*

The adaline was formally defined by eq. (2-5) and Figure 2-4 with an "input" $x_0 \equiv +1$. Figure 3-2 above then is really a two dimensional slice of the $\Re^3$ input space at $x_0 = 1$. To simplify the present discussion, this "input" is ignored and the threshold term θ is used. Thus, the original adaline description is temporarily adopted: the adaline in this example has two inputs, $\mathbf{x} = [x_1\ x_2]^T$, two weights, $\mathbf{w} = [w_1\ w_2]^T$, and a threshold, denoted θ here.

If the weight vector, $\mathbf{w} = [1\ 1]^T$, is drawn on the input space of Figure 3-2, the association between that vector and the decision hyperplane is readily determined: they are perpendicular (Figure 3-3).

Of course, this is not really that remarkable, it is a simple matter of geometry. The hyperplane is determined by solving the equation $\Sigma x_i w_i = \theta$, or equivalently,

$$\mathbf{x} \circ \mathbf{w} = \theta \tag{3-1}$$

For a fixed $\mathbf{w}$ and θ, eq. (3-1) represents the set of all vectors, $\mathbf{x}$, in the input space which have the same projection on $\mathbf{w}$. The projection is $\frac{\theta}{\|\mathbf{w}\|}$. This is shown in two dimensions in

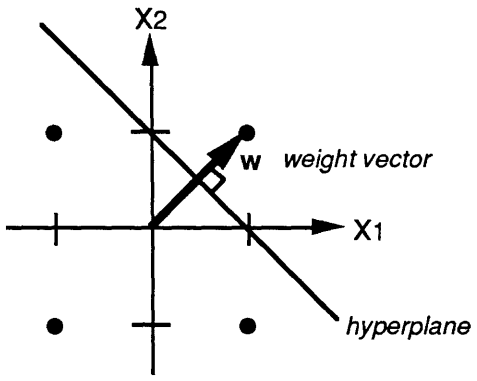

Figure 3-3: *Weight Vector Perpendicular to the Hyperplane*

Figure 3-4a. This array of input vectors creates a hyperplane — in two dimensions, a line — perpendicular to **w**. If $\theta = 0$, the projection is zero and the hyperplane includes the origin. More intuitively, if $\theta = 0$, the dot product of the weight and the input vectors is zero, so the vectors must be perpendicular. This is shown in Figure 3-4b.

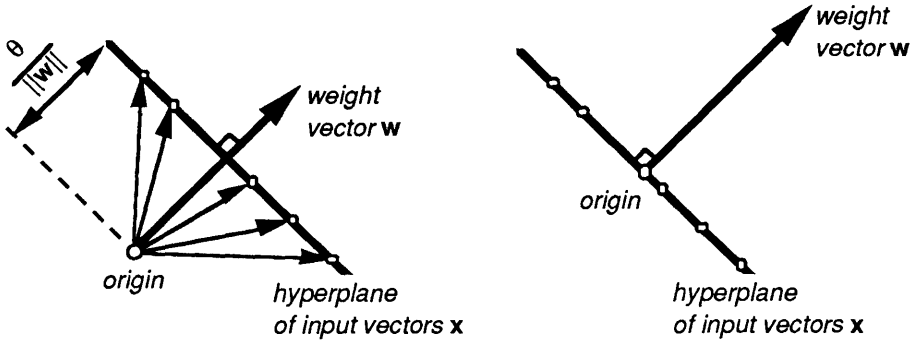

a: $\theta > 0$ *b:* $\theta = 0$

Figure 3-4: *Projection of Vectors* x *on* w, $x \circ w = \theta$

Returning to the formal definition of an adaline, $y = SGN\{\mathbf{x} \circ \mathbf{w}\}$, where $\mathbf{x} = [x_0\ x_1\ \ldots\ x_n]^T$, $\mathbf{w} = [w_0\ w_1\ \ldots\ w_n]^T$. If $x_0 \equiv 1$ is considered to be an "input", $\Re^{n+1}$ is required to describe the entire input space. It is clear that the weight vector is perpendicular to a decision hyperplane which passes through the origin of that input space. For a two input adaline, the input space is three dimensional and the decision boundary is defined by a 2-dimensional plane. Figure 3-5 depicts the input space of the two-input adaline example. Note the $x_0 = +1$ plane is the same as Figure 3-2 and the weight vector, $\mathbf{w} = [+1\ +1\ -1]^T$, which

was previously determined in §2.1, is perpendicular to the decision plane.

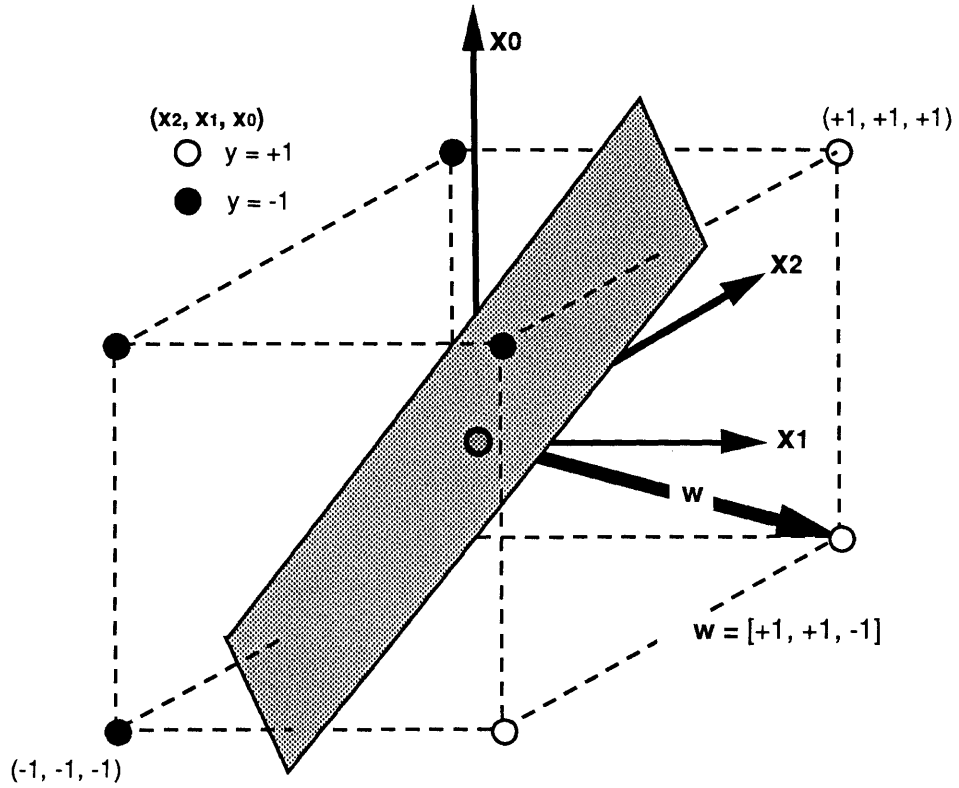

***Figure 3-5:** Decision Hyperplane and Weight Vector for the 2-Input Adaline Example*

From the figure, one sees that all inputs to one side of the plane are classified as y = +1; inputs to the other side are classified as y = -1. Given the weight vector, it is easy to determine the proper classifications: since y is determined by the sign of the dot product of the input vector and the weight vector, inputs **x** which have a positive projection on **w** are classified as y = +1. These are the inputs on the same side of the plane as the weight vector. Figure 3-6 portrays a simpler two-dimensional view (a separate example).[6] There the projection of **x** on **w** is negative, so y = -1 and **x** is categorized as "-1".

6. 2-dimensional input space is quite uninteresting if x_0 is considered to be an "input". The adaline described in this space would have only 1 true input, x_1.

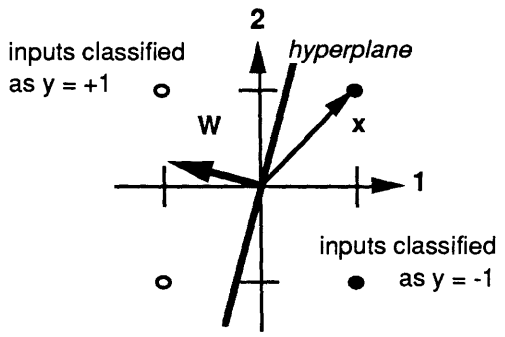

Figure 3-6: *Weight Vector and Decision Hyperplane in 2-Dimensional Input Space*

A few remaining definitions and formulas are required before the failure model based upon this spatial analysis of adaline classification can be constructed. The n-input adaline requires (n+1)-dimensional space ($\Re^{n+1}$) for complete spatial description. Familiar terms which describe one-, two-, and three-dimensional geometric structures must be extended to n (or n+1) dimensions. Description of these higher order geometric entities can be found in fundamental texts on the subject [48, 68].[7] Figure 3-7 presents a two-dimensional depiction of them.

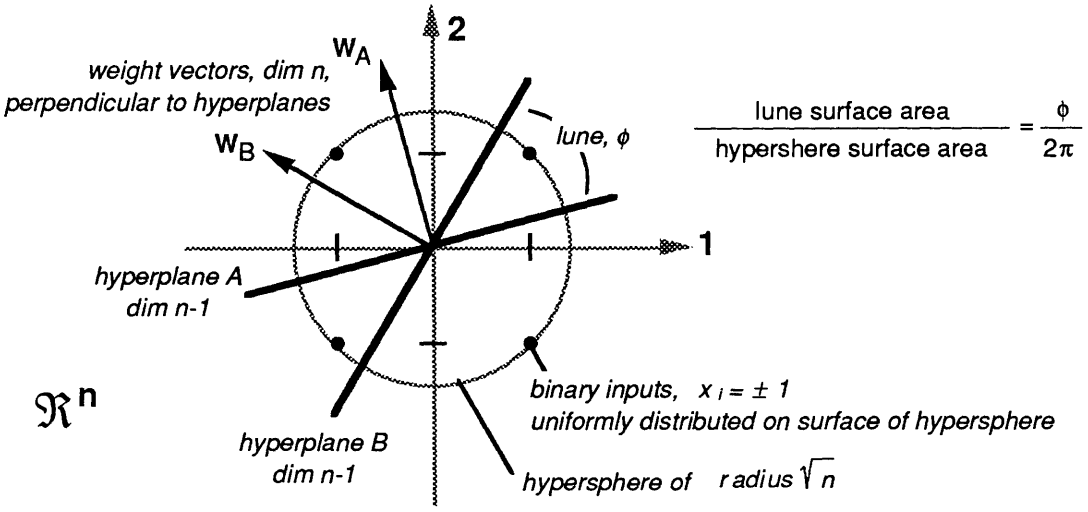

Figure 3-7: *Two-dimensional Depiction of n-dimensional Adaline Input Geometry*

The inputs to an adaline are strictly binary, that is, $x_i \in \{-1, +1\}$. In $\Re^2$, these points are distributed over a circle of radius $r = \sqrt{2}$ and in $\Re^3$, they are distributed over a sphere of

7. The reader is also referred to the entertaining discussion of higher geometry in *Flatland: A Romance of Many Dimensions* [1].

radius $r = \sqrt{3}$. In $\Re^n$, the points are distributed over a *hypersphere* of radius $r = \sqrt{n}$.

The term hyperplane has already been introduced. If the input space of an adaline requires only one dimension, the decision hyperplane is a point. For $\Re^2$ input space, as shown in Figure 3-6, the hyperplane is a line, and in $\Re^3$ it is a two-dimensional plane. The general n-input adaline space spanning $\Re^{n+1}$ will be bisected by an n-dimensional hyperplane.

The intersection of two hyperplanes at the origin form a solid angle, ϕ, in the hypersphere. Technically, this is called a *lune* [23]. The ratio of the surface area subtended by a lune of magnitude ϕ to the surface area of the hypersphere is given by $\frac{\phi}{2\pi}$. For example, in two dimensions, the lune is an angle, ϕ, which is subtended by an arc on the circumference of the circle. The ratio of the area of this arc to the surface area (circumference) of the circle is $\frac{\phi}{2\pi}$.

Hoff [21] showed that as the number of inputs grows large, the set of input vectors, $\mathbf{x} = [x_0\ x_1\ \ldots\ x_n]^T$, $x_i \in \{-1, +1\}$, become uniformly distributed over the surface of the hypersphere. The implication of this fact coupled with the surface area ratio of a lune to its hypersphere is that the percentage of input vectors contained in a lune of magnitude ϕ is simply given by $\frac{\phi}{2\pi}$. This is often referred to as the *Hoff hypersphere-area approximation.*[8]

Two hyperplanes intersecting at the origin actually form two lunes, one the spherical reflection of the other. Thus, the percent of input vectors contained in these lunes is $2 \cdot \frac{\phi}{2\pi} = \frac{\phi}{\pi}$.

Since the x_0 "input" is always +1, the input vectors which need to be considered for classification are distributed on only half of the hypersphere, called a *hemihypersphere*. For

---

8. Spatial analysis of classification has been used by Widrow for over three decades. Adaptive classifiers were first addressed by his students Buzzard [9] and Mattson [29] at MIT in the late 1950's. During Widrow's tenure at Stanford since then, his students Hoff [21], Glanz [19], Winter [67] and, most recently, Stevenson [50] have extended the analyses. Stevenson's work is used as the foundation for this work. The adaline was formally presented first in 1960 [60] and the madaline in two years later [56]. An excellent review of all the work has recently been published, appropriately entitled "30 Years of Neural Networks" [61].

example, in Figure 3-5 the points below the horizontal x_1-x_2 plane ($x_0 = -1$) are irrelevant since those vectors can never be applied to the adaline for classification. In all circumstances then, exactly half of the possible input vectors are relevant for classification. At the same time, of those vectors contained in the two lunes created by two intersection hyperplanes, exactly half will be in the $x_0 = +1$ hemihypersphere and thus relevant for classification. This means that *the percent of relevant input vectors contained in the two lunes created by the intersection of two hyperplanes at the origin is still* $= \frac{\phi}{\pi}$ [50]. Figure 3-8 presents two examples.

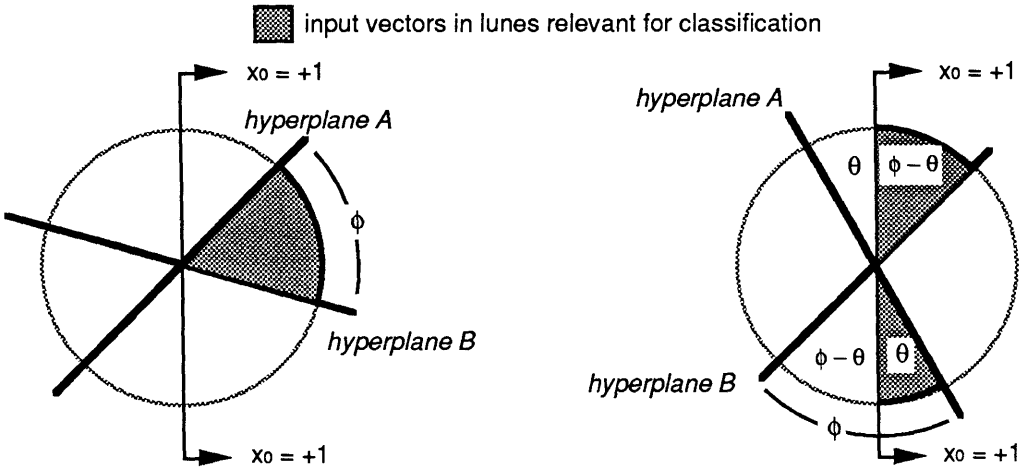

Figure 3-8: *Relevant Input Vectors in Two Lunes Formed by Two Hyperplanes*

A final note for the perceptive reader who may have noticed that requiring the decision hyperplane to pass through the origin prevents it from implementing all possible linearly separable classifications of the input space. Such a hyperplane cannot implement those classifications for the entire set of input vectors, $\mathbf{x} = [x_0\ x_1\ \ldots\ x_n]^T$, but it can implement such a classification for set of input vectors, $\mathbf{x} = [+1\ x_1\ \ldots\ x_n]^T$, which is all that is required here. That fact is not merely coincidental: $x_0 \equiv +1$ is simply a mathematical tool for implementing the threshold θ, by setting $w_0 = -\theta$, and treating $x_0 w_0$ as any other weighted input. By considering only the $x_0 = +1$ plane in Figure 3-5, one can visualize any linearly separating decision line which is the intersection of that $x_0 = +1$ plane and a decision plane which passes through the origin.

3.3 SINGLE ADALINE FAILURE MODEL

With a spatial analysis of adaline classification in hand, the effect of altering the weight vector can be determined. This section defines the probability of adaline failure (misclassification) given the insertion of a specific weight fault.

The non-faulty adaline has a specific hyperplane, H, which classifies its input vectors. If a fault is inserted in the weight vector, a new decision hyperplane, H_F, is created. The new hyperplane will reclassify the input space. Some of the inputs originally classified as y = +1 with hyperplane H will be erroneously classified as y = -1 with hyperplane H_F. Similarly, some of the inputs originally classified as y = -1 will be erroneously classified as y = +1. If any of the inputs which have become misclassified are applied to the adaline, the output is in error: the adaline has failed.

The faulty hyperplane H_F forms two lunes each of magnitude ϕ with the original hyperplane H. Input vectors in both of these lunes will be misclassified: one lune will misclassify $y(\mathbf{x}) = +1 \rightarrow y(\mathbf{x}) = -1$ and the other will misclassify $y(\mathbf{x}) = -1 \rightarrow y(\mathbf{x}) = +1$. From the Hoff hypersphere-area approximation, the percent of input vectors in these two lunes is $\frac{\phi}{\pi}$. In the section above, it was shown that the percent of relevant input vectors in these two lunes is also $\frac{\phi}{\pi}$. Thus, $\frac{\phi}{\pi}$ percent of the vectors will be misclassified. Given a uniform distribution of input vectors[9], then, this is also the probability of adaline failure. The task is to determine the lune magnitude, ϕ.

If both hyperplanes are known, the lune can be calculated and the adaline failure probability can be readily determined. In the general case, the original hyperplane is not known. Its expected value, that is, the expected value of the weight vector, can be determined from a probability distribution of the weight vector. Since the faulty hyperplane is created from

---

9. Stevenson has reported that this is not a necessary condition. Assuming randomly oriented weight vectors (that is, a randomly oriented hyperplanes) any input has a probability of (ϕ/π) of being misclassified.

the original hyperplane via insertion of a known weight fault, the expected value of the lune between the two hyperplanes can also be determined. The expected value of the percentage of input vectors which will be misclassified is thus $\frac{E\{\phi\}}{\pi}$, where $E\{x\}$ is the expected value of x. This is the probability of adaline failure, denoted P_F, in the general case:

$$P_F = \frac{E\{\phi\}}{\pi} \tag{3-2}$$

The weight vector, **w**, is associated with the original hyperplane and a faulty weight vector, $\mathbf{w}_F$, is associated with the faulty hyperplane. Since the weight vectors are perpendicular to their respective hyperplanes, the angle between the vectors will be equal to the magnitude of the lune between the hyperplanes (Figure 3-9). This means that the weight vectors alone can be used to determine ϕ.

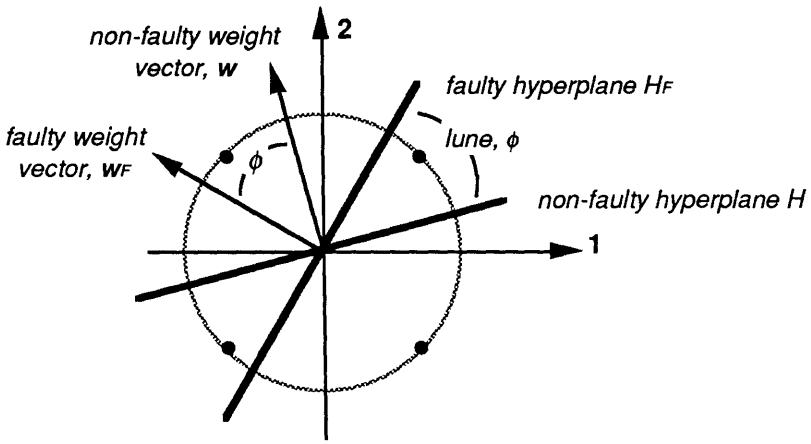

Figure 3-9: *Equivalence of Angle Between Weight Vectors and Lune Between Hyperplanes*

The transformation from **w** to $\mathbf{w}_F$ is determined by the weight fault which is inserted. The three fault modes identified in §3.1 (rail fault, zeroed-weight fault, and sign-change fault) manifest four faults $\{w_i \rightarrow +1,\ w_i \rightarrow -1,\ w_i \rightarrow 0,$ and $w_i \rightarrow -w_i\}$ which are separately inserted to corrupt weight components w_i. Mixed fault modes are not considered, but the method described here can be used to model any particular fault scenario. A single weight fault is first inserted; m multiple faults, $(1 < m \leq n+1)$ are then inserted. The expected value of the angle **w** and $\mathbf{w}_F$ is calculated for each mode and eq. (3-2) is used to determine P_F.

The results are functions of the weight component magnitudes, w_i, and the number of

inserted faults, m. The magnitudes of the weight components, in turn, are functions of the dimension of the weight vector, n.[10] Thus, the analysis will derive a set of equations for P_F which are dependent upon the fault mode and the number of inserted faults, with notation as tabulated below, Figure 3-10.

Inserted Fault	Single Fault	m Multiple Faults
+1 Rail Fault	$P_F^{+1}(n)$	$P_F^{+M}(n,m)$
-1 Rail Fault	$P_F^{-1}(n)$	$P_F^{-M}(n,m)$
Zeroed-Weight Fault	$P_F^{0}(n)$	$P_F^{0M}(n,m)$
Sign-Change Fault	$P_F^{\Delta S}(n)$	$P_F^{\Delta SM}(n,m)$

***Figure 3-10**: Notation for Adaline Probability of Failure*

As expected values of functions of random variables (w_i), the solutions to these equations require the probability density functions for the weight components. These are derived in §3.4. Closed-form solutions are presented in §3.5.

Spatial analysis is employed to derive $E\{\phi\}$. Since P_F is determined only by the amount of input vectors contained in the lune ϕ, only the magnitude of the angle between $\mathbf{w}$ and $\mathbf{w}_F$ is required.[11] Geometric axioms in the $\mathbf{w}$-$\mathbf{w}_F$ (hyper)plane are used to determine the magnitude of ϕ.

Simplification of the geometry of the problem greatly reduces the complexity of the solutions for P_F. Since the adaline decision hyperplane is perpendicular to the weight vector, the magnitude of the vector is irrelevant. Only the direction of the weight vector is important.

---

10. More accurately, the dimension is n+1.

11. Furthermore, since $P_F = \frac{E\{\phi\}}{\pi}$, eq. (5-3), $E\{\phi\}$ must be in the first two quadrants, that is, $\phi \in [0,\pi]$.

By normalizing the vector, that is, requiring $\|\mathbf{w}\| = 1$, the geometry of the problem of finding ϕ is simplified. Thus, for the derivations in this section the weight vector $\mathbf{w}$ is defined as

$$\mathbf{w} = [w_0\ w_1\ \ldots\ w_n]^T \tag{3-3}$$

such that $$\|\mathbf{w}\| \equiv 1 \tag{3-4}$$

Eq. (3-4) is paramount to the simplification of solutions for P_F.

3.3.1 Single Weight Fault

In this section, one of the n+1 adaline weights, w_k, is corrupted with one of the four faults enumerated in Figure 3-10. The approach is to determine the angle ϕ between the original weight vector, $\mathbf{w}$, and the corrupted weight vector, $\mathbf{w}_F$. As discussed above, this leads directly to the probability of adaline failure:

$$P_F = \frac{E\{\phi\}}{\pi} \tag{3-2}$$

For the cases below, the weight vector $\mathbf{w}$ is defined by eqs. (3-3) and (3-4) and a corrupting weight vector, $\Delta\mathbf{w}$ is defined such that

$$\mathbf{w}_F = \mathbf{w} + \Delta\mathbf{w}$$

or $$\Delta\mathbf{w} = \mathbf{w}_F - \mathbf{w} \tag{3-5}$$

as shown in Figure 3-11. With these terms defined, ϕ for all cases is determined.

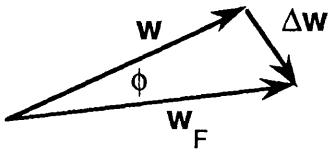

Figure 3-11: *Relationship Between $\mathbf{w}$, $\mathbf{w}_F$, and $\Delta\mathbf{w}$*

Single Zeroed-Weight Fault

For a zeroed-weight fault, $\mathbf{w}_F$ is

$$\mathbf{w}_F = [w_0\ w_1\ \ldots\ w_{k-1}\ 0\ w_{k+1}\ \ldots\ w_n]^T$$

so that,

$$\Delta \mathbf{w} = [0\ 0\ \ldots\ 0\ -w_k\ 0 \ldots\ 0\ ]^T \tag{3-6}$$

Notice that

$$\mathbf{w}_F \circ \Delta \mathbf{w} = 0$$

which means that $\mathbf{w}_F$ and $\Delta \mathbf{w}$ are perpendicular. Figure 3-12 illustrates the relationship.

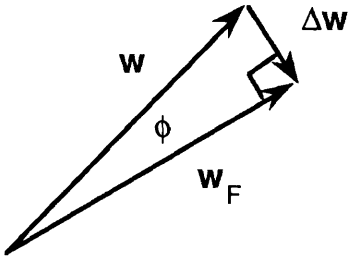

Figure 3-12: *Relationship Between* $\mathbf{w}$, $\mathbf{w}_F$, *and* $\Delta \mathbf{w}$ *for Zeroed-Weight Fault*

Clearly from the figure,

$$\sin \phi = \frac{\|\Delta \mathbf{w}\|}{\|\mathbf{w}\|}$$

which from eqs. (3-4) and (3-6) reduces to

$$\sin \phi = |w_k|$$

so that

$$\phi = \sin^{-1} |w_k|$$

Eq. (3-2) leads to a result of

$$P_F^0(n) = \frac{1}{\pi} E\left\{ \sin^{-1} |w_k| \right\} \tag{3-7}$$

Single +1 Rail Fault

For this case, the dot product between the two vectors $\mathbf{w}$ and $\mathbf{w}_F$ is used to determine ϕ. Here $\mathbf{w}_F$ is

$$\mathbf{w}_F = [w_0\ w_1\ \ldots\ w_{k-1}\ \ 1\ \ w_{k+1}\ \ldots\ w_n]^T$$

The angle between $\mathbf{w}$ and $\mathbf{w}_F$ is

$$\begin{aligned} \phi &= \cos^{-1}\left(\frac{\mathbf{w} \circ \mathbf{w}_F}{\|\mathbf{w}\|\ \|\mathbf{w}_F\|} \right) \\ &= \cos^{-1}\left(\frac{(w_0)^2 + \ldots + (w_{k-1})^2 + w_k + (w_{k+1})^2 + \ldots + (w_n)^2}{\left((w_0)^2 + \ldots + (w_{k-1})^2 + 1 + (w_{k+1})^2 + \ldots + (w_n)^2\right)^{1/2}} \right) \end{aligned} \tag{3-8}$$

Now, by definition, from eq. (3-4)

$$1 \equiv \|\mathbf{w}\| = \sqrt{\sum_{i=0}^{n}(w_i)^2}$$

or

$$\sum_{i=0}^{n}(w_i)^2 = 1 \tag{3-9}$$

so

$$(w_0)^2 + \ldots + (w_{k-1})^2 + (w_{k+1})^2 + \ldots + (w_n)^2 = 1 - (w_k)^2$$

and eq. (3-8) becomes

$$\phi = \cos^{-1}\left(\frac{1 - (w_k)^2 + w_k}{(2 - (w_k)^2)^{1/2}}\right) \tag{3-10}$$

so that

$$P_F^{+1}(n) = \frac{1}{\pi} E\left\{\cos^{-1}\left(\frac{1 - (w_k)^2 + w_k}{(2 - (w_k)^2)^{1/2}}\right)\right\} \tag{3-11}$$

Single -1 Rail Fault

For the -1 rail fault, the faulty weight vector is

$$\mathbf{w}_F = [w_0\ w_1\ \ldots\ w_{k-1}\ -1\ w_{k+1}\ \ldots\ w_n]^T$$

A derivation identical to the +1 rail fault case leads to

$$\phi = \cos^{-1}\left(\frac{1 - (w_k)^2 - w_k}{(2 - (w_k)^2)^{1/2}}\right) \tag{3-12}$$

resulting in

$$P_F^{-1}(n) = \frac{1}{\pi} E\left\{\cos^{-1}\left(\frac{1 - (w_k)^2 - w_k}{(2 - (w_k)^2)^{1/2}}\right)\right\} \tag{3-13}$$

Equivalence of $P_F^{+1}(n)$ and $P_F^{-1}(n)$

Intuitively, for the general case, the weight component magnitude should be symmetrically distributed around 0, that is, equally to take on a positive value $+w_k$ as a negative value $-w_k$. Thus, the probability that a +1 rail fault in a weight component causes adaline failure should be the same as the probability that a -1 rail fault causes adaline failure.

This indeed is the case. The equations for ϕ for the +1 rail fault (ϕ^+) and ϕ for the -1 rail fault (ϕ^-) are ordinate reflections of each other:

$$\phi^+(w_k) = \cos^{-1}\left(\frac{1 - (w_k)^2 + w_k}{(2 - (w_k)^2)^{1/2}}\right) \tag{3-10}$$

$$\phi^-(w_k) = \cos^{-1}\left(\frac{1 - (w_k)^2 - w_k}{(2 - (w_k)^2)^{1/2}}\right) \tag{3-12}$$

The functions are shown in Figure 3-13. Because they are ordinate reflections, the area under their curves will be equal. As long as w_k is distributed symmetrically around 0, the functions will have the same expected value. As the reader will see in §3.4, w_k is distributed symmetrically (its probability density function is even), so $E\{\phi^+\} = E\{\phi^-\}$; or $P_F^{+1}(n) = P_F^{-1}(n)$. Figure 3-14 illustrates the symmetry. For w_k symmetrically distributed, $E\{\phi^+\} = E\{\phi^-\}$.

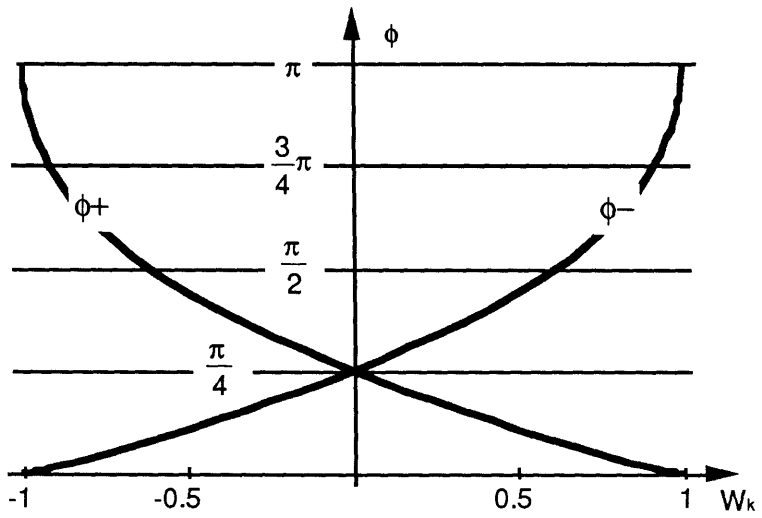

Figure 3-13: *ϕ+ and ϕ- as Functions of w_k*

Because $P_F^{+1}(n) = P_F^{-1}(n)$, the notation is condensed to $P_F^{\pm 1}(n)$ and one, $P_F^{+1}(n)$, is chosen as the equation for a ± 1 rail fault:

$$P_F^{\pm 1}(n) \equiv P_F^{+1}(n) = \frac{1}{\pi} E\left\{\cos^{-1}\left(\frac{1 - (w_k)^2 + w_k}{(2 - (w_k)^2)^{1/2}}\right)\right\} \tag{3-14}$$

	+1 Rail Fault $\phi = \cos^{-1}\left(\frac{1 - w_k^2 + w_k}{\sqrt{2-w_k^2}}\right)$ (•) = argument of $\cos^{-1}$		**-1 Rail Fault** $\phi = \cos^{-1}\left(\frac{1 - w_k^2 - w_k}{\sqrt{2-w_k^2}}\right)$ (•) = argument of $\cos^{-1}$	
range of w_k	Ranges of (•) and ϕ	Two-Dimensional Depiction	Ranges of (•) and ϕ	Two-Dimensional Depiction
$w_k = -1$	(•) = -1 $\phi = \pi$	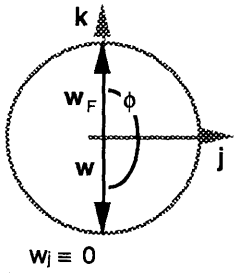	(•) = 1 $\phi = 0$	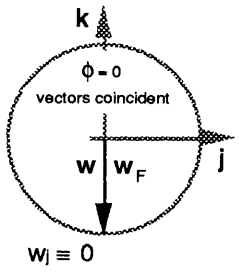
$-1 < w_k < 0$	$-1 < (\bullet) < \frac{1}{\sqrt{2}}$ $\pi > \phi > \frac{\pi}{4}$	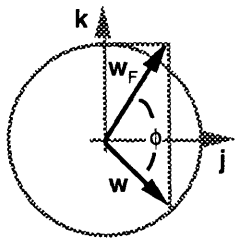	$+1 > (\bullet) > \frac{1}{\sqrt{2}}$ $0 < \phi < \frac{\pi}{4}$	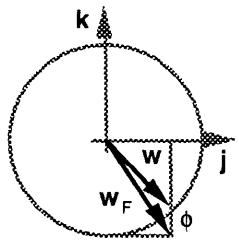
$w_k = 0$	$(\bullet) = \frac{1}{\sqrt{2}}$ $\phi = \frac{\pi}{4}$	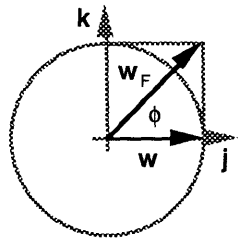	$(\bullet) = \frac{1}{\sqrt{2}}$ $\phi = \frac{\pi}{4}$	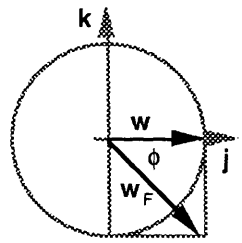
$0 < w_k < +1$	$\frac{1}{\sqrt{2}} < (\bullet) < +1$ $\frac{\pi}{4} > \phi > 0$	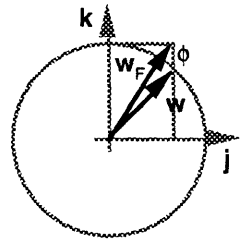	$\frac{1}{\sqrt{2}} > (\bullet) > -1$ $\frac{\pi}{4} < \phi < \pi$	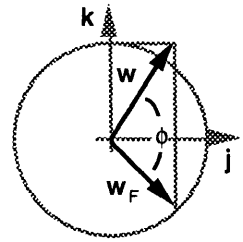
$w_k = +1$	(•) = +1 $\phi = 0$	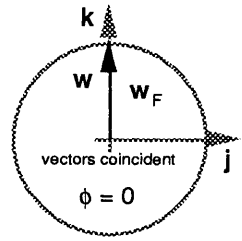	(•) = -1 $\phi = \pi$	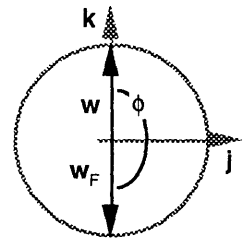

Figure 3-14: Inverse Symmetry of ϕ for +1 Rail Fault and -1 Rail Fault

Single Sign-Change Fault

For the case of a single weight component changing sign, the faulty weight vector is

$$\mathbf{w}_F = [w_0 \ldots w_{k-1} \ -w_k \ w_{k+1} \ldots w_n]^T$$

Note that it still has magnitude of 1, $\|\mathbf{w}_F\| = 1$. The corrupting weight vector is

$$\Delta\mathbf{w} = [0 \ldots 0 \ -2w_k \ 0 \ldots 0]^T$$

and it has magnitude $\|\Delta\mathbf{w}\| = 2|w_k|$. The three vectors, $\mathbf{w}$, $\mathbf{w}_F$, and $\Delta\mathbf{w}$ form the isoceles triangle shown in Figure 3-15.

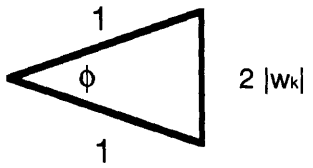

Figure 3-15: *Isoceles Triangle Formed by Sign-Change Fault*

The Law of Cosines is used to determine ϕ:

$$a^2 = b^2 + c^2 - 2bc \cdot \cos(\alpha)$$

where α is the angle subtended by a. From the figure,

$$4(w_k)^2 = 2 - 2\cos(\phi)$$

$$\cos(\phi) = 1 - 2(w_k)^2$$

$$\phi = \cos^{-1}\left(1-2(w_k)^2\right)$$

Resulting in

$$P_F^{\Delta S}(n) = \frac{1}{\pi} E\left\{\cos^{-1}\left(1-2(w_k)^2\right)\right\} \tag{3-15}$$

3.3.2 Multiple Weight Faults

Approaches identical to those in the previous section are used to derive the probability of failure when multiple faults are inserted into an adaline. In this section a single adaline is corrupted with m weight faults of one of the four fault modes. The faults are considered separately — mixed fault modes are left for further study.

As in the previous section, the task is to determine the angle, ϕ, between the original weight vector and the faulty weight vector. For a single fault, ϕ is a function of w_k, $\phi = g(w_k)$, where w_k is a single weight component. In the case of m multiple faults, $\phi = g(w_{k1}, w_{k2}, \ldots w_{km})$, where w_{kj} are m different weight components. In the general case, the value of ϕ is not dependent upon which weight components have been corrupted, but rather the number of weight components (m) which have been corrupted. For mathematical uniformity and clarity, the faulty weight vector will be assumed corrupted in its first m terms, that is, the elements $w_0 \ldots w_{m-1}$ will be considered to be the faulty components.

As before, the weight vector is assumed normalized, $\|\mathbf{w}\| \equiv 1$, and a corrupting weight vector $\Delta\mathbf{w}$ is defined as $\Delta\mathbf{w} \equiv \mathbf{w}_F - \mathbf{w}$. The derivations mimic the procedures of §3.3.1.

Also, the same arguments for the equivalence of $P_F^{+1}(n)$ and $P_F^{-1}(n)$ apply to $P_F^{+M}(n,m)$ and $P_F^{-M}(n,m)$. For those reasons, the two multiple rail fault cases are condensed to one, denoted $P_F^{\pm M}(n,m)$ and assigned, arbitrarily, to the form of $P_F^{+M}(n,m)$:

$$P_F^{\pm M}(n,m) \equiv P_F^{+M}(n,m) = P_F^{-M}(n,m) \tag{3-16}$$

Multiple Zeroed-Weight Faults

For m zeroed-weight faults, the faulty weight vector is

$$\mathbf{w}_F = [0 \ldots 0\ w_m\ w_{m-+1} \ldots w_n]^T$$

so that $$\Delta\mathbf{w} = [-w_0\ -w_1\ \ldots\ -w_{m-1}\ 0\ 0 \ldots 0]^T$$

Again, $\mathbf{w}_F$ and $\Delta\mathbf{w}$ are perpendicular, so

$$\sin\phi = \frac{\|\Delta\mathbf{w}\|}{\|\mathbf{w}\|}$$

which reduces to

$$\sin\phi = \sqrt{\sum_{i=0}^{m-1}(w_i)^2}$$

so that

$$\phi = \sin^{-1}\left(\left(\sum_{i=0}^{m-1} (w_i)^2 \right)^{1/2} \right)$$

and

$$P_F^{0M}(n,m) = \frac{1}{\pi} E\left\{ \sin^{-1}\left(\left(\sum_{i=0}^{m-1} (w_i)^2 \right)^{1/2} \right) \right\} \tag{3-17}$$

Multiple ±1 Rail Faults

The equation for multiple ±1 rail faults was assigned to the form of the $P_F^{+M}(n,m)$, that is the form for the multiple +1 rail faults. In this case

$$\mathbf{w}_F = [1\ 1\ \ldots\ 1\ w_m\ \ w_{m-+1}\ \ldots\ w_n]^T$$

and the angle between $\mathbf{w}$ and $\mathbf{w}_F$ is found from their dot product:

$$\begin{aligned} \phi &= \cos^{-1}\left(\frac{\mathbf{w} \circ \mathbf{w}_F}{\|\mathbf{w}\|\ \|\mathbf{w}_F\|} \right) \\ &= \cos^{-1}\left(\frac{w_0 + \ldots + w_{m-1} + (w_m)^2 + (w_{m+1})^2 + \ldots + (w_n)^2}{\left(m + (w_m)^2 + (w_{m+1})^2 + \ldots + (w_n)^2\right)^{1/2}} \right) \end{aligned} \tag{3-18}$$

But from eq. (3-9)

$$\sum_{i=0}^{m-1} (w_i)^2 + \sum_{i=m}^{n} (w_i)^2 = 1$$

so

$$\sum_{i=m}^{n} (w_i)^2 = 1 - \sum_{i=0}^{m-1} (w_i)^2$$

and eq. (3-18) becomes

$$\phi = \cos^{-1}\left(\frac{\sum_{i=0}^{m-1} w_i + 1 - \sum_{i=0}^{m-1} (w_i)^2}{\left(m + 1 - \sum_{i=0}^{m-1} (w_i)^2 \right)^{1/2}} \right)$$

resulting in

$$P_F^{\pm M}(n,m) = \frac{1}{\pi} E\left\{ \cos^{-1}\left(\frac{\sum_{i=0}^{m-1} w_i + 1 - \sum_{i=0}^{m-1}(w_i)^2}{\left(m + 1 - \sum_{i=0}^{m-1}(w_i)^2 \right)^{1/2}} \right) \right\} \tag{3-19}$$

Multiple Sign-Change Fault

As with the single sign-change fault, the faulty weight vector has unit magnitude,

$$\mathbf{w}_F = [-w_0 \; -w_1 \ldots \; -w_{m-1} \;\; w_m \;\; w_{m+1} \ldots \; w_n]^T$$

and the corrupting vector $\Delta\mathbf{w}$ is

$$\Delta\mathbf{w} = [-2w_0 \; -2w_1 \ldots \; -2w_{m-1} \; 0 \ldots \; 0]^T$$

with magnitude

$$\|\Delta\mathbf{w}\| = 2\sqrt{\sum_{i=0}^{m-1}(w_i)^2}$$

Again the vectors $\mathbf{w}$, $\mathbf{w}_F$, and $\Delta\mathbf{w}$ form an isoceles triangle with two sides equal to unity. Using the Law of Cosines,

$$\|\Delta\mathbf{w}\| = 4\sum_{i=0}^{m-1}(w_i)^2 = 2 - 2\cos(\phi)$$

so that

$$\phi = \cos^{-1}\left(1 - 2\sum_{i=0}^{m-1}(w_i)^2 \right)$$

resulting in

$$P_F^{\Delta SM}(n,m) = \frac{1}{\pi} E\left\{ \cos^{-1}\left(1 - 2\sum_{i=0}^{m-1}(w_i)^2 \right) \right\} \tag{3-20}$$

Notice that if all vector components change sign, that is, $m = n+1$, $P_F = 1$. This is sensible: if all weights change sign, the weight vector reverses direction. It creates the same decision hyperplane but reverses the classification of all input vectors.

3.3.3 Summary of Model Equations

The table below, Figure 3-16, provides a summary of the formulas for the four failure models considered in this section.

Failure Model	Notation	Formula
Single Zeroed-Weight Fault Probability an adaline misclassifies given one of its input weights, w_k, has been forced to zero.	$P_F^0(n)$	$\frac{1}{\pi} E\left\{ \sin^{-1}\lvert w_k \rvert \right\}$
Single Rail Fault Probability an adaline misclassifies given one of its input weights,w_k, has been forced to ± 1.	$P_F^{\pm 1}(n)$	$\frac{1}{\pi} E\left\{ \cos^{-1}\left(\frac{1 - (w_k)^2 + w_k}{(2 - (w_k)^2)^{1/2}} \right) \right\}$
Single Sign-Change Fault Probability an adaline misclassifies given one of its input weights,w_k, changes sign, $w_k \rightarrow -w_k$.	$P_F^{\Delta S}(n)$	$\frac{1}{\pi} E\left\{ \cos^{-1}\left(1-2(w_k)^2\right) \right\}$
Multiple Zeroed-Weight Fault Probability an adaline misclassifies given m of its input weights have been forced to zero.	$P_F^{0M}(n,m)$	$\frac{1}{\pi} E\left\{ \sin^{-1}\left(\left(\sum_{i=0}^{m-1} (w_i)^2 \right)^{1/2} \right) \right\}$
Multiple Rail Fault Probability an adaline misclassifies given m of its input weights have been forced to ± 1.	$P_F^{\pm M}(n,m)$	$\frac{1}{\pi} E\left\{ \cos^{-1}\left(\frac{\sum_{i=0}^{m-1} w_i + 1 - \sum_{i=0}^{m-1} (w_i)^2}{\left(m + 1 - \sum_{i=0}^{m-1} (w_i)^2 \right)^{1/2}} \right) \right\}$
Multiple Sign-Change Fault Probability an adaline misclassifies given m of its input weights change sign.	$P_F^{\Delta SM}(n,m)$	$= \frac{1}{\pi} E\left\{ \cos^{-1}\left(1 - 2\sum_{i=0}^{m-1} (w_i)^2 \right) \right\}$

***Figure 3-16**: Summary of Formulas for Failure Modes*

3.4 WEIGHT DISTRIBUTIONS

The probabilities of adaline failures derived for the various fault modes in the previous section all involve expected values of functions of the adaline weights. To evaluate the failure probabilities, the probability distributions of the weight components must be determined. More specifically, the probability density function of the weight components must be derived.

The adaline weight vector has n+1 dimensions, $\mathbf{w} = [w_0\ w_1\ \ldots\ w_n]^T$. If each component can take on any value, determining probability distributions for the general case is an intractable problem — specific statistics of the weight vector must be provided. However, as discussed in §3.3, normalization of the weight vector to unit value has no effect on the adaline decision function, yet limits the range of vector components. Furthermore, a normalized weight vector was used to derive the equation for adaline probability and so must be used here as well. Thus, for the analysis here, **w** is assumed to be normalized to unit value, that is:

$$\begin{aligned} \|\mathbf{w}\|^2 &\equiv (w_0)^2 + (w_1)^2 + \ldots + (w_n)^2 \\ &= \sum_{i=0}^{n} (w_i)^2 = 1 \end{aligned} \tag{3-21}$$

Eq. (3-21) is also the equation of a unit hypersphere. *Normalization of* ***w*** *to unit length requires it to lie on the unit hypersphere.*

Since the vector represents the statistical information of the input classifications, the values of each component are highly dependent upon the classification function. The analysis in this thesis is intentionally general[12], so the vector must be considered "randomly oriented"; that is, the vector is assumed to be equally likely to be pointed in any direction. Thus, **w** is distributed on the unit hypersphere such that the probability that it lies on any patch of the

12. For specific cases where the weight probability distributions may be known, those distributions can be used to solve the equations of P_F. If the specific weight vector is known, the lune magnitude ϕ can be determined for all cases and the mean value of ϕ should be used for $E\{\phi\}$.

hypersphere is equal for equally-sized patches.

The vector components w_i, i = 0, 1, ..., n, are each dependent random variables on the interval [-1, +1], with eq. (3-21) imposing the interdependence. Evaluation of the equations for P_F thus requires evaluation of the expected value of functions of random variables. The expected value of any function of random variables $g(x_1, x_2, \ldots, x_n)$, where x_i are the random variables, can be determined using the joint probability density function of the random variables:

$$E\{g(x_1, x_2, \ldots, x_n)\} =$$

$$\int_{\Omega_X} g(x_1, x_2, \ldots, x_n)\, f_{x_1 x_2 \ldots x_n}(x_1, x_2, \ldots, x_n) dx_1 dx_2 \ldots dx_n \qquad (3\text{-}22)$$

where $f_{x_1 x_2 \ldots x_n}(x_1, x_2, \ldots, x_n)$ is the joint probability density function[13] and Ω_X is the range of the random variables. The expected value of a function of only one random variable g(x) is simply given by

$$E\{g(x)\} = \int_{\Omega_X} g(x) f_x(x) dx \qquad (3\text{-}23)$$

where $f_x(x)$ is the probability density function of x.

The equations for the probability of failure of an adaline with only one fault require the evaluation of the expected value of a function of one random variable, w_k. Those cases can be solved using eq. (3-23) and the probability density function for w_k. The equations for the probability of failure of a multi-fault adaline require that the joint probability density function of $w_0, w_1, \ldots, w_{m-1}$ be used in eq. (3-22). In this section, these probability density functions are derived.

Thus the problem is: given an n-dimensional[14] random vector $\mathbf{w} = [w_1\ w_2\ \ldots\ w_n]^T$ distributed uniformly over the unit hypersphere, determine the probability density function of a

---

13. Notation based loosely on Drake [14]. $F_x(x) = P\{x \leq x\}$; $f_x(x) = \frac{dF_x(x)}{dx}$.

14. This can obviously be extended to the n+1 dimensional vector $\mathbf{w} = [w_0\ w_1\ \ldots\ w_n]^T$.

single vector component w_i, denoted $f_w(w)$, and the joint probability density function of m components $w_1, w_2, \ldots, w_m$, denoted $f_w(w_1 \ldots w_m)$. Because $f_w(w)$ is a special case of $f_w(w_1 \ldots w_m)$, i.e., $f_w(w) = f_w(w_1 \ldots w_m)$ for $m = 1$, $f_w(w_1 \ldots w_m)$ is first derived.

The key to deriving the probability density function is to properly interpret the meaning of the vector being "distributed uniformly over the unit hypersphere." Since the goal is to have all directions equally likely, patches on the unit hypersphere of equal surface area (technically, of equal surface "content" [48]), must be equally likely to contain the vector. Patches of unequal area will have unequal probabilities of containing the vector and the ratio of those probabilities will be equal to the ratio of the surface areas.

The probability that the vector lies on the patch which covers the entire hypersphere is clearly unity. So, the probability that the vector lies in a smaller surface patch of area ds is simply the ratio of ds to the surface area of the hypersphere:

$$\text{Prob}\{\mathbf{w}_o < \mathbf{w} \le \mathbf{w}_o + \Delta\mathbf{w}\} = \frac{ds}{S_n} \tag{3-24}$$

where $\mathbf{w}_o$ is an arbitrary vector, $\Delta\mathbf{w}$ is an incremental vector, such that both $\mathbf{w}_o$ and $\mathbf{w}_o + \Delta\mathbf{w}$ meet the constraints of eq. (3-21), ds is the surface area of the patch subtending $\Delta\mathbf{w}$, and S_n is the surface area of an n-dimensional hypersphere. S_n is readily available[15] [41, 48]:

$$S_n = \frac{2\pi^{n/2}}{\Gamma\left(\frac{n}{2}\right)} \tag{3-25}$$

where $\Gamma(y)$ is the gamma function[16]:

---

15. The meaning of the term S_n varies by discipline. For this thesis, S_n will denote the surface area of the unit hypersphere which occupies n-dimensional space. For example, S_3 is surface area of the conventional sphere. It has surface area, from eq. (5-25), of $S_3 = 4\pi$. Mathematicians [41] often denote the surface area of a hypersphere which occupies n-dimensional space as S_{n-1}, since the *surface* is a manifold of n-1 dimensions in $\Re^n$. Of course the area is the same; only the notation and formula for S_n are different.

16. Three important properties of the gamma function are useful for evaluating $\Gamma\left(\frac{n}{2}\right)$ [03370]:

    $\Gamma(x) = (x-1)!$, for x an integer; $\Gamma\left(\frac{1}{2}\right) = \sqrt{\pi}$; and $\Gamma(y+1) = y\Gamma(y)$.

$$\Gamma(y) = \int_0^1 x^{y-1} e^{-x}\, dx \tag{3-26}$$

Equation (3-24) is the essence of the derivations to follow.

A note on symmetry is in order before the density functions are derived. Since the hypersphere is symmetrical in all directions and the components of **w** are numbered arbitrarily (or, the axes of $\Re^n$ are labelled arbitrarily), the probability density function for the single vector component is independent of the particular component chosen. Thus, $f_w(w)$ will be identical for all components. Similarly, the joint probability density function for the first m elements is identical to the joint probability density function for any m elements. The recognition of the equivalences of these functions simplifies the derivations.

3.4.1 Joint Probability Density Function of Several Weights

As stated in eq. (3-24), the ratio of the surface area of a "patch" on the unit hypersphere to the total hypersphere surface area is the probability that a unit vector distributed uniformly over the hypersphere lies in that patch. For a patch which subtends only differential elements, the surface area ratio gives a probability density function. For a patch which subtends m differential elements, a joint probability density function of m components is found. (For m = 1, the single probability density function for one component is found.) Finding the probability density functions thus requires finding the surface area of the "patch".

By definition, the probability that the vector **w** lies in a patch which subtends m differential components is the joint probability density function times the differential area of the subtending components:

$$\text{Prob}\left\{\begin{array}{l} w_1 < w_1 \le w_1 + dw_1 \\ w_2 < w_2 \le w_2 + dw_2 \\ \cdots \\ w_m < w_m \le w_m + dw_m \end{array}\right\} = f_w(w_1 \ldots w_m)\, dw_1\, dw_2 \ldots dw_m \tag{3-27}$$

The probability is also equal to the ratio of the surface area of the patch to the surface area of hypersphere, eq. (3-24):

$$\text{Prob}\left\{\begin{array}{l} w_1 < w_1 \le w_1 + dw_1 \\ w_2 < w_2 \le w_2 + dw_2 \\ \quad \cdots \\ w_m < w_m \le w_m + dw_m \end{array}\right\} = \frac{ds}{S_n} \tag{3-28}$$

where ds is the area of the patching subtending $dw_1\ dw_2 \ldots dw_m$. Equating the right sides of the above probabilities,

$$f_w(w_1 \ldots w_m) = \frac{ds}{S_n\ dw_1 dw_2 \ldots dw_m} \tag{3-29}$$

The problem is now to determine the ds, the area of a patch on a unit hypersphere which subtends m differential components. Figure 3-17 provides an illustration.

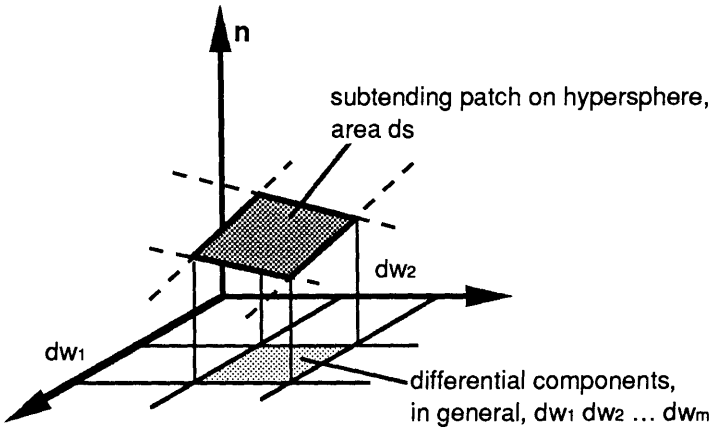

***Figure 3-17**: Patch of Area ds Subtending m Differential Components*

Determining the patch area requires considering the higher order space $\Re^n$. Excellent, if dated, texts are available on the subject [48, 68], but by decomposing the space into smaller dimensional spaces which can be more easily expressed, the patch area can be described here.

The n-dimensional space $\Re^n$ is spanned by the unit vectors $\mathbf{u}_1, \mathbf{u}_2, \ldots, \mathbf{u}_n$. This space can be considered as two orthogonal spaces, one spanned by $\mathbf{u}_1, \mathbf{u}_2, \ldots, \mathbf{u}_m$, and the other spanned by $\mathbf{u}_{m+1}, \mathbf{u}_{m+2}, \ldots, \mathbf{u}_n$. This is shown in Figure 3-18, with a horizontal vector $\mathbf{x} = \mathbf{u}_1 + \mathbf{u}_2 + \ldots + \mathbf{u}_m$ and a vertical vector $\mathbf{y} = \mathbf{u}_{m+1} + \mathbf{u}_{m+2} + \ldots + \mathbf{u}_n$. In this depiction, the unit hypersphere filling $\Re^n$ is a 2-dimensional circle, as shown, with radius r = 1. The vector $\mathbf{w}$ must lie on that circle; it too can be decomposed into $\mathbf{w} = w_x\,\mathbf{x} + w_y\,\mathbf{y}$.

A patch on the unit hypersphere which subtends m differential components $dw_1, dw_2, \ldots, dw_m$ at w_x, as shown in Figure 3-19, has an m-dimensional arc length da. The area of the

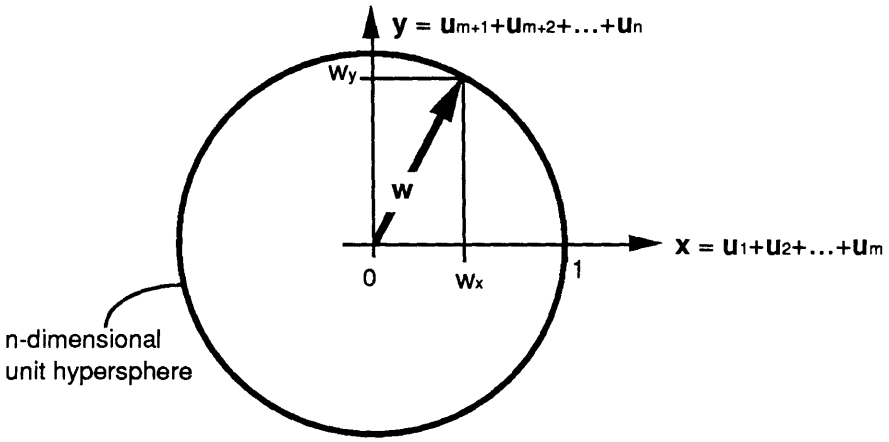

Figure 3-18: *Unit Hypersphere in a Simplified* $\Re^n$

patch, ds, is equal to the arc length times the area, A, of the underlying surface.

$$ds = da \bullet A \tag{3-30}$$

That underlying surface spans the remaining n-m dimensions and has dimension n-m-1 (n-m-1 degrees of freedom). The patch will have dimension n-1; m dimensions from da and n-m-1 dimensions from A.

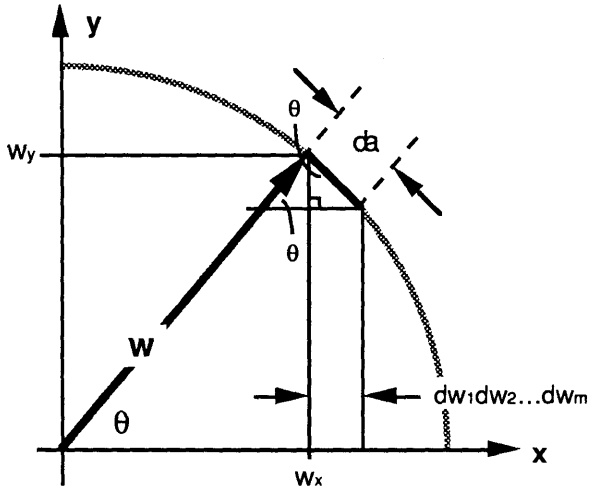

Figure 3-19: *Patch Arc Length, da*

To understand the meaning of eq. (3-30), consider Figure 3-19 as a cross-section of a conventional 3-dimensional sphere. The area of the patch which subtends a single differential component dx at w_x is the arc length da above w_x times the circumference of the circle at w_x which is perpendicular to **x**. The "circumference of the circle" is simply the "area" of the

underlying surface which spans the other 2 dimensions. Here, m=1, so the arc length has dimension 1 and the underlying surface has dimension 3-1-1 = 1 as well. The patch itself has dimension 2: it is a differential ring.

The first step is to find the arc length da. From Figure 3-19, the relationship between da and $dw_1\ dw_2 \ldots dw_m$ can be directly determined:

$$\frac{dw_1 dw_2 \ldots dw_m}{da} = \sin\theta \tag{3-31}$$

where θ is the angle between **w** and **x**. But,

$$\sin\theta = \frac{w_y}{\|\mathbf{w}\|}$$

and since $\|\mathbf{w}\| = 1$,

$$\sin\theta = w_y \tag{3-32}$$

Now, w_x is the length of the first m components of **w**:

$$w_x = \sqrt{\sum_{i=1}^{m} (w_i)^2} \tag{3-33}$$

by using $\|\mathbf{w}\| = 1$ and Pythagoras

$$w_y = \sqrt{1 - (w_x)^2}$$

$$= \sqrt{1 - \sum_{i=1}^{m} (w_i)^2} \tag{3-34}$$

Combining eq. (3-31), (3-32), and (3-34), yields an equation for da:

$$da = \frac{dw_1 dw_2 \ldots dw_m}{\sqrt{1 - \sum_{i=1}^{m} (w_i)^2}} \tag{3-35}$$

Although the patch will always subtend $dw_1\ dw_2 \ldots dw_m$, it will also span a surface over the remaining n-m dimensions. To see this, expand the 2-dimensional depiction to 3 dimensions, one spanned by $\mathbf{u}_1, \mathbf{u}_2, \ldots, \mathbf{u}_m$ as before, one spanned by only $\mathbf{u}_{m+1}$, and one spanned by the remaining unit vectors, $\mathbf{u}_{m+2}, \mathbf{u}_{m+3}, \ldots, \mathbf{u}_n$. Define the spanning vectors **x** =

$\mathbf{u}_1 + \mathbf{u}_2 + \ldots + \mathbf{u}_m$, $\mathbf{y} = \mathbf{u}_{m+1}$, and $\mathbf{z} = \mathbf{u}_{m+2} + \mathbf{u}_{m+3} + \ldots + \mathbf{u}_n$, shown in Figure 3-20. As before, $\mathbf{w}$ can be decomposed into $\mathbf{w} = w_x\mathbf{x} + w_{m+1}\mathbf{y} + w_z\mathbf{z}$.

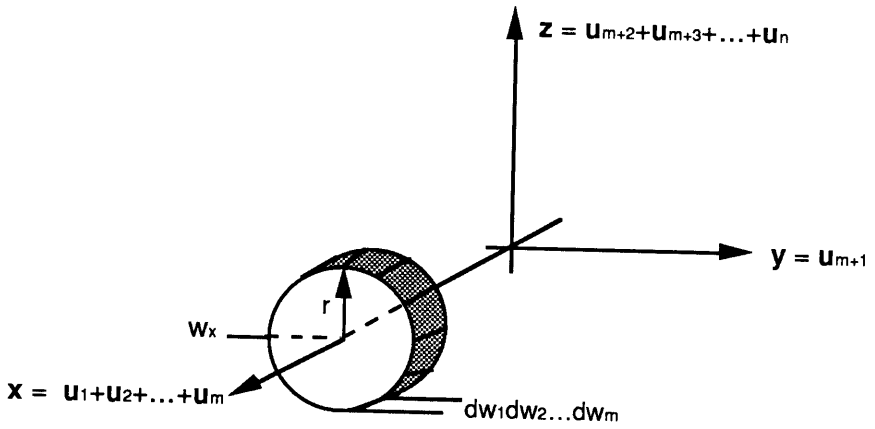

Figure 3-20: *3-dimensional Depiction of the Hypersphere Slice in* $\Re^n$

The differential slice in Figures 5-18 and 5-19 becomes a differential ring in Figure 3-20. It has a radius, r, equal to distance between the arc da and $\mathbf{x}$. From Figure 3-19,

$$r = w_y = \sqrt{1 - \sum_{i=1}^{m}(w_i)^2} \tag{3-36}$$

To see this formally, remember that the vector $\mathbf{w} = w_x\mathbf{x} + w_{m+1}\mathbf{y} + w_z\mathbf{z}$ must always satisfy the equation of the unit hypersphere:

$$\sum_{i=1}^{n}(w_i)^2 = 1$$

which expands to

$$\sum_{i=1}^{m}(w_i)^2 + (w_{m+1})^2 + \sum_{i=m+2}^{n}(w_i)^2 = 1 \tag{3-37}$$

but $(w_x)^2 = \sum_{i=1}^{m}(w_i)^2$ and $(w_z)^2 = \sum_{i=m+2}^{n}(w_i)^2$, so eq. (3-37) becomes

$$(w_x)^2 + (w_{m+1})^2 + (w_z)^2 = 1$$

or

$$(w_{m+1})^2 + (w_z)^2 = 1 - (w_x)^2 \tag{3-38}$$

For a fixed w_x, eq. (3-38) has the form of an equation of a circle in the $\mathbf{y}$-$\mathbf{z}$ plane:

$$(w_{m+1})^2 + (w_z)^2 = r^2$$

Thus, at a fixed w_x the surface of the hypersphere is a circle parallel to the **y-z** plane, centered on the **x** axis with radius r,

$$r = \sqrt{1 - (w_x)^2}, \text{ or}$$

or
$$r = \sqrt{1 - \sum_{i=1}^{m} (w_i)^2}$$

which is eq. (3-36). Of course, the surface is a circle because only 2 dimensions, **y** and **z**, are depicted. In the vernacular of higher geometry, a circle is a hypersphere of 2 dimensions.

To go beyond 2 dimensions and obtain the general surface of n-m dimensions, eq. (5-38) is re-expanded with r given by eq. (3-36):

$$(w_{m+1})^2 + (w_{m+2})^2 + \ldots (w_n)^2 = r^2 \qquad (3\text{-}39)$$

This is the equation of an n-m dimensional hypersphere with radius r. *Thus, the surface spanned by the remaining n-m components of* ***w*** *is an n-m dimensional hypersphere with radius given by eq. (3-36),* $r = \left(1 - \sum_{i=1}^{m} (w_i)^2 \right)^{1/2}$.

As stated by eq. (3-30), the area of the patch subtending m differential components is the m-dimensional arc length, da, times the area of the underlying (n-m)-dimensional hypersphere, A. Using the 3 dimensional sphere as an example again, the patch above a single differential component dw_1 at w_1 is a differential ring with area equal to the arc length times the circumference of the ring at w_1, shown in Figure 3-21[17]. The "circumference of the ring" is technically the area of a 2-dimensional hypersphere.

The surface area of n-dimensional hypersphere with a radius other than unity, denoted A_n, is given by [48]:

---

17. In this case, $da = \frac{dw_1}{\sqrt{1-(w_1)^2}}$ and the circumference $= 2\pi r$, $r = \sqrt{1-(w_1)^2}$. Thus, the area of the patch is the constant $2\pi dw$. This interesting well-known result [53] reveals that if a sphere is sliced into equal widths perpendicular to one axis, each slice will have equal surface area. For example, an orange cut up in such a way would yield slices with equal peel area.

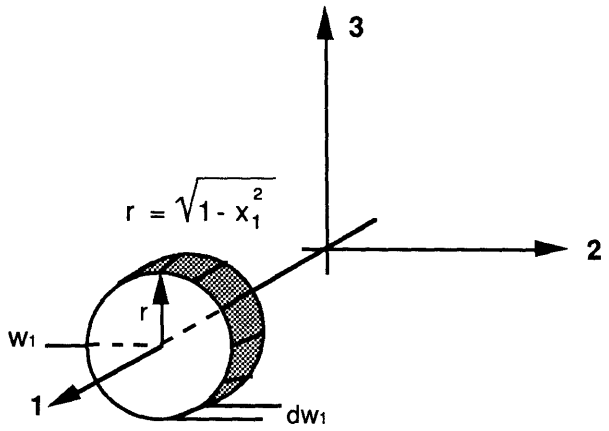

Figure 3-21: *Slice of a Sphere at One Fixed Component, w_1*

$$A_n = S_n r^{n-1} \tag{3-40}$$

where S_n is the surface area of the unit n-dimensional hypersphere, given by eq. (3-25). The area of the underlying (n-m)-dimensional hypersphere with radius r given by eq. (3-36) is thus

$$A = S_{n-m}\left(1-\sum_{i=1}^{m}(w_i)^2\right)^{(n-m-1)/2} \tag{3-41}$$

Combining this result with length of the arc da, eq. (3-35), the area of the patch is finally obtained:

$$ds = dw_1 dw_2 \ldots dw_m \, S_{n-m} \frac{\left(1-\sum_{i=1}^{m}(w_i)^2\right)^{(n-m-1)/2}}{\left(1-\sum_{i=1}^{m}(w_i)^2\right)^{1/2}}$$

which reduces to

$$ds = dw_1 dw_2 \ldots dw_m \, S_{n-m}\left(1-\sum_{i=1}^{m}(w_i)^2\right)^{(n-m-2)/2} \tag{3-42}$$

The patch area is substituted into eq. (3-29) to obtain the joint probability density function:

$$f_w(w_1 \ldots w_m) = \frac{dw_1 dw_2 \ldots dw_m \, S_{n-m}\left(1-\sum_{i=1}^{m}(w_i)^2\right)^{(n-m-2)/2}}{dw_1 dw_2 \ldots dw_m \, S_n}$$

which simplifies nicely to

$$f_w(w_1 \ldots w_m) = \frac{S_{n-m}}{S_n}\left(1 - \sum_{i=1}^{m}(w_i)^2\right)^{(n-m-2)/2} \tag{3-43}$$

Using eq. (3-25), the fraction $\frac{S_{n-m}}{S_n}$ is reduced for easier computation:

$$f_w(w_1 \ldots w_m) = \frac{\Gamma\left(\frac{n}{2}\right)}{\Gamma\left(\frac{n-m}{2}\right)(\pi)^{m/2}}\left(1 - \sum_{i=1}^{m}(w_i)^2\right)^{(n-m-2)/2} \tag{3-44}$$

Behavior of the Joint Probability Density Function

With the joint probability density function in hand, some comments on its behavior are in order. First, note that despite its complicated form in eq. (3-44), the function of eq. (3-43) is actually quite elegant. It reveals that the joint probability density function of m components is given by a constant term times the radius of a particular hypersphere raised to a power. The constant is the ratio of the surface area of an (n-m)-dimensional unit hypersphere, Sn-m, to the surface area of an n-dimensional unit hypersphere, Sn. The radius, $r = \left(1 - \sum_{i=1}^{m}(w_i)^2\right)^{1/2}$, is that of an (n-m)-dimensional hypersphere on the surface of the n-dimensional unit hypersphere. The power (n-m-2) is simply two less than the difference in dimensions.

A relevant question is the validity of the form of eq. (3-43) when m=n; can the joint probability density function of m components be used to determine the probability density function of all n components? The answer is yes, with some appropriate interpretation.

First the density function of eq. (3-43) must be formally stated to account for the constraints on the range of the components. Formally, the probability density function is non-zero only when the components are within the n dimensional unit hypersphere:

$$f_w(w_1 \ldots w_m) = \begin{cases} \frac{S_{n-m}}{S_n} \left(1 - \sum_{i=1}^{m} (w_i)^2 \right)^{(n-m-2)/2} & \text{iff } \sum_{i=1}^{m} (w_i)^2 \leq 1 \\ 0 & \text{otherwise} \end{cases} \quad (3\text{-}45)$$

For m=n, the density function is non-zero only when the components are within the n-dimensional unit hypersphere[18]. From eq. (3-45),

$$f_w(w_1 \ldots w_n) = \begin{cases} \frac{S_0}{S_n \left(1 - \sum_{i=1}^{n} (w_i)^2 \right)} & \text{iff } \sum_{i=1}^{n} (w_i)^2 \leq 1 \quad (3\text{-}46a) \\ 0 & \text{otherwise} \quad (3\text{-}46b) \end{cases}$$

Now, $S_0 = 0^{\dagger}$, so $f_w(w_1 \ldots w_n) = 0$, unless $\sum_{i=1}^{n} (w_i)^2 = 1$, in which case the denominator of eq. (3-46a) is zero as well. But, this condition holds in all cases: it is the requirement of **w** being a unit vector. Cancelling the zeros in the numerator and denominator at $\sum_{i=1}^{n} (w_i)^2 = 1$, eq. (5-46) becomes:

$$f_w(w_1 \ldots w_n) = \begin{cases} \frac{1}{S_n} & \text{iff } \sum_{i=1}^{n} (w_i)^2 = 1 \\ 0 & \text{otherwise} \end{cases} \quad (3\text{-}47)$$

Eq. (3-47) states that the n components of a unit vector are simply distributed uniformly over the surface of the unit hypersphere — which was the original statement guiding the derivations of this section. The S_n in the denominator is a normalizing factor so that the density over the surface integrates to 1.

---

18. The components must actually be on the n-dimensional unit hypersphere. This condition is met by the resulting equation.

† $S_0 = \frac{2}{\Gamma(0)}$ and $\frac{1}{\Gamma(0)} = 0$.

For example, for n = 2:

$$f_w(w_1 w_2) = \begin{cases} \frac{1}{S_n} = \frac{1}{2\pi} & \text{iff } w_1^2 + w_2^2 = 1 \\ 0 & \text{otherwise} \end{cases}$$

The density is illustrated in Figure 3-22. It is an infinitesimally thin, hollow cylinder of radius 1 and height $\frac{1}{2\pi}$, centered at the origin. The "area" under the density (which must equal 1) is simply the circumference of the unit circle times the height of the cylinder: $2\pi \bullet \frac{1}{2\pi} = 1$.

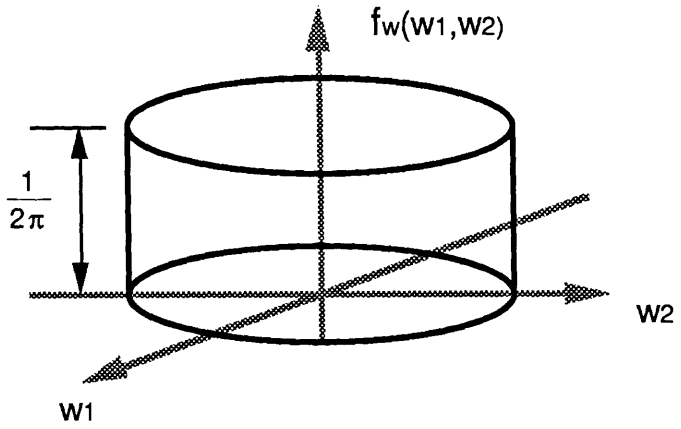

Figure 3-22: *Joint density of Both components of a Vector on the Unit Circle*

The density for a single component can be determined by integrating out the density of the other component. The area under the density contributed by w_2 for each dw_1 is 2da times the height $\frac{1}{2\pi}$, where da is the arc length at w, shown in Figure 3-23. From Figure 3-19,

$$da = \frac{dw_1}{\sqrt{1-w_1^2}}$$

so

$$f_w(w_1) = \frac{1}{\pi\sqrt{1-w_1^2}}$$

which agrees with eq. (3-43) for n=2 and m=1.

It is often instructive to study the behavior of a probability density function by identifying its first two central moments, i.e., its mean and variance. Since eq. (3-43) is an even function of all of its arguments, all variables have zero mean. This reduces the covariance matrix to

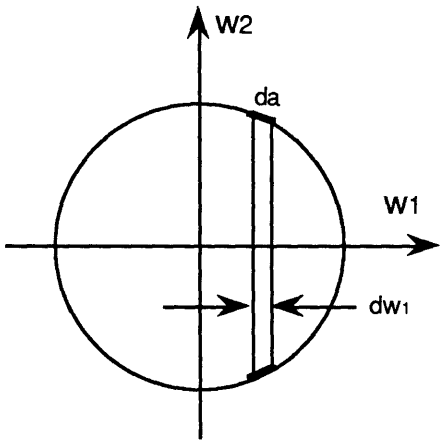

Figure 3-23: Calculation of Probability Density of Single Component on the Unit Circle

$$\mathbf{R} = \begin{bmatrix} E\{(w_1)^2\} & E\{w_1w_2\} & \dots & E\{w_1w_m\} \\ E\{w_2w_1\} & E\{(w_2)^2\} & \dots & E\{w_2w_m\} \\ \dots & \dots & \dots & \dots \\ E\{w_mw_1\} & E\{w_mw_2\} & \dots & E\{(w_m)^2\} \end{bmatrix} \tag{3-48}$$

Clearly by the symmetry of the problem $E\{(w_i)^2\} = E\{(w_j)^2\}$ and $E\{w_iw_j\} = E\{w_kw_l\}$. Higher order central moments would reflect the same symmetry. Unfortunately, the expected values in eq. (3-48) will all be functions of n and the remaining m-1 or m-2 variables and their significance may be difficult to interpret. For this reason, the covariance matrix is left in the form of eq. (3-48) and the variance for only the single probability density function, m=1, is derived — in the next section.

As a conclusion to the joint probability density function, Figure 3-24 presents a tabulation of the density functions for n = 2 to 5 and m = 1 to n. Note the uniform distribution for m = (n-2).

3.4.2 Probability Density Function of a Single Weight

The probability density function of a single weight, w, is derived from the joint probability density function for only 1 component. That is, the single probability density function is given by eq. (3-43) with m = 1:

$$f_w(w_1 \ldots w_m) = \frac{S_{n-m}}{S_n}\left(1 - \sum_{i=1}^{m}(w_i)^2\right)^{(n-m-2)/2}$$

n⇒ m⇓	2	3	4	5
1	$\frac{1}{\pi\sqrt{1-(w_1)^2}}$	$\frac{1}{2}$	$\frac{2}{\pi}\sqrt{1-(w_1)^2}$	$\frac{3}{4}\left(1-(w_1)^2\right)$
2	$\frac{1}{2\pi}$	$\frac{1}{2\pi\sqrt{1-(w_1)^2-(w_2)^2}}$	$\frac{1}{\pi}$	$\frac{3}{2\pi}\sqrt{1-(w_1)^2-(w_2)^2}$
3	—	$\frac{1}{4\pi}$	$\frac{2}{\sqrt{1-(w_1)^2-(w_2)^2-(w_3)^2}}$	$\frac{3}{4\pi}$
4	—	—	$\frac{1}{2\pi^2}$	$\frac{3}{4\pi^2\sqrt{1-(w_1)^2-(w_2)^2-(w_3)^2-(w_4)^2}}$
5	—	—	—	$\frac{3}{8\pi^2}$

Figure 3-24: *Tabulation of Joint Density Function*

$$f_w(w_1) = \frac{S_{n-1}}{S_n}\left(1-\sum_{i=1}^{1}w_i^2\right)^{(n-3)/2}$$

which, after dropping the subscript on w and simplifying the notation, becomes

$$f_w(w) = \frac{\Gamma\left(\frac{n}{2}\right)}{\Gamma\left(\frac{n-1}{2}\right)\sqrt{\pi}}(1-w^2)^{(n-3)/2} \tag{3-49}$$

The distribution is an even function with zero mean and, except for the case of n=2, a maximum value (at w = 0) given by the ratio[19] $\frac{\Gamma\left(\frac{n}{2}\right)}{\Gamma\left(\frac{n-1}{2}\right)\sqrt{\pi}}$.

19. Although the ratio $\frac{\Gamma\left(\frac{n}{2}\right)}{\Gamma\left(\frac{n-1}{2}\right)\sqrt{\pi}}$ appears reducible, because n is an integer the function can be calculated relatively easily and the fractional form is easier to use than a reduced form. Appendix B.1 derives a form for the ratio which does not explicitly require the gamma function. For notational convenience, the original fractional form will be used.

It is instructive to see how $f_w(w)$ behaves as n grows large. Because the sum of the squares of the components must equal 1, it seems likely that the probability density function of any component will be amassed near 0 for large n. That is, it is unlikely that the component takes on a value near 1 since all other components must then be much less than 1 but all have identical probability distributions.

Indeed, this is the case. The value of $\frac{\Gamma\left(\frac{n}{2}\right)}{\Gamma\left(\frac{n-1}{2}\right)\sqrt{\pi}}$ increases with n. The variance, calculated in Appendix B.2, is given simply by $\frac{1}{n}$.

The equations of $f_w(w)$ for various values of n are tabulated in Figure 3-25. The actual distributions are plotted in Figure 3-26.

3.5 PROBABILITY OF ADALINE FAILURE

Evaluation of the probability of adaline failure requires the incorporation of the probability density functions derived in the previous section into the formulae for the probability of the adaline failure from §3.3. Those results are repeated here for convenience.

$$P_F^0(n) = \frac{1}{\pi} E\left\{ \sin^{-1}|w_k| \right\} \tag{3-50}$$

$$P_F^{\pm 1}(n) = \frac{1}{\pi} E\left\{ \cos^{-1}\left(\frac{1 - (w_k)^2 + w_k}{\left(2 - (w_k)^2\right)^{1/2}} \right) \right\} \tag{3-51}$$

$$P_F^{\Delta S}(n) = \frac{1}{\pi} E\left\{ \cos^{-1}\left(1-2(w_k)^2\right) \right\} \tag{3-52}$$

$$P_F^{0M}(n,m) = \frac{1}{\pi} E\left\{ \sin^{-1}\left(\left(\sum_{i=0}^{m-1} (w_i)^2 \right)^{1/2} \right) \right\} \tag{3-53}$$

$$P_F^{\pm M}(n,m) = \frac{1}{\pi} E\left\{ \cos^{-1}\left(\frac{\sum_{i=0}^{m-1} w_i + 1 - \sum_{i=0}^{m-1} (w_i)^2}{\left(m + 1 - \sum_{i=0}^{m-1} (w_i)^2 \right)^{1/2}} \right) \right\} \tag{3-54}$$

n	$f_w(w)$	n	$f_w(w)$
2	$\frac{1}{\pi\sqrt{1-w^2}}$ (see note 20)	20	$1.72(1-w^2)^{8.5}$
3	$\frac{1}{2}$ (see note 21)	50	$2.78(1-w^2)^{23.5}$
4	$\frac{2}{\pi}\sqrt{1-w^2}$	100	$3.96(1-w^2)^{48.5}$
5	$\frac{3}{4}(1-w^2)$	500	$8.92(1-w^2)^{298.5}$
10	$\frac{128}{35\pi}(1-w^2)^{7/2} \approx 1.16(1-w^2)^{7/2}$	1000	$12.6(1-w^2)^{498.5}$

***Figure 3-25**: Tabulation of Single Probability Density Function*

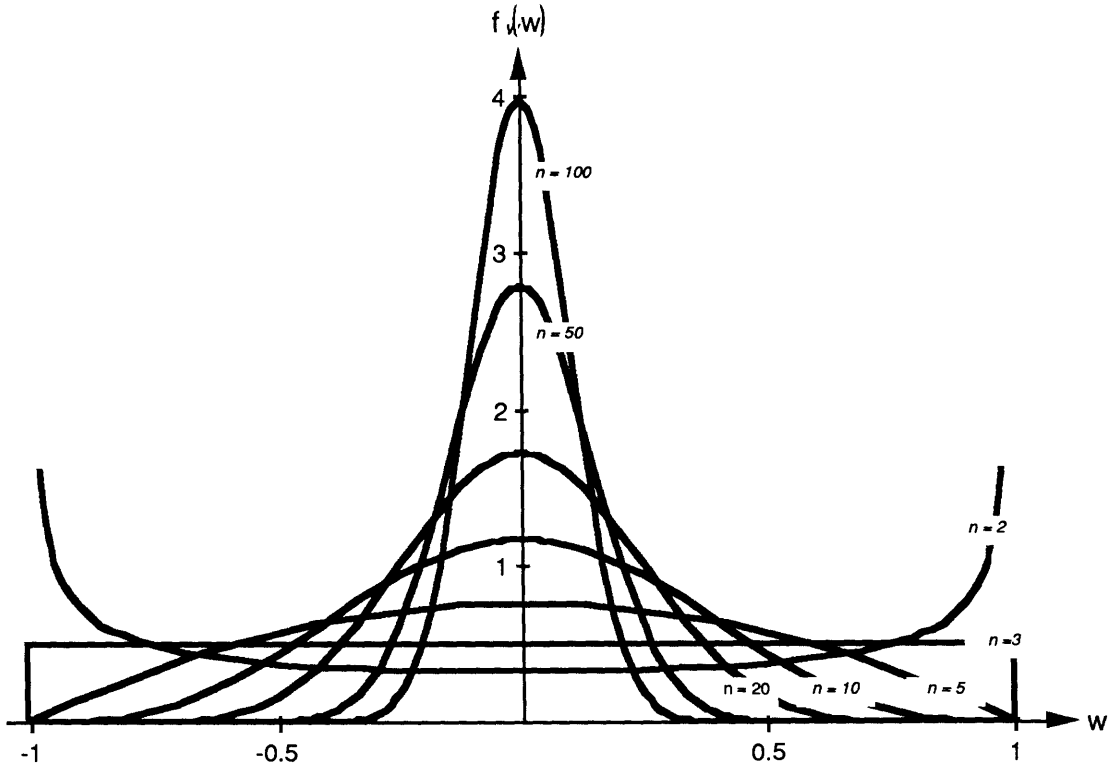

***Figure 3-26**: Probability Density Function for Values of Vector Dimension, n*

---

20. The result for n=2 agrees with the result conventionally derived when w is one of the two vector components on the unit circle [34]. Note that despite the fact that fw(1) = ∞, there are no impulses at w = 1 and therefore the probability of w =1 is zero. A similar phenomenon occurs in all cases of the joint density function when m = n - 1.

21. For n=3, the uniform distribution is a well-known paradigm; see note 17.

$$P_F^{\Delta SM}(n,m) = \frac{1}{\pi} E\left\{\cos^{-1}\left(1 - 2\sum_{i=0}^{m-1}(w_i)^2\right)\right\} \tag{3-55}$$

Recall that for notational convenience, the density functions of §3.4 were derived for an n-dimensional vector, $\mathbf{w} = [w_1\ w_2\ \ldots\ w_n]^T$. The weight vector of interest, however, has n+1 elements, where n is the number of true adaline inputs, $\mathbf{w} = [w_0\ w_1\ \ldots\ w_n]^T$. Thus, the density functions for the weight vector of an adaline with n inputs are:

$$f_w(w) = \frac{\Gamma\left(\frac{n+1}{2}\right)}{\Gamma\left(\frac{n}{2}\right)\sqrt{\pi}}(1-w^2)^{(n-2)/2} \tag{3-56}$$

$$f_w(w_1 \ldots w_m) = \frac{\Gamma\left(\frac{n+1}{2}\right)}{\Gamma\left(\frac{n-m+1}{2}\right)(\pi)^{m/2}}\left(1 - \sum_{i=0}^{m-1}(w_i)^2\right)^{(n-m-1)/2} \tag{3-57}$$

The problem is now to use eq. (3-22) and eq. (3-23) to solve eqs. (3-50) through (3-55). In all cases, $P_F = \frac{E\{\phi\}}{\pi}$ and $\phi = g(w_0,\ldots,w_{m-1},n)$, so

$$P_F(n) = \frac{1}{\pi}\int_{-1}^{1} g(w_0,\ldots,w_{m-1},n)\, f_w(w_0,\ldots,w_{m-1})dw_0 \ldots dw_{m-1} \tag{3-58}$$

The particular instantiations of eq. (3-58) are as follows:

$$P_F^0(n) = \frac{\Gamma\left(\frac{n+1}{2}\right)}{\Gamma\left(\frac{n}{2}\right)\pi^{3/2}}\int_{-1}^{1}\sin^{-1}|w|\,(1-w^2)^{(n-2)/2}dw \tag{3-59}$$

$$P_F^{\pm 1}(n) = \frac{\Gamma\left(\frac{n+1}{2}\right)}{\Gamma\left(\frac{n}{2}\right)\pi^{3/2}}\int_{-1}^{1}\cos^{-1}\left(\frac{1 - (w)^2 + w}{(2 - (w)^2)^{1/2}}\right)(1-w^2)^{(n-2)/2}dw \tag{3-60}$$

$$P_F^{\Delta S}(n) = \frac{\Gamma\left(\frac{n+1}{2}\right)}{\Gamma\left(\frac{n}{2}\right)\pi^{3/2}}\int_{-1}^{1}\cos^{-1}\left(1-2(w)^2\right)(1-w^2)^{(n-2)/2}dw \tag{3-61}$$

$$P_F^{0M}(n,m) = \frac{\Gamma\left(\frac{n+1}{2}\right)}{\Gamma\left(\frac{n-m+1}{2}\right)\pi^{(m+2)/2}} \cdot \int_{-1}^{1} \sin^{-1}\left(\left(\sum_{i=0}^{m-1} (w_i)^2 \right)^{1/2} \right) \left(1 - \sum_{i=0}^{m-1} (w_i)^2 \right)^{(n-m-1)/2} dw_0 \ldots dw_{m-1} \quad (3\text{-}62)$$

$$P_F^{\pm M}(n,m) = \frac{\Gamma\left(\frac{n+1}{2}\right)}{\Gamma\left(\frac{n-m+1}{2}\right)\pi^{(m+2)/2}} \cdot \int_{-1}^{1} \cos^{-1}\left(\frac{\sum_{i=0}^{m-1} w_i + 1 - \sum_{i=0}^{m-1} (w_i)^2}{\left(m + 1 - \sum_{i=0}^{m-1} (w_i)^2 \right)^{1/2}} \right) \left(1 - \sum_{i=0}^{m-1} (w_i)^2 \right)^{(n-m-1)/2} dw_0 \ldots dw_{m-1} \quad (3\text{-}63)$$

$$P_F^{\Delta SM}(n,m) = \frac{\Gamma\left(\frac{n+1}{2}\right)}{\Gamma\left(\frac{n-m+1}{2}\right)\pi^{(m+2)/2}} \cdot \int_{-1}^{1} \cos^{-1}\left(1 - 2\sum_{i=0}^{m-1} (w_i)^2 \right) \left(1 - \sum_{i=0}^{m-1} (w_i)^2 \right)^{(n-m-1)/2} dw_0 \ldots dw_{m-1} \quad (3\text{-}64)$$

3.5.1 Closed-Form Solutions

Solving eqs. (3-59) through (3-64) is no small task. However, the integrals can be simplified by recognizing that both $g(\bullet)$ and $f_w(\bullet)$ in all cases are even functions of w_i. Since the product of even functions is an even function the integral of eq. (3-58) can be reduced to:

$$P_F(n) = \frac{2^m}{\pi} \int_0^1 g(w_0,\ldots,w_{m-1},n)\, f_w(w_0,\ldots,w_{m-1}) dw_0 \ldots dw_{m-1} \quad (3\text{-}65)$$

and the arguments of $g(\bullet)$ and $f_w(\bullet)$ will all be positive. For example, eq. (3-59) is reduced to:

$$P_F^0(n,m) = \frac{2^m \Gamma\left(\frac{n+1}{2}\right)}{\Gamma\left(\frac{n}{2}\right)\pi^{3/2}} \int_0^1 \sin^{-1}(w)(1-w^2)^{(n-2)/2} dw \tag{3-66}$$

Further simplifications can be made by recognizing similarities in the arguments of g(•) and f$_W$(•) and making clever substitutions.

Despite these simplifications, the integrals are still formidable. Closed-form solutions are attainable, but those forms themselves are complicated functions which are impractical to solve by hand. The single zeroed-weight fault, for example, has the simplest integral to solve, eq. (3-66). That integral can be reduced to

$$\begin{aligned} P_F^0(n,m) &= \frac{2^m \Gamma\left(\frac{n+1}{2}\right)}{\Gamma\left(\frac{n}{2}\right)\pi^{3/2}} \int_0^1 \sin^{-1}(w)(1-w^2)^{(n-2)/2} dw \\ &= \frac{2^m \Gamma\left(\frac{n+1}{2}\right)}{\Gamma\left(\frac{n}{2}\right)\pi^{3/2}} \int_0^{\pi/2} \theta(\cos\theta)^{n-3} d\theta \end{aligned} \tag{3-67}$$

The solution to equation (3-67) derived in Appendix B.3, is non-trivial.

Because the integrals reduce to a form impractical to solve by hand for any reasonably large n, the formulas for the probability of adaline failure are left in the forms of eqs. (3-59) to (3-63). Several computer-aided techniques, including simulation [44], or mechanical quadrature [27] can be used to determine $P_F(n,m)$ for particular values of n and m.

3.5.3 A Monte Carlo Simulation

Instead of integrating the equations (3-59) through (3-64) and solving for the P_F directly, the trend for the failure probabilities as functions of n and m are determined. This is accomplished through simulation of statistical trials, the so-called Monte Carlo method [44]. In this process, N vectors, $\mathbf{x}_j$, j =1... N, with distributions identical to the distributions of the adaline weight vector are constructed. The value of $\phi_j = g(\mathbf{x}_j)$ is then calculated. For large enough N, the average value of ϕ approximates its expected value. That is, according to the Law of Large Numbers

$$\lim_{N\to\infty} \frac{\sum_{j=1}^{N} \phi_j}{N} = E\{\phi\} \tag{3-68}$$

The functions g(•) were developed in §3.3. They are simply the arguments of E{•} in Figure 3-16. The problem is now to construct a vector **x** whose components have the same distribution as the weight vector **w**. That is, the "simulated" vector **x** must have components whose probability density function is given by eq. (3-56):

$$f_x(x) = C_n(1-x^2)^{(n-2)/2} \tag{3-56}$$

where
$$C_n = \frac{\Gamma\left(\frac{n+1}{2}\right)}{\Gamma\left(\frac{n}{2}\right)\sqrt{\pi}} \tag{3-70}$$

Schreider [44] provides a direct method for constructing sample set of numbers with probability density $f_x(x)$. It involves transforming a sample set with uniform distribution into a set with the desired distribution. If $F_x(x)$ is the desired distribution

$$F_x(x) \equiv \int_{-\infty}^{x} f_x(z)dz = P\{x < x\}$$

and $Y = \{y_1, y_2, \ldots\}$ is a sample set whose components are uniformly distributed over [0,1], then a sample set $X = \{ x_1, x_2, \ldots\}$ can be constructed by solving

$$F_x(x_i) = y_i$$

that is, by setting

$$x_i = F_x^{-1}(y_i) \tag{3-71}$$

Unfortunately, for $f_x(x)$ of eq. (3-69), $F_x(x_i)$ is an odd polynominal of order (n/2) [15] and inverting it to apply eq. (3-71) is particularly difficult. Another method must be used in this case.

Fortunately, Schreider provides another method. This involves distributing two variables uniformly in the rectangle which bound the density function. One variable is distributed uniformly on the range of the abscissa, $x \in [-1, 1]$, and the other on the range of

the ordinate, $y \in [0, \max(f_x(x))]$. A test is performed on the pair (x,y): if $y \leq f_x(x)$, then the variable x is placed in the sample set. Otherwise the pair is discarded. The process is repeated until the desired sample set size is obtained.

The process is illustrated in Figure 3-28, with $f_x(x)$ from eq. (3-69) with n=100. For pair A, $y_1 < f_x(x_1)$, so x_1 is saved for the sample set. But, for pair B, $y_2 > f_x(x_2)$, so the pair is discarded and x_2 is not placed into the sample set. If a large number of pairs is generated, the points (x_i,y_i) will be uniformly dispersed in the rectangle $([-1,+1], [0,C_n])$. The process will bias the X sample space; the bias is determined by the probability density function.

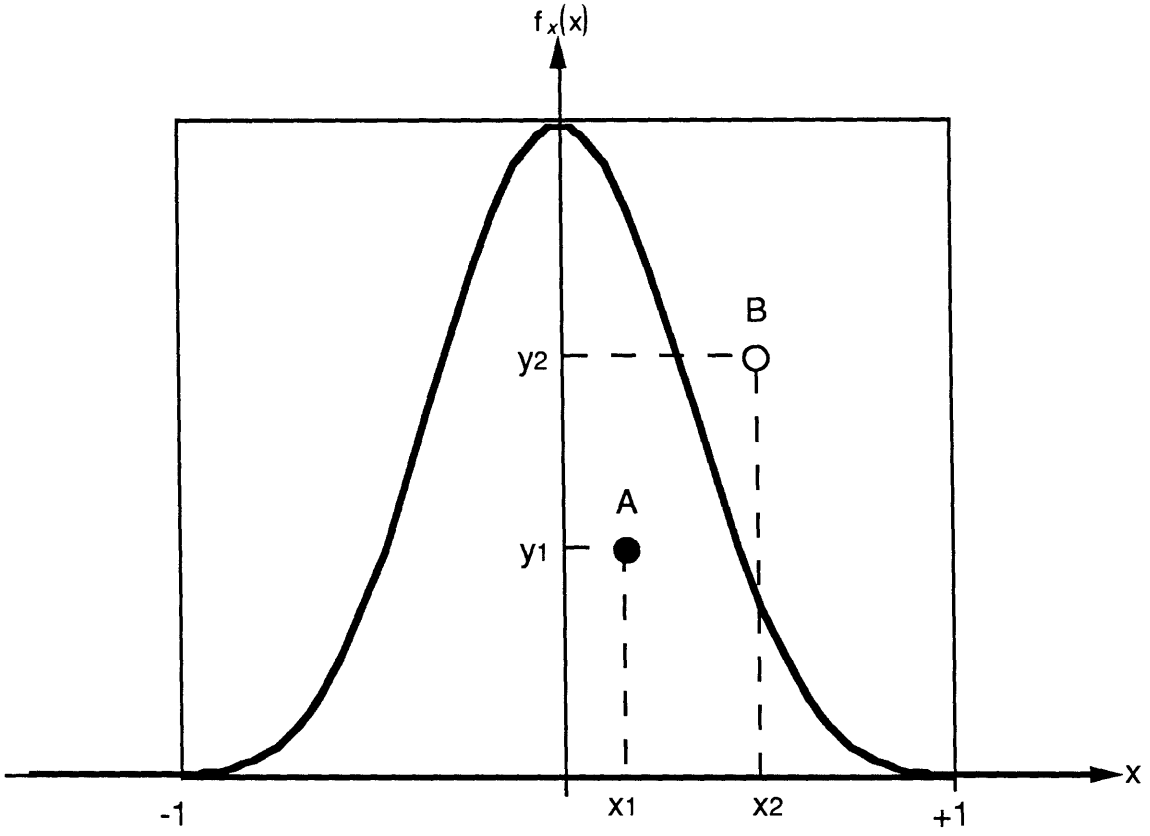

Figure 3-28: *Process for Creating Biased Sample Space*

To code the process for simulation, a pair of random numbers is created. The variable x is distributed uniformly between -1, and +1. The variable y is distributed uniformly between 0 and C_n, where C_n is given by eq. (3-70). If $y \leq C_n(1-x^2)^{(n-2)/2}$, then the variable x is written

to a file representing the sample space.[22] The process is repeated until the sample space is adequate in size.

Monte Carlo simulations were used to estimate adaline failure probability for all of the fault modes previously discussed. To ascertain a trend for likelihood of adaline failure as the number of inputs grow, simulations for n=10, 20, 30, 40, 50, 100, 200, 300, and 500 were performed. For the multiple fault cases, faults were inserted as a percentage of the number of inputs. Three cases were simulated: 1% faulty weights, 10% faulty weights, and 50% faulty weights[23]. For n < 100, the 1% faulty weights case was omitted. The following procedure was used for each case of n:

1. A 100,000 element sample set was created. The elements have a distribution equivalent to components on an n+1 dimensional unit hypersphere (density of eq. (3-56)). The sample set was created using the process described by Figure 3-28.

2. For the single fault case, where $P_F(n) = \frac{1}{\pi} E\{g(w)\}$, P_F was determined as the average of all 100,000 components processed by g(•):

$$P_F = \frac{1}{\pi} \cdot \frac{1}{100{,}000} \sum_{j=1}^{100{,}000} g(x_j)$$

   As a sanity check on the sample set, an average sum of squares for n+1 components was also taken. Ideally this should be equal to 1.

3. For the multiple fault case, m elements were randomly selected from the sample set and processed by g(•). The adaline failure probability was estimated as the average of 100,000 of these trials:

---

22. A coding simplification can be made by eliminating the factor C_n. For y distributed uniformly on [0,1] and a test of $y \le (1-x^2)^{(n-2)/2}$, the same results will be obtained. Elimination of C_n simply scales the density function and the Y sample space both to 1.

23. More accurately the cases were, m=0.01n, m=0.10n, and m=0.50n. The number of inputs is n, but an adaline has n+1 weights.

$$P_F = \frac{1}{\pi} \cdot \frac{1}{100{,}000} \sum_{j=1}^{100{,}000} g([w_0 w_1 \ldots w_m]_j)$$

where $[w_0 w_1 \ldots w_m]_j$ is a set of m randomly selected elements from the sample space.

The size of the sample space, or more specifically the number of trials, in a Monte Carlo simulation determines it accuracy. From the Chebyshev Inequality, the accuracy of a Monte Carlo simulation can be determined: for N trials, the error in predicting an event probability is inversely proportional to the root of N [44] . That is,

$$\delta \equiv \left| \frac{\sum_{j=1}^{N} g(x_j)}{N} - E\{g(x)\} \right| \sim \frac{1}{\sqrt{N}} \tag{3-72}$$

For the simulations here, 100,000 trials were performed, resulting in an error $\approx \pm 0.003$. Thus the results for the adaline failure probability can be assumed accurate in the second decimal point.[24]

The procedure enumerated above provides a quick survey into the trend for adaline failure probability. It suffers, however, from an important statistical inaccuracy: the components on the n-dimensional vector are independent. Ideally, n components should have some measure of dependence upon one another, because in fact they are dependent random variables. A more rigorous method for creating a sample space would be to create m components at a time using the multi-dimensional joint probability density function, eq. (3-44). In this method, m components, x_i, would be drawn from a uniform distribution over [-1,+1]. An additional element, y, distributed over [0, C_n] would also be drawn. If $y \leq f_x(x_1, \ldots, x_m)$, where $f_x(x_1, \ldots, x_m)$ is the joint density of eq. (3-44), then the m x_i components would be used as a sample. 100,000 samples would be then be averaged.

The problem with this more rigorous method is computation time. For any reasonably

---

24. Note that 4,000,000 independent trials would be required to secure the third decimal point.

large m, the probability that $y \leq f_x(x_1, \ldots, x_m)$ is very small.[25] Some tests using this method were attempted: tens of thousands of "bad" samples were found for every good sample, when m was only 20. Computation times of days were required to achieve any reasonable sample size. A positive note, however, is that the preliminary results showed that the dependent samples resulted in statistically insignificant differences from the independent samples (see discussion below).

The source code and results for the simulations are contained in Appendix A. The following section interprets the results.

3.5.3 Simulation Results

The results of the Monte Carlo simulation are tabulated in Figure 3-29. Plots of the data are presented in Figures 3-30 through 5-33. This section contains some interpretative commentary on the data.

The first note of interest is that the sum of the squares for n+1 components behaved very well. In all cases, $\sum_{i=0}^{n}(x_i)^2 = 1.00 \pm 0.009$. This means that the simulation did create a sample set whose elements have a distribution such that the sum of n+1 squares equals unity, which was the original intention. *That is, the independent trials behaved as if they were dependent.*

---

25. At a minimum, the sum of the squares of the x_i components must be less than one. The sample space is an n-dimensional hypercube of volume 2^n. The volume enclosing the elements whose sum of squares is less than 1 is a hypersphere of dimension n and radius 1. Its volume becomes a very small fraction of the volume of the hypercube as n grows large.

		TYPE OF FAULT			
n	m	Zeroed	Rail	Sign-Change	Sum of Squares
10	1	0.081	0.258	0.161	0.996
	5	0.235	0.422	0.469	
20	1	0.057	0.254	0.114	0.998
	2	0.090	0.317	0.180	
	10	0.0243	0.484	0.486	
30	1	0.046	0.252	0.093	0.991
	3	0.093	0.346	0.186	
	15	0.243	0.458	0.488	
40	1	0.040	0.252	0.080	0.992
	4	0.095	0.364	0.190	
	20	0.245	0.462	0.491	
50	1	0.036	0.252	0.072	0.998
	5	0.97	0.378	0.193	
	25	0.247	0.467	0.493	
100	1	0.025	0.251	0.051	0.997
	10	0.099	0.411	0.199	
	50	0.248	0.477	0.496	
200	1	0.018	0.250	0.036	1.000
	2	0.028	0.305	0.056	
	20	0.101	0.437	0.202	
	100	0.249	0.484	0.499	
300	1	0.014	0.250	0.029	0.994
	3	0.029	0.335	0.059	
	30	0.101	0.448	0.202	
	150	0.248	0.486	0.497	
500	1	0.011	0.251	0.023	0.995
	5	0.030	0.367	0.060	
	50	0.102	0.460	0.203	
	250	0.249	0.490	0.498	

Figure 3-29: *Tabulation of Simulation Results*

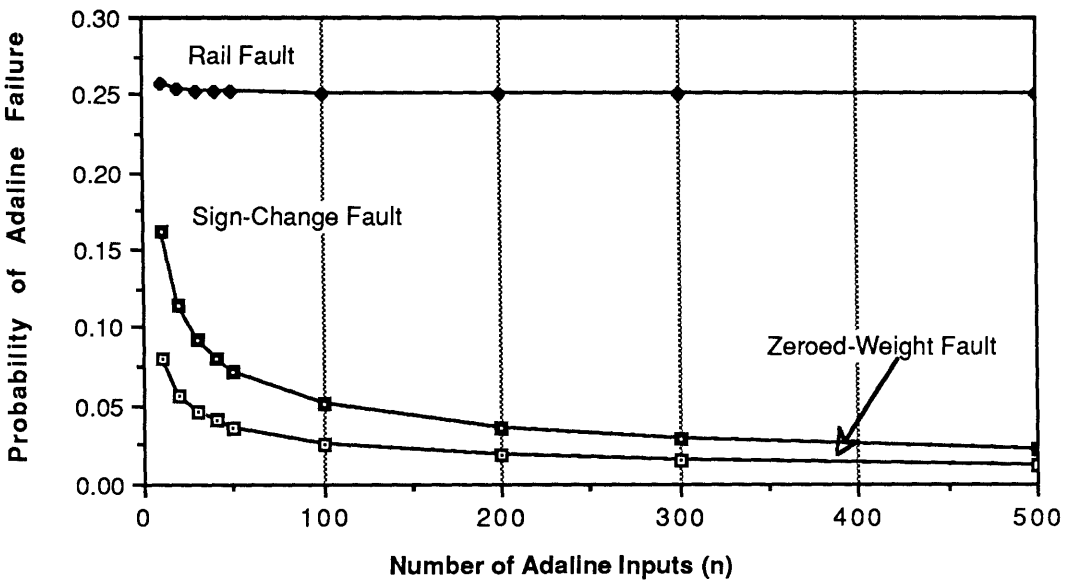

Figure 3-30: Probability of Adaline Failure for Single Fault Cases

For the single fault case, Figure 3-30 shows that the adaline failure probability decreases exponentially with n for both the zeroed-weight and sign-change fault modes. Curve fitting indicates that

$$P_F^0(n) \approx \frac{k}{\sqrt{n}} \tag{3-73}$$

and

$$P_F^{\Delta S}(n) \approx \frac{2k}{\sqrt{n}} \tag{3-74}$$

where $k \approx 0.25$. This is a sensible result: $P_F^0(n) \alpha E\{\sin^{-1}(w_i)\}$ and $P_F^{\Delta S}(n) \alpha E\{\cos^{-1}(1-2w_i^2)\}$; for w_i small, $\sin^{-1}(w_i) \approx w_i$, so $P_F^0(n) \alpha E\{w_i\}$; also for for w_i small, $\cos^{-1}(1-2w_i^2) \approx \sin^{-1}(2w_i) \approx 2w_i$, so $P_F^{\Delta S}(n) \alpha E\{2w_i\}$. Thus, $P_F^{\Delta S}(n) \approx 2P_F^0(n)$. This doubling is also apparent in the raw data (Figure 3-29).

Clearly from the figure, a rail fault is far more likely to cause adaline failure than either of the other two fault modes. This is because **w**, the non-faulty weight vector, is normalized to unit length. For n of any meaningful magnitude, including n =10, the weight components w_i are small. Since the probability of a single rail is given by

$$P_F^{\pm 1}(n) = \frac{1}{\pi} E\left\{\cos^{-1}\left(\frac{1 - (w_k)^2 + w_k}{\left(2 - (w_k)^2\right)^{1/2}}\right)\right\} \tag{3-14}$$

with all w_k small, $P_F^{\pm 1}(n) \approx \frac{1}{\pi} E\left\{\cos^{-1}\left(\frac{1}{\sqrt{2}}\right)\right\} = 0.25$, as indicated.

Interpretation of the multiple fault data is a lesson in asymptotic behavior. This is because for large m the sum

$$\sum_{i=0}^{m-1}(w_i)^2 \approx \frac{m}{n} \tag{3-76}$$

For example, for the multiple zeroed-weight fault,

$$P_F^{0M}(n,m) = \frac{1}{\pi} E\left\{\sin^{-1}\left(\sqrt{\sum_{i=0}^{m-1}(w_i)^2}\right)\right\}$$

which for m large, using eq. (3-76), becomes

$$P_F^{0M}(n,m) \approx \frac{1}{\pi} \sin^{-1}\left(\sqrt{\frac{m}{n}}\right) \tag{3-77}$$

so
$$P_F^{0M}(n,0.01n) \approx \frac{1}{\pi} \sin^{-1}(0.1) = 0.030$$
$$P_F^{0M}(n,0.1n) \approx \frac{1}{\pi} \sin^{-1}(0.32) = 0.102$$
$$P_F^{0M}(n,0.5n) \approx \frac{1}{\pi} \sin^{-1}(0.707) = 0.250$$

These results agree with the data for large n.

Similarly, for the multiple sign-change weight fault,

$$P_F^{\Delta SM}(n,m) = \frac{1}{\pi} E\left\{\cos^{-1}\left(1 - 2\sum_{i=0}^{m-1}(w_i)^2\right)\right\}$$

which for m large becomes

$$P_F^{\Delta SM}(n,m) \approx \frac{1}{\pi} \cos^{-1}\left(1 - \frac{2m}{n}\right) \tag{3-78}$$

so
$$P_F^{\Delta SM}(n,0.01n) \approx \frac{1}{\pi} \cos^{-1}(0.98) = 0.064$$
$$P_F^{\Delta SM}(n,0.1n) \approx \frac{1}{\pi} \cos^{-1}(0.8) = 0.205$$
$$P_F^{\Delta SM}(n,0.5n) \approx \frac{1}{\pi} \cos^{-1}(0.1) = 0.500$$

Again, these results agree with the data.

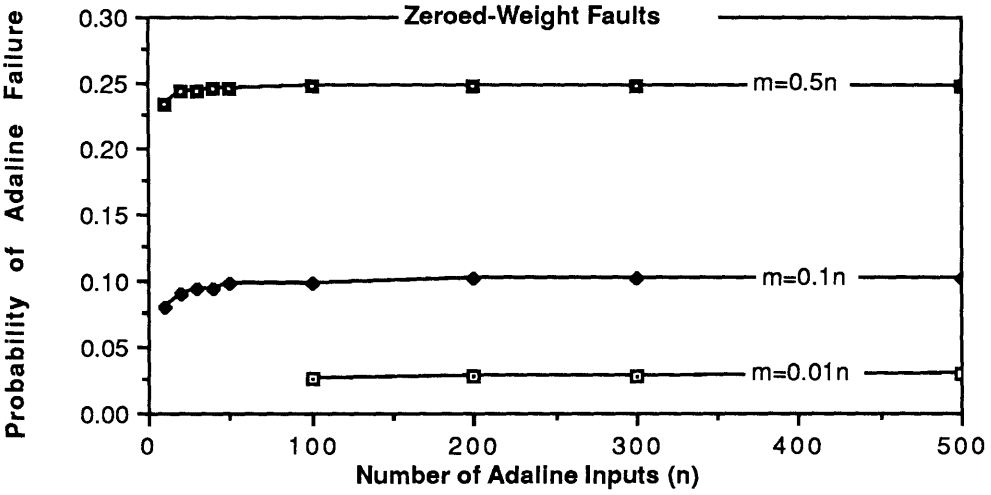

Figure 3-31: Probability of Adaline Failure for Multiple Zeroed-Weight Faults

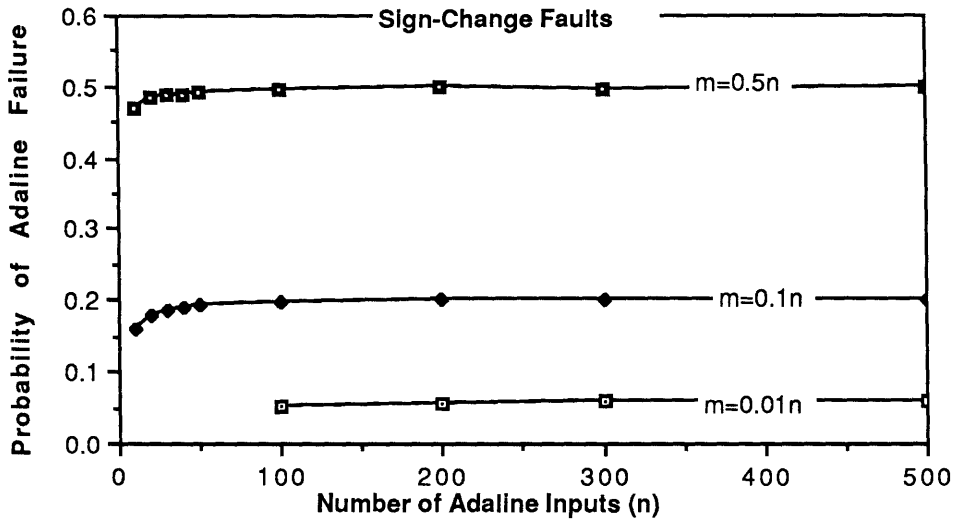

Figure 3-32: Probability of Adaline Failure for Multiple Sign-Change Faults

For the multiple rail fault cases, the asymptote is only clear when m is a large percentage of n. In this case $\|\mathbf{w}_F\|$ is much larger than $\mathbf{w} \circ \mathbf{w}_F$, so the argument of $\cos^{-1}(\bullet)$ vanishes: $\phi \equiv \cos^{-1}\left(\frac{\mathbf{w} \circ \mathbf{w}_F}{\|\mathbf{w}_F\|}\right)$ and ϕ approaches $\frac{\pi}{2}$.

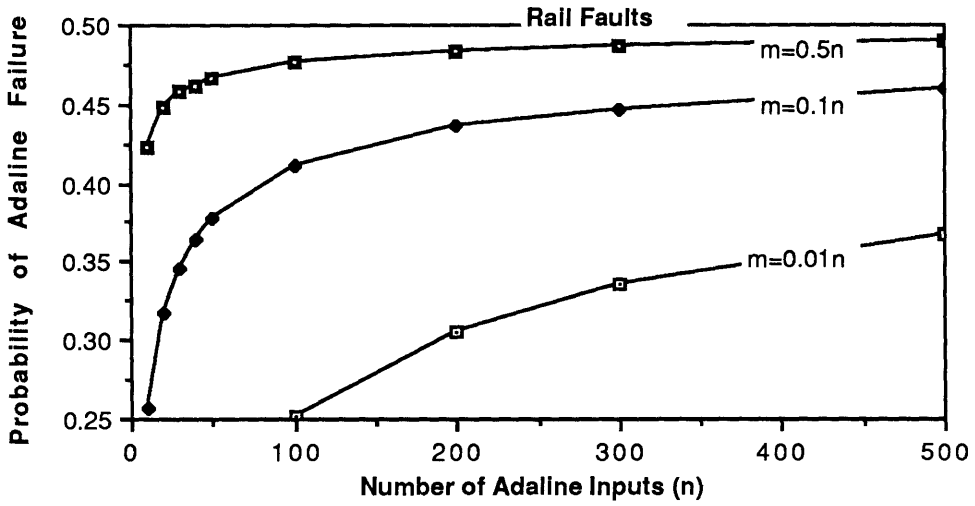

Figure 3-33: Probability of Adaline Failure for Multiple Rail Faults

3.6 PROBABILITY OF MADALINE FAILURE

Extension of the models for adaline failure to a madaline network can be made by propagating the adaline failure probability through the network. In this section, a technique is described for propagating adaline failures. It is based upon the combinatorial probabilities and utilizes the adaline sign change weight fault model.[26]

Since a madaline network consists of connected layers of adalines, an adaline failure in one layer results in an output error which is propagated to the input of the adalines in the subsequent layer. There is some probability that despite being non-faulty an adaline in the subsequent layer produces an output different than it would have if all its inputs were correct. In other words, there is some probability that the "down stream" adalines produce erroneous outputs and behave as if they have failed. The problem is to determine the probability that adalines in the last layer - the output layer - produce erroneous outputs.

---

26. It should be noted that Stevenson [50] developed a different method for propagating failures in a madaline. That method employs an approximation of adaline failure probabilities and is valid when the probabilities are small.

The key to propagating an adaline failure combinatorially through a madaline network is recalling that the probabilities of adaline failure described previously in this chapter are *conditional* probabilities. They stated the probability of adaline failure, or erroneous output, conditioned on the event that a fault occurred. Furthermore, in §3.1 the assumption was made that fault-free adalines do not fail. Thus, the unconditional probability that an adaline fails is:

$$\text{Prob}\{\text{adaline failure}\} = P_F(n,m) \bullet \text{Prob}\{\text{fault occurs}\} \tag{3-80}$$

where $P_F(n,m)$ is the conditional probability of adaline failure. Figure 3-34 illustrates with a Venn diagram.

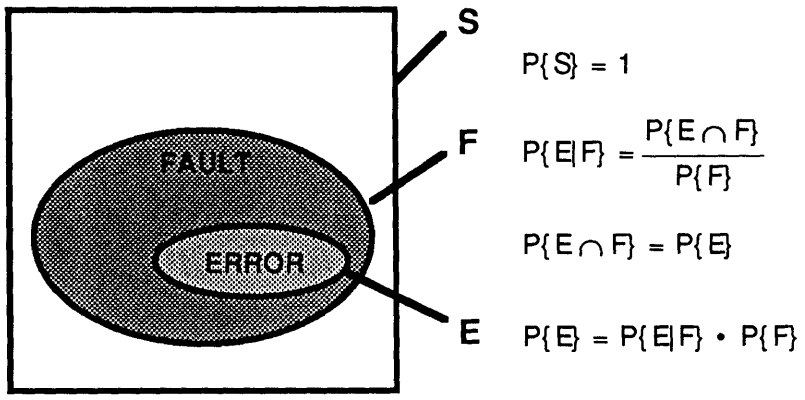

Figure 3-34: *Conditional Probability Venn Diagram*

If an adaline fails, its output has the incorrect sign. The erroneous output is propagated to the inputs of next layer adalines. These adalines operate normally, but have an input with the wrong sign: they behave as if they suffer from a single sign change fault. If the preceding adaline failed with a probability P_F then these adalines will fail with a probability

$$p_1 = P_F \bullet P_F^{\Delta S}(n) \tag{3-81}$$

where n is the number of adalines per layer.

Similarly, non-faulty adalines in the next layer will behave as if they suffer from sign change faults, but in this case <u>all</u> of their weights (except w_0) may have changed sign. The probability that m of them have changed can be approximated[27] by the binomial distribution:

---

27. The probability of m events in n trials can be determined using the binomial distribution when the trials are

$$\binom{n}{m}(p_1)^m (1-p_1)^{n-m} = \frac{n!}{m!\,(n-m!)}(p_1)^m(1-p_1)^{n-m}$$

where p_1 is the probability that the preceding adalines have failed, given in eq. (3-81). Thus, adalines two layers away from the offending fault will fail with probability

$$p_2 = \sum_{i=1}^{n}\left(\binom{n}{i}(p_1)^i (1-p_1)^{n-i} P_F^{\Delta SM}(n,i)\right) \tag{3-82}$$

Propagation of the adaline failure into further layers can be performed by repeatedly applying eq. (3-82), incrementing the indices of p_i each time.

Eq. (3-82) can be estimated using the expected value of n Bermoulli trials (bionomial distribution) and by assuming n is large. In this case, $m=np_1$, that is, np_1 errors are expected in the layer subsequent to the adaline with the offending fault. Using the asymptootic approximation for the multiple sign-change fault, eq. (3-78),

$$P_F^{\Delta SM}(n,m) \approx \frac{1}{\pi}\cos^{-1}\left(1 - \frac{2m}{n}\right) \tag{3-78}$$

eq. (3-82) reduces to

$$p_2 = \approx \frac{1}{\pi}\cos^{-1}(1 - 2p_1) \tag{3-83}$$

Again, equation (3-83) can be used iteratively to determine p_i, the probability of failure of the adaline in layer i from the offending fault.

Notice that eq. (3-83) is independent of n, the size of the layer. Also recall that for $m << n$, $P_F(n,m)$ decreases as n grows, so the original P_F which has been combinatorially propagated ("p_0" in eq. (3-83)) will be smaller for a larger n. These two facts reveal that a "tall" madaline, one with a large number of nodes per layer, will be less likely to fail than a short madaline.

The last layer in a madaline is the output layer. The output adalines encode a recalled

---

independent. Clearly, this is not the case here: an error from a single source is propagating through the network. Nevertheless, if the probability of an event is small, the binomial is a valuable approximation.

pattern which was evoked with the original input vector **x**. Let the output encoding be resilient to a Hamming distance of d, so d adalines in the output layer can be erroneous with the madaline still operational. If the probability of failure of adalines in this last layer P_L, where P_L is determined by eq. (3-82) or eq. (3-83), then the probability that 0 to d adalines have failed is given by the binomial probability:

$$\text{Prob}\{0, 1, \ldots \text{ d adalines failed}\} = \sum_{i=0}^{d} \left(\binom{n}{i} (p_L)^i (1-p_L)^{n-i} \right)$$

Thus the probability the madaline fails is

$$\text{Prob}\{\text{madaline failure}\} = 1 - \sum_{i=0}^{d} \left(\binom{n}{i} (p_L)^i (1-p_L)^{n-i} \right) \tag{3-84}$$

If no output errors can be tolerated, d=0, and eq (3-84) becomes

$$\text{Prob}\{\text{at least 1 output error}\} = 1 - (1-p_L)^n \tag{3-85}$$

Thus, the double-edged sword: for n large, $(1-p_L)^n$ quickly vanishes and the madaline is bound to fail. The madaline output layer, then, should have a large number of inputs but few actual adalines.

Limiting the number of output neurons is a perfectly reasonable requirement. Since the output nodes are binary, n nodes can encode 2^n output classes. As an example, for n = 10, 1024 different classes can be encoded. Thus, the number of input nodes, and possibly hidden nodes, can be large, but the output nodes should be small in number.

3.6.1 An Example

A simple example can be used to evaluate the reliability of a madaline network. In principle a three layer madaline can perform any function that an L layer madaline can perform. Consider, then, a three layer madaline with n=100 neurons in each of the first two layers and 10 output neurons. If a single fault is inserted into the first layer — which is the worst scenario because of error propagation — the adalines in the hidden layer will "fail" with

probability

$$p_1 = P_F \cdot P_F^{\Delta S}(100)$$

$$= 0.05P_F$$

where P_F is the probability of failure of the fault adaline and $P_F^{\Delta S}(100)$ is obtained from Figure 3-29. The adalines in the output layer will fail, using eq. (3-83), with probability

$$p_2 = \approx \frac{1}{\pi}\cos^{-1}(1 - 0.1P_F)$$

Assume no output errors can be tolerated. Using eq. (3-85),

$$\text{Prob}\{\text{madaline failure}\} = 1 - (1-p_2)^{10} \tag{3-86}$$

For a single zeroed-weight fault, $P_F = P_F^0(100) = 0.025$ and eq. (3-86) reveals

$$\text{Prob}\left\{\begin{array}{c}\text{madaline failure} \\ \text{100-100-10 layered configuration} \\ \text{single zeroed-weight fault in layer 1}\end{array}\right\} = 1 - (1 - 0.023)^{10} = 0.21$$

Similarly, for the insertion of a sign-change fault in layer 1, $P_F = P_F^{\Delta S}(100) = 0.051$ and

$$\text{Prob}\left\{\begin{array}{c}\text{madaline failure} \\ \text{100-100-10 layered configuration} \\ \text{single sign-change fault in layer 1}\end{array}\right\} = 1 - (1 - 0.03)^{10} = 0.28$$

The results from the above example are clearly unacceptable.[28] Some design parameters must be altered to reduce the probability of failure.

3.6.2 Some Analysis

One simple method of improving the reliability of a faulty madaline network is to increase the Hamming distance of the output encoding. If the output nodes encode the madaline output vector **y** such that a handful of output errors can be tolerated, the madaline failure probability will decrease. If no Hamming distance can be tolerated, a code should be built in to the network (it can be learned) so that a few errors can be tolerated. That is, coded

---

28. If there were a 100 output nodes, the failure probabilities would be a ridiculous 0.89 and 0.96, respectively.

redundancy should be employed in the output layer. Otherwise, physical redundancy can be employed in the output layer, forcing some acceptable Hamming distance.

Increasing the output Hamming distance, however, does not get to the root of the problem. The architectural impediment which plagues the reliability of a madaline network is the property which is often touted as its chief defense against faults: connectivity. The full connectivity between layers in the madaline neural network acts as a conduit for error propagation. The problem is that full connectivity allows a faulty node to communicate through multiple links with forward nodes. This means that one adaline can inflict multiple sign-change faults in adalines two layers down stream.

The key to isolating a failed element is sparse connectivity. A sparse network will reduce the propagation of errors. The performance penalty which must be paid is network size: a larger network will be required to achieve the same functional capacity. In effect, physical redundancy is being used to isolate faulty elements.

A deliberate topology which isolates failures must be used to reap the full benefits of sparse connectivity. For example, consider the network of Figure 3-35. It has 4 layers. The first three layers have 100 nodes each and the output layer had 10 nodes. Connectivity is restricted so that adalines in Layer 3 are never susceptible to multiple sign-change faults from a single faulty adaline in Layer 1. Each node has a fan-in of 10, so that the layer 3 nodes have a single output.

Suppose a single zero-weight fault is inserted into a first layer neuron. The probability of failure of that neuron, as before, is 0.025 (from the data). Because of the limited connectivity, the probability of failure of a second layer adaline is simply

$$p_1 = (0.025) \bullet P_F^{\Delta S}(10)$$

which from the data is

$$p_1 = (0.025) \bullet (0.161) = 4.025\text{E-}03$$

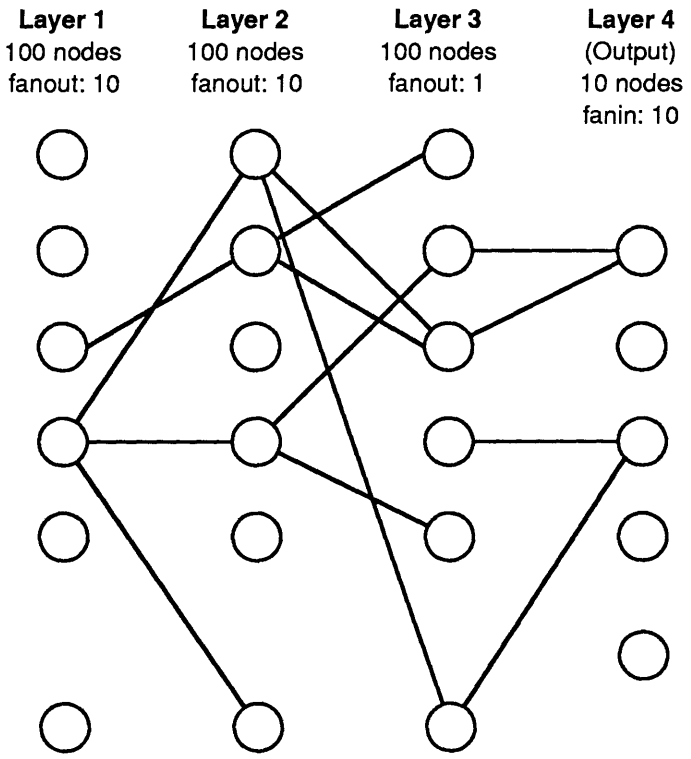

***Figure 3-35**: Sparsely Connected 4-Layer Madaline*

The adalines in the third layer cannot possibly have a multiple sign-change fault. They will fail with probability

$$p_2 = p_1 \bullet P_F^{\Delta S}(10) = (4.025\text{E-}03) \bullet (0.161) = 6.48\text{E-}04$$

Recognizing that these failures are independent makes the calculation of the probability of failure for the output neurons straight forward:

$$\text{Prob}\{\text{a Layer 4 adaline fails}\} = \sum_{j=1}^{10} (6.48\text{E-}04)^j \, P_F^{\Delta S}(10,j)$$

which, to the first order, is approximately

$$\text{Prob}\{\text{a Layer 4 adaline fails}\} \approx 6.48\text{E-}04 \; P_F^{\Delta S}(10,1)$$

$$= (6.48\text{E-}04) \bullet (0.161) = 1.04\text{E-}04$$

Now, tolerating no errors in the output leads to

$$\text{Prob}\left\{\begin{matrix}\text{madaline failure} \\ \text{100-100-100-10 sparse configuration} \\ \text{single zeroed-weight fault in layer 1}\end{matrix}\right\} = 1 - (1 - 1.04\text{E-}04)^{10} = 1.04\text{E-}03$$

Although constructing this network may be impractical, this exercise has shown that sparse connections can drastically reduce the probability of madaline failure.

3.6.3 Multiple Faults in a Network

With a method for propagating of the effect of faults from preceding layers to the output layer developed, a final area requiring examination remains: faults inserted into output adalines. This raises the general question of modelling the behavior of a madaline with multiple faults distributed through the network. Determining madaline failure is these cases is a systematic, if tedious, application of combinatorial probability. The method for analyzing such systems is described below, but formal analysis is left for future work.

Suppose two faults are inserted into two successive layers of a madaline network. Let the faulty adaline in the first layer fail with probability P_{F1} and the faulty adaline in the second layer fail with probability P_{F2}. As discussed above, the non-faulty adalines in the second layer have a probability of producing an erroneous output of $p = P_{F1} \cdot P_F^{\Delta S}(n)$. The faulty adaline in the second layer has an additional probability of failure. This adaline fails with probability given by

$$\text{Prob}\left\{\begin{array}{c}\text{faulty adaline in}\\ \text{second layer fails}\end{array}\right\} = \text{Prob}\left\{\left(\begin{array}{c}\text{erroneous input}\\ \text{causes failure}\end{array}\right) \text{ OR } \left(\begin{array}{c}\text{fault}\\ \text{causes failure}\end{array}\right)\right\}$$

which is

$$\text{Prob}\left\{\begin{array}{c}\text{faulty adaline in}\\ \text{second layer fails}\end{array}\right\} = P_{F1}P_F^{\Delta S}(n) + P_{F2} - P_{F1}\cdot P_F^{\Delta S}(n)\cdot P_{F2}$$

Using such simple statements of combinatorial probability and careful bookkeeping, the error caused by a faulty adaline can be propagated through the network and multiple faults in a madaline can be considered.

Next suppose f faults, each causing an adaline to fail with probability P_F, are distributed randomly in a madaline network with L layers and n adalines per layer. Assuming that the faults are uniformly distributed and no single adaline receives more than one fault

(although the models developed previously can account for this), the probability that any adaline fails because of an inserted fault only is

$$P_{F,FAULT} = \frac{f}{nL} P_F$$

For n large, the number of failures in the first layer can be assumed to be $n \cdot \left(\frac{f}{nL} P_F\right) = \frac{f}{L} P_F$. The adalines in the second layer thus see $m = \frac{f}{L} P_F$ erroneous inputs. From these erroneous inputs alone the second layer adalines will fail with a probability $P_{F,EI}$

$$P_{F,EI} = P_F^{\Delta SM}(n,m) \tag{3-86}$$

But, $\frac{f}{nL}$ in the second layer will also have faults of their own; those faulty adalines will have a probability of failure of $(P_{F,EI} + P_F - P_{F,EI} \cdot P_F)$. The number of expected failures in the second layer will thus be

$$\left(n - \frac{f}{nL}\right) P_{F,EI} + \frac{f}{nL} (P_{F,EI} + P_F - P_{F,EI} \cdot P_F) \tag{3-87}$$

The third layer will see m erroneous inputs, where m is given by eq. (3-87). The probability of failure for non-faulty third layer adalines from these erroneous inputs is determined using eq. (3-86). Third layer faults must also counted.

This iterative process continues until the probability of failure of the output layer adalines can be determined. Using this method and careful accounting of the combinatorial probabilities, the madaline failure can be assessed.

CHAPTER FOUR
CONCLUSION

Those readers seeking a short answer to the question, "Are neural networks fault-tolerant?", must wait. The work described here represents a first step in a rigorous journey towards quantifying the fault-tolerance of these systems. Some conclusions can be drawn from the data of Chapter Three, but, by and large, the models which were developed are building blocks for future work.

To provide some concluding remarks, the work is briefly reviewed and future work to be performed is identified.

6.1 SUMMARY

In this thesis, a particular neural network was selected and its operation under faulty conditions was modelled. The paradigm is the madaline, a feed-forward binary element neural network which is well-suited for pattern classification tasks. The madaline consists of many processing nodes, called adalines, which adaptively place linear decision boundaries in their input space.

An adaline decision is determined by the sign of the dot product of the input vector and an adaline weight vector. Thus, the weight vector provides the specification for the adaline decision. With all adaline failures modelled as weight faults, a spatial analysis of the adaline was utilized to determine the probability of a faulty weight vector misclassifying the input space.

Three fault modes were examined. The *zeroed-weight fault* modelled the effect of a synaptic disconnection in a madaline network. The *rail fault* examined the effect of a weight component saturating to its minimum or maximum value. The *sign-change fault* considered the effect of a weight component changing sign. Although implausible from a practical perspective, this latter fault mode was used to model the propagation of errors in a madaline.

Rigorous closed-form solutions for the probability of adaline failure were pursued for the

three fault modes. The models were purposely general and assumed a uniform distribution of a weight vector normalized to unit length. Determining the expected probabilities of failure for each fault mode required deriving the probability density function of the components of an n-dimensional unit vector. This result, on its own, may be useful in other applications.

Although closed-form solution for adaline failure probability models were obtained, computer simulation through statistical trials provided a better interpretation of the results. For both single zeroed-weight and sign-change faults, the probability of adaline failure was proportional to the inverse root of the number of adaline inputs, n:

$$P_F^0(n) \approx \frac{1}{4\sqrt{n}}$$

$$P_F^{\Delta S}(n) \approx \frac{1}{2\sqrt{n}}$$

For m multiple faults, a similar result was obtained:

$$P_F^{0M}(n,m) \approx \frac{1}{\pi} \sin^{-1}\left(\frac{\sqrt{m}}{\sqrt{n}}\right)$$

$$P_F^{\Delta SM}(n,m) \approx \frac{1}{\pi} \cos^{-1}\left(1 - \frac{2m}{n}\right)$$

The probability of adaline failure for rail faults was significantly higher but not as well behaved. However, for a uniformly distributed weight vector, the range of the probability for the rail fault can be shown to be between 0.25 and 0.50.

The probability of failure of a madaline network was determined by propagating errors caused by adaline failures through the network. Since an adaline output is binary ±1, an adaline failure produces an output with the wrong sign. Erroneous adaline outputs in one layer become erroneous inputs in the next layer and errors are propagated using the sign-change fault. Madaline failure can be determined through a systematic, if tedious, application of combinatorial probability.

The madaline analyses reveal that full connectivity can be a nemesis to neural networks because it allows the propagation of multiple copies of errors to down stream neurons. Sparse topologies appear to be worthy of consideration from a reliability viewpoint, although more rigorous analyses must be performed before claims can be made.

6.2 FUTURE WORK

As with any research endeavor, there is more work to do. Using the spatial models and stochastic methods developed in this thesis, future work can continue to pursue the quantification of the fault-tolerance of neural networks. Below are four areas of research of interest.

Weight Component Distributions

The classification function of a neural network is highly dependent upon the statistical nature of the synaptic weights. It would be folly to expect that the distribution of the weights for a particular neural network could be employed to predict a general result. In this work the weight vectors associated with each neuron (adaline) were assumed to be randomly oriented. The validity of this assumption has been reported [43], but further investigation is necessary. The distribution of the weights in a trained network should be examined and compared to the uniform distribution assumed here. Also, other distributions can be tested to determine the robustness of a network as a function of the weight distributions.

Simplification of the Closed-Form Solutions.

The closed-form equations for the adaline failure probability were deemed too involved to solve by hand. Approximations which rely on the weight components, w_i, being small should be made to obtain reasonable forms for these equations.

Madaline Simulation.

The Monte Carlo methods should be used to determine the probability of failure for a madaline network. In §5.6, some approximations for analyzing complete networks were made. A simulation would provide insight to the validity of those approximations. Note that this would <u>not</u> be the simulation of a neural network; it would be the statistical evaluation of the failure model of a neural network.

The credible results from the brief analysis of a sparsely connected network indicate a need for additional work in madaline topologies. This work should examine the trade-offs of network size and functional capacity versus increased reliability.

Sigmoidal Threshold Units

The next logical research step would be to extend the models developed here to neurons which utilize a sigmoidal threshold function in place of the step function. A sigmoidal function may be more forgiving of faults since outputs will not fail hard to the opposite sign. This may be especially useful to prohibit the propagation of errors because the sigmoid has the capability of "squashing" errors before they become large. The popularity of the back-propagation learning rule, which requires a sigmoidal threshold function, would make this research widely applicable.

CHAPTER FIVE
BIBLIOGRAPHY

1. Abbot, E., *Flatland: A Romance of Many Dimensions*, Little, Brown: Boston, 1941.
2. Abu-Mostafa, Y. S. "Neural Networks for Computing?" in Denker, J. S., ed., *AIP Conference Proceedings 151: Neural Networks for Computing*, American Institute of Physics: New York, 1986, pp. 1-6.
3. Anderson, J. A. and E. Rosenfeld, *Neurocomputing: Foundations of Research*, MIT Press: Cambridge, MA, 1988.
4. Andes, D., B. Widrow & et. al., "MRIII: A Robust Algorithm for Training Analog Neural Networks," *Proceedings of the IJCNN-90-Wash*, 1990, pp. I: 533-536.
5. Avižieniz, A. and J. C. Laprie, "Dependable Computing: From Concepts to Design Diversity," *Proceedings of the IEEE*, v. 74 (1986) pp. 629-638.
6. Barnett, S. and Cronin, T. M., *Mathematical Formulae for Engineering and Science Students*, 4th Ed., Bradford Univerity Press, 1986.
7. Borsuk, K., *Multidimensional Analytic Geometry*, Państwowe Wydawnictwo Naukowe (PWN – Polish Scientific Publishers): Warsaw, 1969.
8. Brown, R. G., *Introduction to Random Signal Analysis and Kalman Filtering*, John Wiley and Sons: New York, 1983.
9. Buzzard, R. D., *Design and Analysis of an Adaptive System*, Master of Science Thesis, MIT Department of Electrical Engineering, 1958.
10. Carpenter, G. A. and S. Grossberg, "Absolutely Stable Learning of Recognition Codes by a Self-Organizing Neural Network," in Denker, J. S. ed., *AIP Conference Proceedings 151: Neural Networks for Computing*, American Institute of Physics: New York, 1986, pp. 77-85.
11. Carter, M. J., F. J. Rudolph, and A. J. Nucci, "Operational Fault Tolerance of CMAC Networks," in D. S. Touretzky, ed., *Advances in Neural Information Processing Systems 2*, Morgan Kaufman: San Mateo, CA, 1990, pp. 340-347.
12. Carter, M. J., "The 'Illusion' of Fault-Tolerance in Neural Networks for Pattern Recognition and Signal Processing," *Technical Session on Fault-Tolerant Integrated Systems*, University of New Hampshire, Durham, NH, March 1988.
13. Chalkley, H. W., J. Cornfield, and H. Park, "A Method for Estimating Volume-Surface Ratios," *Science*, v. 110 (1949), pp. 295-297.
14. Drake, A.W., *Fundamentals of Applied Probability Theory*, McGraw-Hill: New York, 1967.
15. Dwight, H.B., *Tables of Integrals and Other Mathematical Data*, 4th Ed., Macmillan: New York, 1961.
16. Gallagher, R. G., *Information Theory and Reliable Communication*, John Wiley and Sons: New York, 1968.
17. Gazzaniga, M. S., D. Steen, and B. T. Volpe, *Functional Neuroscience*, Harper and Row: New York, 1979.
18. Gelb, A., ed., *Applied Optimal Estimation*, MIT Press: Cambridge, MA, 1974.
19. Glanz, F. H., *Statistical Extrapolation in Certain Adaptive Pattern-Recognition Systems*, Ph.D. Dissertation, Department of Electrical Engineering, Stanford University, 1965.
20. Hecht-Nielsen, R., *Neurocomputing*, Addison-Wesley Publishing: Reading, MA, 1990.
21. Hoff, Jr., M. E., *Learning Phenomena in Networks of Adaptive Switching Ciruits*, Ph.D. Dissertation, Department of Electrical Engineering, Stanford University, 1962.
22. James, G., *Mathematics Dictionary*, 4th Ed., Von Nostrand Reinhold: New York, 1976.
23. Karush, W., *Webster's New World Dictionary of Mathematics*, Simon and Schuster: New York, 1989.

24. Kendall, M. G. and P. A. P. Moran, *Geometrical Probability*, Charles Griffin and Co: London, 1963.

25. Kohonen, T., *Self-Organization and Associative Memory*, 3rd Ed., Springer-Verlag: New York, 1989.

26. Kohonen, T., "The Self-Organizing Map," *Proceedings of the IEEE*, v. 78 (1990), pp. 1464-1480.

27. Krylov, V.I., *Approximate Calculation of Integrals*, Macmillan: New York, 1962.

28. Lippmann, R.P., "An Introduction to Computing with Neural Networks," *IEEE Acoustics, Speech, and Signal Processing Magazine*, v. 4 #2 (April 1987), pp. 4-22.

29. Mattson, R.L., *The Design and Analysis of an Adaptive System for Statistical Classification*, Master of Science Thesis, Department of Electrical Engineering, Massachusetts Institute of Technology, May 1959.

30. McCulloch, W. S. and W. H. Pitts, "A Logical Calculus of Ideas Immanent in Nervous Activity," Bulletin of Mathematical Biophysics, vol. 5 (1943), pp. 115-133. Reprinted in [3], pp. 15-27.

31. Minsky, M. *Computation: Finite and Infinite Machines*, Prentice-Hall: New York, 1967.

32. Minsky, M. L. and Papert, S.A., *Perceptrons: An Introduction to Computational Geometry*, 3rd Ed., MIT Press: Cambridge MA, 1988.

33. Nijhuis, J., B. Höfflinger, A. van Schaik, and L. Spaanenburg, "Limits to the Fault-Tolerance of a Feedforward Neural Network with Learning," *Digest of Papers, Fault-Tolerant Computing: The Twentieth International Symposium (FTCS-20)*, June 1990, pp. 228-235.

34. Papoulis, A., *Probability, Random Variables, and Stochastic Processes*, McGraw-Hill: New York, 1965.

35. Petsche, T. and B. W. Dickinson, "Trellis Codes, Receptive Fields, and Fault Tolerant Self-Repairing Neural Networks," *IEEE Transactions on Neural Networks*, v. 1 (1990), pp. 154-166.

36. Protzel, P., D. Palumbo, and M. Arras, "Fault-Tolerance of a Neural Network Solving the Traveling Salesman Problem," *NASA Contractor Report 181798*, February, 1989.

37. Prudnikov, A. P., Yu. A. Brychkov, and O. I. Marichev, *Integrals and Series; Volume 1: Elementary Functions*, Gordon and Breach Science Publishers: New York, 1986.

38. Rosenblatt, F. *Principles of Neurodynamics*, Spartan Books: Washington, DC, 1961.

39. Roth, M. W., "Survey of Neural Network Technology for Automatic Target Recognition," *IEEE Transactions on Neural Networks*, v. 1 (1990), pp. 28-43.

40. Rumelhart, D. E., G. E. Hinton and R. J. Williams, "Learning Internal Representations by Error Propagation," in D. E. Rumelhart, J. L. McClelland, eds., *Parallel Distributed Processing: Explorations in the Microstructure of Cognition; Volume 1: Foundations*, MIT Press: Cambridge, MA, 1986, pp. 318-362.

41. Santaló, L. A., *Integral Geometry and Geometric Probability*, Addison-Wesley: Reading, MA, 1976.

42. Santaló, L. A., *Introduction to Integral Geometry*, Hermann and Cie Éditeurs: Paris, 1953.

43. Schneider, R., personal communicatiuon cited in [45].

44. Schreider, Yu. A., ed., *The Monte Carlo Method*, Pergamon Press: New York, 1966.

45. Shoemaker, P. A., "Weight Errors in Layered Networks of Threshold Logic Units," *Neural Network Review*, v. 4, #1, pp. 24-26.

46. Simpson, P. K., *Artificial Neural Systems: Foundations, Paradigms, Applications, and Implementations*, Pergamon Press: New York, 1990.

47. Solomon, H., *Geometric Probability*, Society for Industrial and Applied Mathematics: Philadelphia, 1978.

48. Sommerville, D. M. Y., *An Introduction to the Geometry of n Dimensions*, Dover Publications: New York, 1958.

49. Spanier, J. and Oldham, K. B., *An Atlas of Functions*, Hemisphere Publishing: New York, 1987.

50. Stevenson, M., R. Winter, and B. Widrow, "Sensitivity of Feedforward Neural Networks to Weight

Errors," *IEEE Transactions on Neural Networks*, v. 1 (1990), pp. 71-80.

51. Stone, G.O., "An Analysis of the Delta Rule and the Learning of Statistical Associations," in D. E. Rumelhart, J. L. McClelland, eds., *Parallel Distributed Processing: Explorations in the Microstructure of Cognition; Volume 1: Foundations*, MIT Press: Cambridge, MA, 1986, pp. 444-459.

52. Stork, D.G., "Self-Organization, Pattern Recognition, and Adaptive Resonance Networks," *Journal of Neural Network Computing*, v. 1 (1989), pp. 26-42.

53. Strang, G., personal communication, November, 1990.

54. Wasserman, P. D., *Neural Computing: Theory and Practice*, Van Nostrand Reinhold: New York, 1989.

55. White, H., "Learning in Artificial Neural Networks: A Statistical Approach," *Neural Computation*, v. 1 (1989), pp. 425-464.

56. Widrow, B. "Generalization and Information Storage in Networks of Adaline 'Neurons'," in M. C. Yovits, G. T. Jacobi, and G. D. Goldstein, eds., *Self-Organizing Systems 1962*, Spartan Books: Washington, DC, 1962, pp. 435-461.

57. Widrow, B., *Lectures on Neural Networks, Lecture Notes from Tutorial Number 5*, IJCNN 90, June 1990.

58. Widrow, B., ed., *DARPA Neural Network Study*, AFCEA Press: Fairfax VA, 1988.

59. Widrow, B., J. R. Glover, Jr., J. M. McCool, J. Kaunitz, C. S. Williams, R. H. Hearn, J. R. Ziedler, E. Dong, Jr., and R. C. Goodlin, "Adaptive Noise Cancelling: Principles and Applications," *Proceedings of the IEEE*, v. 63 (1975), pp. 1692-1716.

60. Widrow, B. and M. E. Hoff, "Adaptive Switching Circuits," *IRE WESCON Convention Record*, Part 4, August 1960, pp. 96-104. Reprinted in [3], pp. 126-134.

61. Widrow, B. and M. Lehr, "30 Years of Neural Networks: Perceptron, Madaline, and Backpropagation," *Proceedings of the IEEE*, v. 78 (1990), pp. 1415-1442.

62. Widrow, B., J. M. McCool, M. G. Larimore, and C. R. Johnson, Jr., "Stationary and Nonstationary Learning Characteristics of the LMS Adaptive Filter," *Proceedings of the IEEE*, v. 64 (1976), pp. 1151-1162.

63. Widrow, B. and S. D. Stearns, *Adaptive Signal Processing*, Prentice-Hall: New York, 1985.

64. Widrow, B. and R. Winter, "Neural Nets for Adaptive Filtering and Adaptive Pattern Recognition," *Computer*, v. 21, #3 (March 1988), pp. 25-39.

65. Widrow, B., R. G. Winter and R. A. Baxter, "Learning Phenomena in Layered Neural Networks," *Proceedings of the First IEEE International Conference on Neural Networks*, June 1987, pp. II:411-430.

66. Widrow, B., R. G. Winter, and R. A. Baxter, "Layered Neural Nets for Pattern Recognition," *IEEE Transactions on Acoustics, Speech, and Signal Processing*, v. 36 (1988), pp. 1109-1118.

67. Winter, R.G., *Madaline Rule II: A New Method for Training Networks of Adalines*, Ph. D Thesis, Stanford University, January 1989.

68. Woods, F.S., *Higher Geometry: An Introduction to Advanced Methods in Analytical Geometry*, Ginn and Co: Boston, 1922.

APPENDIX A: MONTE CARLO SIMULATION CODE AND RESULTS

Three programs, all written in C for the VAX/VMS operating system, were used for the Monte Carlo simulations of adaline failure probability. This Appendix contains the source code for those three files and the resulting output files.

The process was to create a sample set of numbers which have the distribution of the components of an (n+1)-dimensional unit vector. Separate sample sets of 100,000 numbers each were created for n=10, 20, 30, 40, 50, 100, 200, 300, and 500. The sample sets were then stored in separate files. The first program in this Appendix, COMGEN.C, created the sample sets.

The two other programs, SINGLEPF.C and MULTIPLEPF.C, used the sample sets to estimate the probability of adaline failure. For single fault cases, all 100,000 data points were used individually as arguments in the equations for adaline failure. Their average was then taken as the expected value of the probability of adaline failure for the particular case. As a check on the validity of the sample space, the average sum of n+1 of the elements squared was also computed. The results were written to SINGLEPF.OUT.

For the multiple fault case, m random selections from the sample space were made. These m elements were used as arguments in the equations for adaline failure. This process was repeated 100,000 times and the average result was posted to MULTIPLEPF.OUT. For each dimension, n, three values of m were chosen: m = 0.01n (1% faulty weights), m = 0.1n (10% faulty weights) and m = 0.5n (50% faulty weights). For $n < 100$, the case of m = 0.01n was excluded.

A.1 COMGEN.C

```
/* COMGEN.C: Component Generator
This program creates 10,000 components of an n+1 dimensional vector
which is distributed uniformly on the unit n+1 dim hypersphere.

The procedure is to generate a pair of uniformly distributed random
numbers, x and y.  If y <= f(x), where f(x) is the density function
of interest then keep x as part of the sample space.

For a large number of samples, the set {x1, x2, ...} will have a
distribution of f(x).

The components are stored in a file for later recall to determine
expected values of functions of them.

Created: 24 October 1990, 21:00, MDz
Updated: 15 December 1990 14:00, MDz */

#include <stdio.h>                    /* for file & printing output */
#include <math.h>                              /* for real work */
#include <time.h>                         /* for timing execution */

main()
{

/* Declare variables */

int     n;                        /* the dim - 1, # of adaline inputs */
int     nCase;                          /* the different cases for n */
int     CompNum = 0;              /* count of # of components created */

double  theX, theY;                      /* the pair of random numbers*/

time_t  thetime;                /* time stamp for performance checks */
FILE    *outFile;                                 /* output data file */

printf("COMPONENT GENERATION BEGUN.\n");

for (nCase = 1; nCase <= 9; nCase++) {

   switch(nCase) {
      case 1:                                                    /* n=10 */
        n = 10;
        outFile = fopen("COMP10.DAT", "w");
        printf("\n \tFile COMP10.DAT opened.");
        break;

      case 2:                                                    /* n=20 */
        n = 20;
        outFile = fopen("COMP20.DAT", "w");
        printf("\n \tFile COMP20.DAT opened.");
        break;

      case 3:                                                    /* n=30 */
        n = 30;
        outFile = fopen("COMP30.DAT", "w");
        printf("\n \tFile COMP30.DAT opened.");
```

```
        break;

      case 4:                                                    /* n=40 */
        n = 40;
        outFile = fopen("COMP40.DAT", "w");
        printf("\n \tFile COMP40.DAT opened.");
        break;

      case 5:                                                    /* n=50 */
        n = 50;
        outFile = fopen("COMP50.DAT", "w");
        printf("\n \tFile COMP50.DAT opened.");
        break;

      case 6:                                                   /* n=100 */
        n = 100;
        outFile = fopen("COMP100.DAT", "w");
        printf("\n \tFile COMP100.DAT opened.");
        break;

      case 7:                                                   /* n=200 */
        n = 200;
        outFile = fopen("COMP200.DAT", "w");
        printf("\n \tFile COMP200.DAT opened.");
        break;

      case 8:                                                   /* n=300 */
        n = 300;
        outFile = fopen("COMP300.DAT", "w");
        printf("\n \tFile COMP300.DAT opened.");
        break;

      case 9:                                                   /* n=500 */
        n = 500;
        outFile = fopen("COMP500.DAT", "w");
        printf("\n \tFile COMP500.DAT opened.");
        break;

     default:                                  /* something's wrong */
        printf("Something is Wrong!\n");
        break;}

   printf("\nVector Dimension: %d", n+1);

/* Start the computation. */
   thetime = time(NULL);
   printf(" ... Starting Computation (n = %d)\n", n);
   CompNum = 0;

   while (CompNum < 100000) {               /* get 100,000 numbers */

      theX = rand() % 200001;          /* rand # from 0 to 200,000 */
      theX = theX/100000.0;            /* scale down, 4 dec places */
      theX = theX - 1.0;              /* change range to: -1 to +1 */

      theY = rand() % 1000001;       /* rand # from 0 to 1,000,000 */
      theY = theY/1000000.0;           /* scale down, 5 dec places */
```

```
      /* Check for y <= f(x); keep if true; else try again*/
      if (theY <= pow(sqrt(1.0 - (theX * theX)) , (n-2) ))

         {CompNum = CompNum + 1;
          fprintf(outFile, "%f\n", theX);          /* save to file */
          if ((CompNum % 100) == 0)          /* monitor every 1000 */
            {printf("Component %d: ", CompNum);
             printf("%f, (y = %f)\r", theX, theY);
            }                                    /* end of printing */
          }                                  /* end of saving number */

      }                  /* 100,000 components for 1 dim generated. */
   fclose(outFile);

   printf("\n\n 10,000 components generated (n = %d).\n", n);
   thetime = time(NULL) - thetime;
   printf("%d vectors in %d seconds.\n", CompNum, (int)thetime);
   printf("File Closed.\n");

   }                                             /* end of all cases */

}                                                  /* end of program */
```

A.2 SINGLEPF.C

```
/* PROBABILITY OF ADALINE FAILURE FOR SINGLE FAULT CASE
Mark Dzwonczyk, Created: Dec 15, 1990, Updated: Dec 16, 1990 13:00

This program reads in a set of numbers with distribution f(x)
and determines the expected values of functions of them using
the Law of Large Numbers:
E{g(x)} = sum(g(x))/N, for N large.  Here, n = 100,000.

This program is used only for the single fault cases */


#include <stdio.h>                    /* for file & printing output */
#include <math.h>                                 /* for real work */

main() {

/* Declare Variables First */

int     n = 0;              /* dim-1 of vector; # of adaline inputs */
int     CompNum = 0;                 /* count of number of vectors */
int     nCase = 0;                             /* an index for PFs */

FILE    *inFile;                                    /* Input Data */
FILE    *outFile;                                  /* Output Data */

double  SOS[10];               /* Sum of Squares, n+1 should be 1. */
double  PFSZWF[10];              /* PF - Single Zeroed-Weight Fault*/
double  PFSRF[10];                       /* PF - Single Rail Fault */
double  PFSSCF[10];               /* PF - Single Sign Change Fault */
double  PI = 3.1415926;
double  w;                     /* the element from the sample space */
double  w2;                                          /* w squared */
double  theArg;                  /* an argument for trig functions */

   outFile = fopen("SINGLEPF.OUT", "w");
   fprintf (outFile, "Calculation of Adaline Failures as functions of
      dim, n\n");

   printf("FUNCTION CALCULATION BEGUN.\n");

   for (nCase = 1; nCase < 10; nCase++) {

      PFSZWF[nCase] = 0.0;             /* initialize the variables */
      PFSRF[nCase] = 0.0;
      PFSSCF[nCase] = 0.0;
      SOS[nCase] = 0.0;

      switch(nCase) {
         case 1:                                                /* n=10 */
           inFile = fopen("COMP10.DAT", "r");
           printf("\n \tFile COMP10.DAT opened.");
           n = 10;
           break;

         case 2:                                                /* n=20 */
           inFile = fopen("COMP20.DAT", "r");
```

```
      printf("\n \tFile COMP20.DAT opened.");
      n = 20;
      break;

    case 3:                                                  /* n=30 */
      inFile = fopen("COMP30.DAT", "r");
      printf("\n \tFile COMP30.DAT opened.");
      n = 30;
      break;

    case 4:                                                  /* n=40 */
      inFile = fopen("COMP40.DAT", "r");
      printf("\n \tFile COMP40.DAT opened.");
      n = 40;
      break;

    case 5:                                                  /* n=50 */
      inFile = fopen("COMP50.DAT", "r");
      printf("\n \tFile COMP50.DAT opened.");
      n = 50;
      break;

    case 6:                                                 /* n=100 */
      inFile = fopen("COMP100.DAT", "r");
      printf("\n \tFile COMP100.DAT opened.");
      n = 100;
      break;

    case 7:                                                 /* n=200 */
      inFile = fopen("COMP200.DAT", "r");
      printf("\n \tFile COMP200.DAT opened.");
      n = 200;
      break;

    case 8:                                                 /* n=300 */
      inFile = fopen("COMP300.DAT", "r");
      printf("\n \tFile COMP300.DAT opened.");
      n = 300;
      break;

    case 9:                                                 /* n=500 */
      inFile = fopen("COMP500.DAT", "r");
      printf("\n \tFile COMP500.DAT opened.");
      n = 500;
      break;

   default:                                 /* something's wrong! */
      inFile = fopen("COMPXX.DAT", "r");
      printf("Something is Wrong!\n");
      break;}

printf("...Vector Dimension: %d\n", n+1);

/* Read the components */
for (CompNum = 1; CompNum <= 100000; CompNum++) {
   fscanf(inFile, "%f\n", &w);
   w2 = w * w;
```

```
        SOS[nCase] = SOS[nCase] + w2;

        theArg = sqrt(w2);       /* no abs val function for floats*/
        PFSZWF[nCase] = PFSZWF[nCase] + asin(theArg);

        theArg = (1 - w2 + w)/sqrt(2 - w2);
        PFSRF[nCase] = PFSRF[nCase] + acos(theArg);

        theArg = 1 - (2 * w2);
        PFSSCF[nCase] = PFSSCF[nCase] + acos(theArg);

        if ( ( (CompNum % 10000)== 0 ) && (CompNum > 10) )
                                          /* monitor some results */
          {printf("\nComputation at Number %d for n = %d.
              RESULTS:\n", CompNum, n);
           printf("\tPROB FAIL, SINGLE ZEROED-WEIGHT FAULT: %f\n",
              PFSZWF[nCase]/(CompNum * PI));
           printf("\tPROB FAIL, SINGLE RAIL-FAULT: %f\n",
              PFSRF[nCase]/(CompNum * PI));
           printf("\tPROB FAIL, SINGLE SIGN-CHANGE FAULT: %f\n",
              PFSSCF[nCase]/(CompNum * PI));
           printf("\tSum of %d Squares: %f\n",n+1, (SOS[nCase] *
              (n+1))/(CompNum));
          }                              /* Close printing commands */

      }                                  /* File completely read */
    fclose(inFile);

    CompNum = 100000;          /* adjust for auto index increment */

    printf("\n\nComputation Complete for n = %d.  RESULTS FOR %d
       TRIALS:\n", n, CompNum);
    printf("\tPROB FAIL, SINGLE ZEROED-WEIGHT FAULT: %f\n",
       PFSZWF[nCase]/(CompNum * PI));
    printf("\tPROB FAIL, SINGLE RAIL-FAULT: %f\n",
       PFSRF[nCase]/(CompNum * PI));
    printf("\tPROB FAIL, SINGLE SIGN-CHANGE FAULT: %f\n",
       PFSSCF[nCase]/(CompNum * PI));
    printf("\tSum of %d Squares: %f\n",n+1, (SOS[nCase] *
       (n+1))/(CompNum));

    fprintf(outFile, "\n\nComputation Complete for n = %d.  RESULTS
       FOR %d TRIALS:\n", n, CompNum);
    fprintf(outFile, "\tPROB FAIL, SINGLE ZEROED-WEIGHT FAULT:
       %f\n", PFSZWF[nCase]/(CompNum * PI));
    fprintf(outFile, "\tPROB FAIL, SINGLE RAIL-FAULT: %f\n",
       PFSRF[nCase]/(CompNum * PI));
    fprintf(outFile, "\tPROB FAIL, SINGLE SIGN-CHANGE FAULT: %f\n",
       PFSSCF[nCase]/(CompNum * PI));
    fprintf(outFile, "\tSum of %d Squares: %f\n",n+1, (SOS[nCase] *
       (n+1))/(CompNum));

  }                                      /* Completed all nCases */

}                                                /* End of Main */
```

A.3 MULTIPLEPF.C

```
/* PROBABILITY OF ADALINE FAILURE FOR MULTIPLE FAULT CASE
Mark Dzwonczyk, Created: Dec 15, 1990, Updated: Dec 16, 1990 15:00

This program reads in a set of numbers with distribution f(x)
and determines the expected values of functions of them
using the Law of Large Numbers:
E{g(x)} = sum(g(x))/N, for N large.  Here, n = 100,000.

This program is used only for the multiple fault cases.
For these, a sample set of 100,000 numbers is read
and m numbers are randomly selected from the set.

An average over 100,000 trials is used for E{g(x)}.*/


#include <stdio.h>                    /* for file & printing output */
#include <math.h>                                /* for real work */

main() {

/* Declare Variables First */

int     n = 0;              /* dim-1 of vector; # of adaline inputs */
int     m[4] = 0;                    /* number of faults inserted */
int     nCase = 0;                             /* an index for PFs */
int     mCase = 0;                    /* an index for differents m's */
int     NumOfTrials;           /* will be 100,000, used for testing */
int     randIndex = 0;        /* a random index into the sample set */
int     CompNum = 0;                 /* count of number of vectors */
int     counter = 0;                             /* simple counter */

FILE    *inFile;                                    /* Input Data */
FILE    *outFile;                                  /* Output Data */

double  theX[100000];                             /* The sample set */
double  PFMZWF[4][10];        /* PF -  Multiple Zeroed Weight Fault */
double  PFMRF[4][10];                 /* PF -- Multiple Rail Fault */
double  PFMSCF[4][10];          /* PF - Multiple Sign Change Fault */
double  PI = 3.1415926;
double  sum1, sum2;                    /* a sum and sum of squares */
double  temp1, temp2;          /* some temp vars for trig functions */
double  theArg;                /* some temp vars for trig functions */

   NumOfTrials = 100000;

   outFile = fopen("MULTIPLEPF.OUT", "w");

   fprintf (outFile, "Calculation of Adaline Failures as functions of
      dim, n\n");
   fprintf(outFile, "Multiple Fault Cases\n");

   printf("FUNCTION CALCULATION BEGUN.\n");

   for (nCase = 1; nCase < 10; nCase++) {

      switch(nCase) {
```

```
case 1:                                                    /* n=10 */
  inFile = fopen("COMP10.DAT", "r");
  printf("\n \tFile COMP10.DAT opened.");
  n = 10;
  break;

case 2:                                                    /* n=20 */
  inFile = fopen("COMP20.DAT", "r");
  printf("\n \tFile COMP20.DAT opened.");
  n = 20;
  break;

case 3:                                                    /* n=30 */
  inFile = fopen("COMP30.DAT", "r");
  printf("\n \tFile COMP30.DAT opened.");
  n = 30;
  break;

case 4:                                                    /* n=40 */
  inFile = fopen("COMP40.DAT", "r");
  printf("\n \tFile COMP40.DAT opened.");
  n = 40;
  break;

case 5:                                                    /* n=50 */
  inFile = fopen("COMP50.DAT", "r");
  printf("\n \tFile COMP50.DAT opened.");
  n = 50;
  break;

case 6:                                                   /* n=100 */
  inFile = fopen("COMP100.DAT", "r");
  printf("\n \tFile COMP100.DAT opened.");
  n = 100;
  break;

case 7:                                                   /* n=200 */
  inFile = fopen("COMP200.DAT", "r");
  printf("\n \tFile COMP200.DAT opened.");
  n = 200;
  break;

case 8:                                                   /* n=300 */
  inFile = fopen("COMP300.DAT", "r");
  printf("\n \tFile COMP300.DAT opened.");
  n = 300;
  break;

case 9:                                                   /* n=500 */
  inFile = fopen("COMP500.DAT", "r");
  printf("\n \tFile COMP500.DAT opened.");
  n = 500;
  break;

default:                              /* something's wrong! */
  inFile = fopen("COMPXX.DAT", "r");
  printf("Something is Wrong!\n");
  break;}
```

```
  printf("...Vector Dimension: %d\n", n+1);

  m[1] = n/100;                          /* mCase = 1, 1% faults */
  m[2] = n/10;                          /* mCase = 2, 10% faults */
  m[3] = n/2;                           /* mCase = 3, 50% faults */

/* Read the components */
  printf("(reading file for n = %d ...(%d trials)...", n,
     NumOfTrials);
  for (CompNum = 0; CompNum < NumOfTrials; CompNum++)
    fscanf(inFile, "%f\n", &theX[CompNum]);
  fclose(inFile);              /* Now theX[] is the sample set */
  printf("file closed\n");

  for(mCase = 1; mCase < 4; mCase++) {

     PFMZWF[mCase][nCase] = 0.0;          /*initialize variables*/
     PFMRF[mCase][nCase] = 0.0;
     PFMSCF[mCase][nCase] = 0.0;

     for(CompNum = 1; CompNum <= NumOfTrials; CompNum++) {
                                          /* do 100,000 trials */
        sum1 = 0.0;
        sum2 = 0.0;

        for(counter=1; counter <= m[mCase]; counter++)
                                              /* get m samples */
          {randIndex = rand() % NumOfTrials;
           sum1 = sum1 + theX[randIndex];         /* need a sum */
           sum2 = sum2 + (theX[randIndex] * theX[randIndex]);
                                       /* and a sum of squares */

        theArg = sqrt(sum2);
        if (theArg > 1.0) theArg = 1.0;

                 /* The line above is required in case by chance
                           the sum of sqaures is greater than 1.
                           The function asin will gag otherwise.
                    This is only relevant for n small (10, 20) */

        PFMZWF[mCase][nCase] = PFMZWF[mCase][nCase] +
           asin(theArg);

        temp1 = 1 + sum1 - sum2;
        temp2 = m[mCase] + 1 - sum2;
        theArg = temp1/sqrt(temp2);
        if (theArg > 1.0) theArg = 1.0;
        if (theArg < -1.0) theArg = -1.0;

                /* the lines above is required in case by chance
                           the sum of sqaures is greater than 1.
                           The function acos will gag otherwise.
                    This is only relevant for n small (10, 20) */

        PFMRF[mCase][nCase] = PFMRF[mCase][nCase] + acos(theArg);

        theArg = 1 - (2 * sum2);
```

```
      if (theArg <-1.0) theArg = -1.0;

                /* the line above is required in case by chance
                          the sum of sqaures is greater than 1.
                          The function acos will gag otherwise.
                  This is only relevant for n small (10, 20) */

       PFMSCF[mCase][nCase] = PFMSCF[mCase][nCase] +
         acos(theArg);

      if (((CompNum % (NumOfTrials/10))==0) && (CompNum > 10))
                                        /* monitor some results */
        {printf("\nComputation at Number %d for n = %d.
          RESULTS:\n", CompNum, n);

         printf("\tPROB FAIL, MUL. ZEROED-WEIGHT FAULT:\n");
         printf("\t\tm = %d: %f\n", m[mCase],
          PFMZWF[mCase][nCase]/(CompNum * PI));

         printf("\tPROB FAIL, MUL. RAIL-FAULT:\n");
         printf("\t\tm = %d: %f\n", m[mCase],
          PFMRF[mCase][nCase]/(CompNum * PI));

         printf("\tPROB FAIL, MUL. SIGN-CHANGE FAULT:\n");
         printf("\t\tm = %d: %f\n", m[mCase],
          PFMSCF[mCase][nCase]/(CompNum * PI));

        }                              /* Close printing commands */

     }                                    /* Completed the trials */

  }                      /* Completed 3 cases for m, specific n */

CompNum = NumOfTrials;     /* adjust for indexed being bumped */

printf("\n\nComputation Complete for n = %d.  RESULTS FOR %d
   TRIALS:\n", n, CompNum);

printf("\tPROB FAIL, MUL. ZEROED-WEIGHT FAULT:\n");
  for(mCase = 1; mCase < 4; mCase++)
  printf("\t\tm = %d: %f\n", m[mCase],
    PFMZWF[mCase][nCase]/(CompNum * PI));

printf("\tPROB FAIL, MUL. RAIL-FAULT:\n");
  for(mCase = 1; mCase < 4; mCase++)
  printf("\t\tm = %d: %f\n", m[mCase],
    PFMRF[mCase][nCase]/(CompNum * PI));

printf("\tPROB FAIL, MUL. SIGN-CHANGE FAULT:\n");
   for(mCase = 1; mCase < 4; mCase++)
   printf("\t\tm = %d: %f\n", m[mCase],
    PFMSCF[mCase][nCase]/(CompNum * PI));

/* Print to File */

fprintf(outFile, "\n\nComputation Complete for n = %d.  RESULTS
   FOR %d TRIALS:\n", n, CompNum);
```

```
      fprintf(outFile, "\tPROB FAIL, MUL. ZEROED-WEIGHT FAULT:\n");
        for(mCase = 1; mCase < 4; mCase++)
        fprintf(outFile, "\t\tm = %d: %f\n", m[mCase],
          PFMZWF[mCase][nCase]/(CompNum * PI));

      fprintf(outFile, "\tPROB FAIL, MUL. RAIL-FAULT:\n");
        for(mCase = 1; mCase < 4; mCase++)
        fprintf(outFile, "\t\tm = %d: %f\n", m[mCase],
          PFMRF[mCase][nCase]/(CompNum * PI));

      fprintf(outFile, "\tPROB FAIL, MUL. SIGN-CHANGE FAULT:\n");
         for(mCase = 1; mCase < 4; mCase++)
         fprintf(outFile, "\t\tm = %d: %f\n", m[mCase],
          PFMSCF[mCase][nCase]/(CompNum * PI));

   }                                          /* Completed all nCases */
fclose(outFile);
}                                                    /* End of Main */
```

A.4 SINGLEPF.OUT

```
Calculation of Adaline Failures as functions of dim, n

Computation Complete for n = 10.  RESULTS FOR 100000 TRIALS:
      PROB FAIL, SINGLE ZEROED-WEIGHT FAULT: 0.080718
      PROB FAIL, SINGLE RAIL-FAULT: 0.258036
      PROB FAIL, SINGLE SIGN-CHANGE FAULT: 0.161436
      Sum of 11 Squares: 0.996311

Computation Complete for n = 20.  RESULTS FOR 100000 TRIALS:
      PROB FAIL, SINGLE ZEROED-WEIGHT FAULT: 0.056952
      PROB FAIL, SINGLE RAIL-FAULT: 0.254418
      PROB FAIL, SINGLE SIGN-CHANGE FAULT: 0.113903
      Sum of 21 Squares: 0.998735

Computation Complete for n = 30.  RESULTS FOR 100000 TRIALS:
      PROB FAIL, SINGLE ZEROED-WEIGHT FAULT: 0.046256
      PROB FAIL, SINGLE RAIL-FAULT: 0.252875
      PROB FAIL, SINGLE SIGN-CHANGE FAULT: 0.092513
      Sum of 31 Squares: 0.990914

Computation Complete for n = 40.  RESULTS FOR 100000 TRIALS:
      PROB FAIL, SINGLE ZEROED-WEIGHT FAULT: 0.040086
      PROB FAIL, SINGLE RAIL-FAULT: 0.251698
      PROB FAIL, SINGLE SIGN-CHANGE FAULT: 0.080172
      Sum of 41 Squares: 0.992254

Computation Complete for n = 50.  RESULTS FOR 100000 TRIALS:
      PROB FAIL, SINGLE ZEROED-WEIGHT FAULT: 0.035947
      PROB FAIL, SINGLE RAIL-FAULT: 0.251584
      PROB FAIL, SINGLE SIGN-CHANGE FAULT: 0.071894
      Sum of 51 Squares: 0.997678

Computation Complete for n = 100.  RESULTS FOR 100000 TRIALS:
      PROB FAIL, SINGLE ZEROED-WEIGHT FAULT: 0.025370
      PROB FAIL, SINGLE RAIL-FAULT: 0.250707
      PROB FAIL, SINGLE SIGN-CHANGE FAULT: 0.050741
      Sum of 101 Squares: 0.996765

Computation Complete for n = 200.  RESULTS FOR 100000 TRIALS:
      PROB FAIL, SINGLE ZEROED-WEIGHT FAULT: 0.017980
      PROB FAIL, SINGLE RAIL-FAULT: 0.250371
      PROB FAIL, SINGLE SIGN-CHANGE FAULT: 0.035960
      Sum of 201 Squares: 1.000242

Computation Complete for n = 300.  RESULTS FOR 100000 TRIALS:
      PROB FAIL, SINGLE ZEROED-WEIGHT FAULT: 0.014626
      PROB FAIL, SINGLE RAIL-FAULT: 0.250226
      PROB FAIL, SINGLE SIGN-CHANGE FAULT: 0.029253
      Sum of 301 Squares: 0.994071

Computation Complete for n = 500.  RESULTS FOR 100000 TRIALS:
      PROB FAIL, SINGLE ZEROED-WEIGHT FAULT: 0.011327
      PROB FAIL, SINGLE RAIL-FAULT: 0.250191
      PROB FAIL, SINGLE SIGN-CHANGE FAULT: 0.022654
      Sum of 501 Squares: 0.995233
```

A.5 MULTIPLEPF.OUT

```
Calculation of Adaline Failures as functions of dim, n
Multiple Fault Cases

Computation Complete for n = 10.  RESULTS FOR 100000 TRIALS:
     PROB FAIL, MUL. ZEROED-WEIGHT FAULT:
          m = 0: 0.000000
          m = 1: 0.080431
          m = 5: 0.234702
     PROB FAIL, MUL. RAIL-FAULT:
          m = 0: 0.000000
          m = 1: 0.257499
          m = 5: 0.422430
     PROB FAIL, MUL. SIGN-CHANGE FAULT:
          m = 0: 0.000000
          m = 1: 0.160861
          m = 5: 0.469404

Computation Complete for n = 20.  RESULTS FOR 100000 TRIALS:
     PROB FAIL, MUL. ZEROED-WEIGHT FAULT:
          m = 0: 0.000000
          m = 2: 0.089945
          m = 10: 0.243087
     PROB FAIL, MUL. RAIL-FAULT:
          m = 0: 0.000000
          m = 2: 0.317708
          m = 10: 0.448419
     PROB FAIL, MUL. SIGN-CHANGE FAULT:
          m = 0: 0.000000
          m = 2: 0.179891
          m = 10: 0.486174

Computation Complete for n = 30.  RESULTS FOR 100000 TRIALS:
     PROB FAIL, MUL. ZEROED-WEIGHT FAULT:
          m = 0: 0.000000
          m = 3: 0.093300
          m = 15: 0.243773
     PROB FAIL, MUL. RAIL-FAULT:
          m = 0: 0.000000
          m = 3: 0.346450
          m = 15: 0.458082
     PROB FAIL, MUL. SIGN-CHANGE FAULT:
          m = 0: 0.000000
          m = 3: 0.186600
          m = 15: 0.487545

Computation Complete for n = 40.  RESULTS FOR 100000 TRIALS:
     PROB FAIL, MUL. ZEROED-WEIGHT FAULT:
          m = 0: 0.000000
          m = 4: 0.095171
          m = 20: 0.245338
     PROB FAIL, MUL. RAIL-FAULT:
          m = 0: 0.000000
          m = 4: 0.364110
          m = 20: 0.461909
     PROB FAIL, MUL. SIGN-CHANGE FAULT:
          m = 0: 0.000000
          m = 4: 0.190342
          m = 20: 0.490676
                                                                    CONTD
```

```
Computation Complete for n = 50.  RESULTS FOR 100000 TRIALS:
     PROB FAIL, MUL. ZEROED-WEIGHT FAULT:
          m = 0: 0.000000
          m = 5: 0.096807
          m = 25: 0.246685
     PROB FAIL, MUL. RAIL-FAULT:
          m = 0: 0.000000
          m = 5: 0.377793
          m = 25: 0.467392
     PROB FAIL, MUL. SIGN-CHANGE FAULT:
          m = 0: 0.000000
          m = 5: 0.193613
          m = 25: 0.493371

Computation Complete for n = 100.  RESULTS FOR 100000 TRIALS:
     PROB FAIL, MUL. ZEROED-WEIGHT FAULT:
          m = 1: 0.025390
          m = 10: 0.099310
          m = 50: 0.247918
     PROB FAIL, MUL. RAIL-FAULT:
          m = 1: 0.250688
          m = 10: 0.411250
          m = 50: 0.476614
     PROB FAIL, MUL. SIGN-CHANGE FAULT:
          m = 1: 0.050780
          m = 10: 0.198621
          m = 50: 0.495836

Computation Complete for n = 200.  RESULTS FOR 100000 TRIALS:
     PROB FAIL, MUL. ZEROED-WEIGHT FAULT:
          m = 2: 0.028232
          m = 20: 0.100999
          m = 100: 0.249260
     PROB FAIL, MUL. RAIL-FAULT:
          m = 2: 0.305295
          m = 20: 0.436569
          m = 100: 0.483615
     PROB FAIL, MUL. SIGN-CHANGE FAULT:
          m = 2: 0.056463
          m = 20: 0.201999
          m = 100: 0.498520

Computation Complete for n = 300.  RESULTS FOR 100000 TRIALS:
     PROB FAIL, MUL. ZEROED-WEIGHT FAULT:
          m = 3: 0.029282
          m = 30: 0.101175
          m = 150: 0.248367
     PROB FAIL, MUL. RAIL-FAULT:
          m = 3: 0.334698
          m = 30: 0.447868
          m = 150: 0.486370
     PROB FAIL, MUL. SIGN-CHANGE FAULT:
          m = 3: 0.058563
          m = 30: 0.202350
          m = 150: 0.496733

Computation Complete for n = 500.  RESULTS FOR 100000 TRIALS:
     PROB FAIL, MUL. ZEROED-WEIGHT FAULT:
          m = 5: 0.030244
          m = 50: 0.101575
          m = 250: 0.248902
     PROB FAIL, MUL. RAIL-FAULT:
          m = 5: 0.367345                                          CONTD
```

```
        m = 50: 0.459844
        m = 250: 0.490417
    PROB FAIL, MUL. SIGN-CHANGE FAULT:
        m = 5: 0.060489
        m = 50: 0.203149
        m = 250: 0.497804
```

APPENDIX B: MATHEMATICAL DERIVATIONS

This appendix presents some of the mathematical detail which was not directly relevant to the principles developed in the body of the text.

B.1 REDUCTION OF GAMMA FUNCTION RATIOS

In §3.4.2, the probability density function for a single weight component, $f_w(w)$ is given by:

$$f_w(w) = \frac{\Gamma\left(\frac{n}{2}\right)}{\Gamma\left(\frac{n-1}{2}\right)\sqrt{\pi}}(1-w^2)^{(n-3)/2} \qquad \text{(3-49), (B1-1)}$$

Since the variable n is an integer, the fraction $\frac{\Gamma\left(\frac{n}{2}\right)}{\Gamma\left(\frac{n-1}{2}\right)\sqrt{\pi}}$ can be reduced to a form not explictly requiring the gamma function. For n even, $\frac{n}{2}$ is also an integer and the gamma function can be calculated directly using as $\Gamma(x) = (x-1)!$, for x an integer. For n even, however, $\frac{n-1}{2}$ is an odd multiple of $\frac{1}{2}$ and the gamma function property $\Gamma(x+1) = x\Gamma(x)$ must be used in conjunction with $\Gamma\left(\frac{1}{2}\right) = \sqrt{\pi}$. The converse is true for n odd.

The formula for the gamma function of an odd multiple of $\frac{1}{2}$ is given by [49]:

$$\Gamma\left(m + \tfrac{1}{2}\right) = (2m-1)!!\,\sqrt{\pi}\,2^{-m} \qquad \text{(B1-2)}$$

where m is an integer and x!! is the semifactorial function

$$x!! = \begin{cases} 1 & x = -1,\ 0 \\ x\bullet(x-2)\bullet(x-4)\bullet\ldots\bullet5\bullet3 & x \text{ odd} \\ x\bullet(x-2)\bullet(x-4)\bullet\ldots\bullet4\bullet2 & x \text{ even} \end{cases} \qquad \text{(B1-3)}$$

The left side of eq. (B1-2) can be rephrased as

$$\begin{aligned} \Gamma\left(m + \tfrac{1}{2}\right) &= \Gamma\left(m - \tfrac{1}{2} + 1\right) \\ &= \Gamma\left(\tfrac{2m-1}{2} + 1\right) \end{aligned} \qquad \text{(B1-4)}$$

Using the property of the gamma function, $\Gamma(y+1) = y\Gamma(y)$, the right side of eq. (B1-4) is:

$$\Gamma\left(\frac{2m-1}{2}+1\right) = \frac{2m-1}{2}\Gamma\left(\frac{2m-1}{2}\right)$$
$$= \frac{2m-1}{2}\Gamma\left(m-\frac{1}{2}\right) \qquad \text{(B1-5)}$$

Concatenating eqs. (B1-4) and (B1-5),

$$\Gamma\left(m+\frac{1}{2}\right) = \frac{2m-1}{2}\Gamma\left(m-\frac{1}{2}\right)$$

or
$$\Gamma\left(m-\frac{1}{2}\right) = \frac{2}{2m-1}\Gamma\left(m+\frac{1}{2}\right)$$

and from eq. (B2-2)

$$\Gamma\left(m-\frac{1}{2}\right) = \frac{2}{2m-1}\left(\frac{(2m-1)!!\sqrt{\pi}}{2^m}\right)$$

$$\Gamma\left(m-\frac{1}{2}\right) = \frac{2\cdot(2m-1)!!\sqrt{\pi}}{2m-1\cdot 2^m}$$

$$\Gamma\left(m-\frac{1}{2}\right) = \frac{(2m-3)!!\sqrt{\pi}}{2^{m-1}} \qquad \text{(B1-6)}$$

So, for n even, n = 2m, (m an integer)

$$\Gamma\left(\frac{n}{2}\right) = \left(\frac{n}{2}-1\right)! = \left(\frac{n-2}{2}\right)! \qquad \text{(B1-7a)}$$

and
$$\Gamma\left(\frac{n-1}{2}\right) = \Gamma\left(m-\frac{1}{2}\right) = \frac{(n-3)!!\sqrt{\pi}}{2^{(n-2)/2}} \qquad \text{(B1-7b)}$$

And, for n odd, n = 2m+1, m = $\frac{n-1}{2}$ (m an integer)

$$\Gamma\left(\frac{n}{2}\right) = \Gamma\left(m+\frac{1}{2}\right) = (n-2)!!\sqrt{\pi}\,2^{-(n-1)/2} \qquad \text{(B1-8a)}$$

and
$$\Gamma\left(\frac{n-1}{2}\right) = \Gamma(m) = (m-1)! = \left(\frac{n-3}{2}\right)! \qquad \text{(B1-8b)}$$

Using eqs. (B1-7) and eqs. (B1-8), the ratio $\dfrac{\Gamma\left(\frac{n}{2}\right)}{\Gamma\left(\frac{n-1}{2}\right)\sqrt{\pi}}$ becomes

$$\frac{\Gamma\left(\frac{n}{2}\right)}{\Gamma\left(\frac{n-1}{2}\right)\sqrt{\pi}} = \begin{cases} \dfrac{\left(\frac{n-2}{2}\right)!\;2^{(n-2)/2}}{\pi(n-3)!!} & \text{n even} \\ \dfrac{(n-2)!!}{2^{(n-1)/2}\left(\frac{n-3}{2}\right)!} & \text{n odd} \end{cases} \qquad \text{(B1-9)}$$

For obvious notational convenience, the left side of eq. (B1-9) is used in the text.

B.2 VARIANCE OF SINGLE COMPONENT PROBABILITY DENSITY FUNCTION

This section derives the variance of a single component of an n-dimensional unit vector. That variable, w, has a probability density function given by

$$f_w(w) = \frac{\Gamma\left(\frac{n}{2}\right)}{\Gamma\left(\frac{n-1}{2}\right)\sqrt{\pi}}(1-w^2)^{(n-3)/2} \qquad \text{(3-49), (B2-1)}$$

By definition, the variance is the second central moment

$$\sigma^2(w) \equiv E\{(w - E\{w\})^2\} \qquad \text{(B2-2)}$$

but $f_w(w)$ is an even function, so $E\{w\} = 0$, and

$$\sigma^2(w) = E\{w^2\} \qquad \text{(B2-3)}$$

The expected value can be found through integration. The range of integration is given by the range of the value of w, $w \in [-1, +1]$.

$$E\{w^2\} = \int_{-1}^{1} \frac{\Gamma\left(\frac{n}{2}\right)}{\Gamma\left(\frac{n-1}{2}\right)\sqrt{\pi}} w^2(1-w^2)^{(n-3)/2}\, dw \qquad \text{(B2-4)}$$

$$= \frac{\Gamma\left(\frac{n}{2}\right)}{\Gamma\left(\frac{n-1}{2}\right)\sqrt{\pi}} \int_{-1}^{1} \left(w^2(1-w^2)^{(n-3)/2}\right) dw \qquad \text{(B2-5)}$$

and since both w^2 and $(1-w^2)^{(n-3)/2}$ are even functions, their product is even and the integral can be reduced to

$$E\{w^2\} = \frac{\Gamma\left(\frac{n}{2}\right)}{\Gamma\left(\frac{n-1}{2}\right)\sqrt{\pi}} 2\int_{0}^{1} \left(w^2(1-w^2)^{(n-3)/2}\right) dw \qquad \text{(B2-6)}$$

From here, integrals tables are used. From Dwight [15], entry 855.41,

$$\int_0^1 x^m(1 - x^2)^p dx = \frac{\Gamma(p+1)\Gamma\left(\frac{m+1}{2}\right)}{2\Gamma\left(p+\frac{m+3}{2}\right)} \qquad \text{(B2-7)}$$

So with $m = 2$ and $p = \frac{n-3}{2}$

$$\int_0^1 \left(w^2(1-w^2)^{(n-3)/2}\right)dw = \frac{\Gamma\left(\frac{n-3}{2}+1\right)\Gamma\left(\frac{2+1}{2}\right)}{2\Gamma\left(\frac{n-3}{2}+\frac{2+3}{2}\right)}$$

$$= \frac{\Gamma\left(\frac{n-1}{2}\right)\Gamma\left(\frac{3}{2}\right)}{2\Gamma\left(\frac{n}{2}+1\right)} \qquad \text{(B2-8)}$$

and using $\Gamma(x+1) = x\Gamma(x)$ and $\Gamma\left(\frac{1}{2}\right) = \sqrt{\pi}$, $\Gamma\left(\frac{3}{2}\right) = \frac{\sqrt{\pi}}{2}$ and $\Gamma\left(\frac{n}{2}+1\right) = \frac{n}{2}\Gamma\left(\frac{n}{2}\right)$:

$$\int_0^1 \left(w^2(1-w^2)^{(n-3)/2}\right)dw = \frac{\Gamma\left(\frac{n-1}{2}\right)\frac{\sqrt{\pi}}{2}}{2\,\frac{n}{2}\Gamma\left(\frac{n}{2}\right)}$$

$$= \frac{\sqrt{\pi}\,\Gamma\left(\frac{n-1}{2}\right)}{2n\,\Gamma\left(\frac{n}{2}\right)} \qquad \text{(B2-9)}$$

Substituting eq. (B2-9) into eq. (B2-6),

$$E\{w^2\} = \frac{2\Gamma\left(\frac{n}{2}\right)}{\Gamma\left(\frac{n-1}{2}\right)\sqrt{\pi}} \frac{\sqrt{\pi}\,\Gamma\left(\frac{n-1}{2}\right)}{2n\,\Gamma\left(\frac{n}{2}\right)} = \frac{1}{n} \qquad \text{(B2-10)}$$

From eq. (B2-3) the result is obtained:

$$\sigma^2(w) = \frac{1}{n} \qquad \text{(B2-11)}$$

B.3 Closed-Form Solution for the Adaline Failure Probability for the Single Zeroed-Weight Fault

In §3.5, the probability of adaline failure for the single zeroed-weight fault is given by

$$P_F^0(n) = \frac{2\Gamma\left(\frac{n+1}{2}\right)}{\Gamma\left(\frac{n}{2}\right)\pi^{3/2}} \int_0^1 \sin^{-1}(w)\left(1-w^2\right)^{(n-2)/2} dw \qquad \text{(3-66), (B3-1)}$$

The integral can be solved by creating a new variable θ, such that

$$w = \sin\theta, \text{ or } \theta = \sin^{-1}(w) \qquad \text{(B3-2)}$$

so that $dw = \cos\theta \, d\theta$

and since $(\sin\theta)^2 + (\cos\theta)^2 = 1$,

$$\cos\theta = \left(1 - w^2\right)^{1/2} \qquad \text{(B3-3)}$$

so $$dw = \left(1 - w^2\right)^{1/2} d\theta \qquad \text{(B3-4)}$$

Setting the constant term in (B3-1) to Cn

$$Cn = \frac{2\Gamma\left(\frac{n+1}{2}\right)}{\Gamma\left(\frac{n}{2}\right)\pi^{3/2}} \qquad \text{(B3-5)}$$

and substituting eqs. (B3-2) through (B3-5) into eq. (B3-1),

$$P_F^0(n) = Cn \int_0^{\pi/2} \theta\left(\cos\theta\right)^{n-3} d\theta \qquad \text{(B3-6)}$$

From here, tables of definite integrals can be used. Entry 2 on p. 386 of Prudnikow et al [37] states for $k \geq 0$:

$$\int_0^{\pi/2} x(\cos x)^k dx = \left(1-k+2\left[\frac{k+1}{2}\right]\right) \frac{A\,(k-1)!!\pi}{4k!!} - \sum_{j=0}^{\left[\frac{k-1}{2}\right]} \left(\frac{\left(\frac{1-k}{2}\right)_j}{\left(\frac{-k}{2}\right)_j (k-2j)^2} \right) \qquad \text{(B3-7)}$$

where $x!!$ is the semifactorial function defined in eq. (B1-3)

$(x)_j = x \cdot (x+1) \cdot \ldots \cdot (x + j - 1)$

[x] is the largest integer up to and including x

$$A = \begin{cases} 1, & k \text{ even} \\ \frac{\pi}{2}, & k \text{ odd} \end{cases}$$

So, for k odd,

$$\left[\frac{k+1}{2}\right] = \frac{k+1}{2} \text{ and } \left[\frac{k-1}{2}\right] = \frac{k-1}{2}$$

and for k even,

$$\left[\frac{k+1}{2}\right] = \frac{k}{2} \text{ and } \left[\frac{k-1}{2}\right] = \frac{k-2}{2}$$

Eq. (B3-7) can be used to solve eq. (B3-6) for $n \geq 3$. The result is

For n odd, $n \geq 3$:

$$P_F^0(n) = \frac{2\Gamma\left(\frac{n+1}{2}\right)}{\Gamma\left(\frac{n}{2}\right)\pi^{3/2}} \left(\frac{\pi^2(n-4)!!}{8(n-3)!!} - \sum_{j=0}^{\frac{(n-5)}{2}} \left(\frac{\left(2 - \frac{n}{2}\right)\left(3 - \frac{n}{2}\right)\cdots\left(j + 1 - \frac{n}{2}\right)}{\left(\frac{3-n}{2}\right)\left(\frac{5-n}{2}\right)\cdots\left(\frac{2j + 1 - n}{2}\right)(n - 3 - 2j)^2} \right) \right) \quad \text{(B3-8a)}$$

and

For n even, $n \geq 3$:

$$P_F^0(n) = \frac{2\Gamma\left(\frac{n+1}{2}\right)}{\Gamma\left(\frac{n}{2}\right)\pi^{3/2}} \left(\frac{\pi(n-4)!!}{2(n-3)!!} - \sum_{j=0}^{\frac{(n-4)}{2}} \left(\frac{\left(2 - \frac{n}{2}\right)\left(3 - \frac{n}{2}\right)\cdots\left(j + 1 - \frac{n}{2}\right)}{\left(\frac{3-n}{2}\right)\left(\frac{5-n}{2}\right)\cdots\left(\frac{2j + 1 - n}{2}\right)(n - 3 - 2j)^2} \right) \right) \quad \text{(B3-8b)}$$

Eqs. (B3-8) support the conclusion that a closed-form solution is not necessarily the best presentation for P_F. Computer-aided solutions, even if approximations, are much more informative.